Addition of Small Electrophiles to NHC-stabilized Disilicon(0): A Revisit of the Isolobal Concept in Low-Valent Silicon Chemistry

Marius I. Arz, Martin Straßmann, Daniel Geiß, Gregor Schnakenburg, and Alexander C. Filippou*

Institute of Inorganic Chemistry, University of Bonn, Gerhard-Domagk-Straße 1, D-53121 Bonn, Germany

E-mail: filippou@uni-bonn.de

Supporting Information

Content

1. Experimental Section – General Part S2

2. Syntheses and analytical data of the compounds S4

2.1 Synthesis of $[Si_2(H)(Idipp)_2][B(Ar^F)_4]$ (**1H**$[B(Ar^F)_4]$) S4

2.2 Synthesis of $[Si_2(D)(Idipp)_2][B(Ar^F)_4]$ (**1D**$[B(Ar^F)_4]$) S11

2.3 Synthesis of $[Si_2(Me)(Idipp)_2][B(Ar^F)_4]$ (**1Me**$[B(Ar^F)_4]$) S12

2.4 Synthesis of $[Si_2(Et)(Idipp)_2][B(Ar^F)_4]$ (**1Et**$[B(Ar^F)_4]$) S16

2.5 Synthesis of $[Si_2(Li)(Idipp)_2][B(C_6F_5)_4]$ (**1Li**$[B(C_6F_5)_4]$) S21

2.6 Synthesis of $[Si_2(Na)(Idipp)_2][B(Ar^F)_4]$ (**1Na**$[B(Ar^F)_4]$) S24

3. Determination of the standard free Gibbs energy of activation for **1H**$[B(Ar^F)_4]$ S28

4. Crystal structure determination S33

5. Electronic structure calculations S37

5.1 Comparison of selected bonding parameters of **1**, $\mathbf{1}_{calc}$, **1H**$[B(Ar^F)_4]$, $\mathbf{1H^+}_{calc}$, $\mathbf{(1H^+)^{TS}}_{calc}$, $\mathbf{(1H^+)'}_{calc}$, $\mathbf{1Me^+}_{calc}$, $\mathbf{(1Me^+)'}_{calc}$ and $\mathbf{1Li^+}_{calc}$ S38

5.2 Selected Kohn-Sham orbitals of the compounds $\mathbf{1H^+}_{calc}$, $\mathbf{(1H^+)'}_{calc}$, $\mathbf{1Me^+}_{calc}$, $\mathbf{(1Me^+)'}_{calc}$ and $\mathbf{1Li^+}_{calc}$ S41

5.3 Results of the natural bond orbital (NBO) and natural resonance theory analysis of $\mathbf{1}_{calc}$, $\mathbf{1H^+}_{calc}$, $\mathbf{(1H^+)^{TS}}_{calc}$, $\mathbf{(1H^+)'}_{calc}$, $\mathbf{1Me^+}_{calc}$, $\mathbf{(1Me^+)'}_{calc}$ and $\mathbf{1Li^+}_{calc}$ S43

5.4 Cartesian coordinates [Å] and SCF energies of the calculated structures of $\mathbf{1}_{calc}$, $\mathbf{1H^+}_{calc}$, $\mathbf{(1H^+)^{TS}}_{calc}$, $\mathbf{(1H^+)'}_{calc}$, $\mathbf{1Me^+}_{calc}$, $\mathbf{(1Me^+)'}_{calc}$, $\mathbf{1Li^+}_{calc}$ S49

5.5 Cartesian coordinates [Å] and SCF energies of the calculated structures of $[(NHC^{Me})(Me)Si{=}Si(NHC^{Me})]^+$, $(NHC^{Me})(Me)Si{=}SiMe$, $Me_2Si{=}Si(NHC^{Me})$, $[Me_2Si{=}SiMe]^-$, $Me_2Si{=}PMe$ and $[Me_2P{=}PMe]^+$ (NHC^{Me} = $C[N(Me)CH]_2$ S64

6. References S67

1. Experimental Section – General Part

All experiments were carried out under strict exclusion of water and oxygen under an atmosphere of argon using Schlenk or glove box techniques. The commercially received argon had a purity of ≥99.999 % and was further passed through an argon purification system to remove traces of O_2 and H_2O. The glassware was dried in an oven at approximately 110 °C and baked under vacuum prior to use. *n*-Hexane was refluxed over sodium wire in the presence of benzophenone and tetraglyme (0.5 vol%), distilled off under argon, and degassed by freeze-pump-thaw cycles. Fluorobenzene was stirred over CaH_2, trap-to-trap condensed and degassed by freeze-pump-thaw cycles. All solvents were stored in the glove box. The compounds $Si_2(Idipp)_2$ (**1**),[S1] $[H(Et_2O)_2][B(Ar^F)_4]$ (Ar^F = C_6H_3-3,5-$(CF_3)_2$),[S2] $[Li(Et_2O)_{2.5}][B(C_6F_5)_4]$[S3] and $Na[B(Ar^F)_4]$[S4] were prepared following the procedures described in the corresponding references. $[D(Et_2O)_2][B(Ar^F)_4]$ was synthesized following the procedure described in ref. [S2] using DCl (97.5 atom % D) instead of HCl. C, H, N elemental analyses were carried out in triplicate for each sample on an Elementar Vario Micro elemental analyser. The C, H, N values did not differ by more than ±0.3 %. The mean C, H, N values are given below for each compound. The melting points were determined in triplicate for each sample using a Büchi melting point B-545 apparatus. The samples were sealed in capillary tubes under vacuum and heated once with a gradient of 5 K min^{-1} for a rough determination and twice with a gradient of 2 K min^{-1}, starting 20 K below the roughly determined melting or decomposition temperature. The decomposition of the compounds was verified by optical inspection or in the case of compounds **1H**$[B(Ar^F)_4]$ and **1Me**$[B(Ar^F)_4]$ by recording the ^1H NMR spectra of the heated samples in THF-d_8. The IR spectra of **1H**$[B(Ar^F)_4]$ and **1D**$[B(Ar^F)_4]$ (4000 – 400 cm^{-1}) were recorded on a Bruker Alpha FT-IR spectrometer in the glovebox with a diamond single-reflection Platinum-ATR module at room temperature. The following abbreviations were used for the intensities of the absorption bands: vs = very strong, s = strong, m = medium, w = weak, vw = very weak. The NMR spectra were recorded on a Bruker Avance DMX-300 or DPX-300 NMR spectrometer in dry deoxygenated THF-d_8 or C_6D_5Cl. THF-d_8 was trap-to-trap condensed after stirring over sodium powder and stored over molecular sieves (4 Å). C_6D_5Cl was stirred over CaH_2, and then trap-to-trap condensed and stored over molecular sieves (4 Å). The ^1H and $^{13}C\{^1H\}$ NMR spectra were calibrated against the residual proton and natural abundance ^{13}C resonances of the deuterated solvent relative to tetramethylsilane (THF-d_8: δ_H = 1.73 ppm and δ_C = 25.3 ppm; C_6D_5Cl: δ_H = 6.96 ppm and δ_C = 126.0 ppm). The ^{29}Si, ^{19}F, ^{11}B and ^7Li NMR spectra were calibrated against external pure $SiMe_4$, $CFCl_3$, $BF_3{\cdot}Et_2O$ and a 1 M aqueous LiCl solution, respectively. The NMR standards were filled in sealed capillaries and measured in vacuum-sealed 5 mm NMR tubes containing THF-d_8, C_6D_5Cl and C_6H_5F,

respectively. The following abbreviations were used for the multiplicities and forms of the NMR signals: s = singlet, d = doublet, t = triplet, q = quartet, qq = quartet of quartets, sept = septet, m = multiplet, dm = doublet of multiplets, br = broad. The full width at half maximum of broad signals was designated with $\Delta\nu_{1/2}$. The ^{1}H and ^{13}C NMR signals of all compounds were assigned by a combination of HMQC, HMBC and DEPT experiments. This allowed an unequivocal assignment of all proton and carbon resonances including those of the diastereotopic methyl groups of the isopropyl substituents, which were labelled with the subscript letters A and B, respectively. The label A was used for the methyl group with the lower ^{1}H chemical shift. ^{1}H-^{29}Si HMBC experiments were carried out to assign the chemically different carbene substituents of **1H**[B(Ar^{F})$_4$] at 213 K and **1Me**[B(Ar^{F})$_4$] and **1Et**[B(Ar^{F})$_4$] at 298 K using the correlation between the C^{4,5}-*H* signals of the carbene substituents and the ^{29}Si NMR signals. The assigned carbene signals were designated with the letters X and Y, respectively. The label X was used to designate the Idipp substituent bonded to the Si atom, which carries the R group (R = H, Me, Et).

2. Syntheses and analytical data of the compounds

2.1 Synthesis of $[Si_2(H)(Idipp)_2][B(Ar^F)_4]$ (1H[B(Ar^F)$_4$])

A solution of $[H(Et_2O)_2][B(Ar^F)_4]$ (425 mg, 0.42 mmol) in 10 mL of C_6H_5F was added dropwise within 10 minutes to a suspension of **1** (350 mg, 0.42 mmol) in 20 mL of C_6H_5F at ambient temperature. A dark red solution containing a small amount of a colourless precipitate was obtained. The solution was stirred for additional 3 hours and then concentrated under vacuum to *ca.* 6 mL and filtered. *n*-Hexane (6 mL) was added to the filtrate. Storage of the filtrate at −30 °C for 8 days afforded dark red crystals of **1H**[B(Ar^F)$_4$]. The crystals were separated from the supernatant with a cannula (Ø = 1 mm) at −30 °C and dried under vacuum ($5 \cdot 10^{-2}$ mbar) at −30 °C for 30 minutes and for additional 2 h at ambient temperature. Yield: 577 mg (0.34 mmol, 80 %). The obtained crystals were suitable for single crystal X-ray diffraction analysis. A red powder was obtained after fine grinding of the crystals. Compound **1H**[B(Ar^F)$_4$] gradually turns dark brown above 173 °C and melts under decomposition at 221 °C.[1] Elemental analysis calcd (%) for $C_{86}H_{85}BF_{24}N_4Si_2$ (1697.57): C 60.84, H 5.05, N 3.30; found: C 60.62, H 5.09, N 3.19 %.

IR (*Figure S1*, solid state, RT, cm^{-1}): 3175 (vw), 3147 (vw), 3076 (vw), 2966 (w), 2932 (w), 2873 (w), 2142 (vw) [ν(Si-H)], 1688 (vw), 1610 (w), 1593 (vw), 1550 (w), 1461 (w), 1409 (vw), 1388 (w), 1353 (s), 1330 (w), 1274 (vs), 1212 (w), 1161 (s), 1118 (vs), 1061 (m), 1043 (m), 947 (w), 933 (w), 900 (w), 885 (m), 838 (m), 800 (m), 773 (w), 754 (m), 744 (m), 713 (m), 681 (m), 667 (m), 637 (vw), 579 (vw), 553 (vw), 536 (vw), 523 (vw), 458 (vw), 447 (w), 435 (vw).[2]

^{1}H NMR (*Figure S2*, 300.1 MHz, THF-d_8, 333 K, ppm): δ = 1.07 (d, 24H, ^3J(H,H) = 6.8 Hz, 4 × C^{2,6}-CH(C*H*$_3$)$_A$(CH$_3$)$_B$), 1.09 (d, 24H, ^3J(H,H) = 6.8 Hz, 4 × C^{2,6}-CH(CH$_3$)$_A$(C*H*$_3$)$_B$), 2.36 (sept, 8H, ^3J(H,H) = 6.8 Hz, 4 × C^{2,6}-C*H*(CH$_3$)$_2$), 5.57 (s, 1H, *J*(Si,H) = 95.4 Hz, *H*-Si), 7.24 (d, 8H, ^3J(H,H) = 7.7 Hz, 4 × C^{3,5}-*H*, C$_6$H$_3$), 7.42 (t, 4H, ^3J(H,H) = 7.7 Hz, 4 × C^4-*H*, C$_6$H$_3$), 7.56 (s, 4H, 4 × C^4-*H*, BAr$^F_4$), 7.72 (s, 4H, 2 × C^{4,5}-*H*), 7.79 (br m, 8H, $\Delta\nu_{½}$ = 9.8 Hz, 4 × C^{2,6}-*H*, BAr$^F_4$).

---

[1] A ^{1}H NMR spectrum in THF-d_8 of the red residue obtained after cooling of the molten sample to room temperature confirmed the unselective decomposition of **2-H**.

[2] The intensity of the ν(Si-H) absorption band of **1H**[B(Ar^F)$_4$] in the solid state is very weak. The ν(Si-H) absorption band could not be detected in the FT-IR spectrum of a concentrated solution of **1H**[B(Ar^F)$_4$] in C_6H_5F at 298 K.

^{1}H NMR (300.1 MHz, THF-d_8, 298 K, ppm): δ = 1.05 (d, 24H, ^{3}J(H,H) = 6.8 Hz, 4 × $C^{2,6}$-CH(CH_3)$_A$(CH$_3$)$_B$), 1.09 (d, 24H, ^{3}J(H,H) = 6.8 Hz, 4 × $C^{2,6}$-CH(CH$_3$)$_A$(CH_3)$_B$), 2.33 (sept, 8H, ^{3}J(H,H) = 6.8 Hz, 4 × $C^{2,6}$-C*H*(CH$_3$)$_2$), 5.62 (s, 1H, *J*(Si,H) = 94.8 Hz, *H*-Si), 7.25 (d, 8H, ^{3}J(H,H) = 7.7 Hz, 4 × $C^{3,5}$-*H*, C$_6$H$_3$), 7.43 (t, 4H, ^{3}J(H,H) = 7.7 Hz, 4 × C^{4}-*H*, C$_6$H$_3$), 7.59 (s, 4H, 4 × C^{4}-*H*, BAr$^{F}_4$), 7.82 (s + br m, 12H, 2 × $C^{4,5}$-*H,* Idipp + 4 × $C^{2,6}$-*H*, BAr$^{F}_4$).

^{1}H NMR (*Figure S3*, 300.1 MHz, THF-d_8, 213 K, ppm): δ = 0.97 (br d, 12H, ^{3}J(H,H) = 6.1 Hz, 2 × $C^{2,6}$-CH(CH_3)$_A$(CH$_3$)$_B$, (Idipp)$_X$), 1.05 – 1.10 (overlapping doublets, 36H, 2 × $C^{2,6}$-CH(CH$_3$)$_A$(CH_3)$_B$, (Idipp)$_X$ + 2 × $C^{2,6}$-CH(CH_3)$_A$(CH$_3$)$_B$, (Idipp)$_Y$ + 2 × $C^{2,6}$-CH(CH$_3$)$_A$(CH_3)$_B$, (Idipp)$_Y$), 2.22 (br sept, 4H, ^{3}J(H,H) = 6.1 Hz, 2 × $C^{2,6}$-C*H*(CH$_3$)$_2$, (Idipp)$_X$), 2.33 (br sept, 4H, ^{3}J(H,H) = 6.1 Hz, 2 × $C^{2,6}$-C*H*(CH$_3$)$_2$, (Idipp)$_Y$), 5.85 (s, 1H, ^{1}J(Si,H) = 204.2 Hz, *H*-Si),[3] 7.28 (d, 4H, ^{3}J(H,H) = 7.7 Hz, 2 × $C^{3,5}$-*H*, C$_6$H$_3$, (Idipp)$_Y$), 7.33 (d, 4H, ^{3}J(H,H) = 7.7 Hz, 2 × $C^{3,5}$-*H*, C$_6$H$_3$, (Idipp)$_X$), 7.44 (t, 2H, ^{3}J(H,H) = 7.7 Hz, 2 × C^{4}-*H*, C$_6$H$_3$, (Idipp)$_Y$), 7.49 (t, 2H, ^{3}J(H,H) = 7.7 Hz, 2 × C^{4}-*H*, C$_6$H$_3$, (Idipp)$_X$), 7.73 (s, 4H, 4 × C^{4}-*H*, BAr$^{F}_4$), 7.90 (br s, 8H, $\Delta\nu_{½}$ = 9.4 Hz, 4 × $C^{2,6}$-*H*, BAr$^{F}_4$), 8.03 (s, 2H, $C^{4,5}$-*H*, (Idipp)$_Y$), 8.08 (s, 2H, $C^{4,5}$-*H*, (Idipp)$_X$).

^{13}C{^{1}H} NMR (*Figures S4 and S5*, 75.47 MHz, THF-d_8, 333 K, ppm): δ = 23.5 (s, 8C, 4 × $C^{2,6}$-CH(*C*H$_3$)$_A$(CH$_3$)$_B$), 25.2 (s, 8C, 4 × $C^{2,6}$-CH(CH$_3$)$_A$(*C*H$_3$)$_B$),[4] 29.8 (s, 8C, 4 × $C^{2,6}$-*C*H(CH$_3$)$_2$), 118.1 (sept, 4C, ^{3}J(F,C) = 3.8 Hz, 4 × *C*^{4}-H, BAr$^{F}_4$), 125.6 (q, 8C, ^{1}J(F,C) = 272.4 Hz, 4 × $C^{3,5}$-*C*F$_3$, BAr$^{F}_4$), 125.7 (s, 8C, 4 × *C*^{3,5}-H, C$_6$H$_3$), 127.3 (s, 4C, 2 × *C*^{4,5}-H), 130.1 (qq, 8C, ^{2}J(F,C) = 31.3 Hz, ^{3}J(C,^{11}B) = 2.9 Hz, 4 × *C*^{3,5}-CF$_3$, BAr$^{F}_4$), 132.0 (s, 4C, 4 × *C*^{4}-H, C$_6$H$_3$), 134.3 (s, 4C, 4 × *C*^{1}, C$_6$H$_3$), 135.7 (br s, 8C, $\Delta\nu_{½}$ = 9.9 Hz, 4 × *C*^{2,6}-H, BAr$^{F}_4$), 146.2 (s, 8C, 4 × *C*^{2,6}, C$_6$H$_3$), 162.9 (q, 4C, ^{1}J(C,^{11}B) = 49.9 Hz, ^{1}J(C,^{10}B) = 16.6 Hz, 4 × *C*^{1}, BAr$^{F}_4$), 169.7 (br, $\Delta\nu_{½}$ = 135.8 Hz, 2C, 2 × *C*^{2}-Si).

^{13}C{^{1}H} NMR (75.47 MHz, THF-d_8, 298 K, ppm): δ = 23.5 (s, 8C, 4 × $C^{2,6}$-CH(*C*H$_3$)$_A$(CH$_3$)$_B$), 25.3 (s, 8C, 4 × $C^{2,6}$-CH(CH$_3$)$_A$(*C*H$_3$)$_B$),[5] 29.8 (s, 8C, 4 × $C^{2,6}$-*C*H(CH$_3$)$_2$), 118.2 (br sept, 4C, $\Delta\nu_{½}$ = 10.6 Hz, ^{3}J(F,C) = 3.8 Hz, 4 × *C*^{4}-H, BAr$^{F}_4$), 125.5 (q, 8C, ^{1}J(F,C) = 270.7 Hz, 4 × $C^{3,5}$-*C*F$_3$, BAr$^{F}_4$), 125.7 (s, 8C, 4 × *C*^{3,5}-H, C$_6$H$_3$), 127.3 (s, 4C, 2 × *C*^{4,5}-H), 130.1 (qq, 8C, ^{2}J(F,C) = 31.7 Hz, ^{3}J(C,^{11}B) = 2.9 Hz, 4 × *C*^{3,5}-CF$_3$, BAr$^{F}_4$), 131.9 (s, 4C, 4 × *C*^{4}-H, C$_6$H$_3$), 134.2 (s,

[3] The ^{2}J(Si,H) satellite signals could not be resolved in the ^{1}H NMR spectrum at 213 K.

[4] The signal at δ = 25.2 ppm overlaps with that of the deuterated solvent but was easily detected in the ^{13}C{^{1}H} DEPT135 experiment.

[5] The signal at δ = 25.3 ppm overlaps with that of the deuterated solvent but was easily detected in the ^{13}C{^{1}H} DEPT135 experiment.

4C, 4 × C^1, C_6H_3), 135.6 (br s, 8C, $\Delta\nu_{½}$ = 10.2 Hz, 4 × $C^{2,6}$-H, BAr^F_4), 146.1 (s, 8C, 4 × $C^{2,6}$, C_6H_3), 162.9 (q, 4C, ^1J(C,^{11}B) = 49.7 Hz, ^1J(C,^{10}B) = 16.6 Hz, 4 × C^1, BAr^F_4).[6]

$^{13}C\{^1H\}$ NMR (*Figures S6 and S7*, 75.47 MHz, THF-d_8, 213 K, ppm): δ = 22.5 (s, 4C, 2 × $C^{2,6}$-$CH(CH_3)_A(CH_3)_B$, $(Idipp)_Y$), 23.9 (s, 4C, 2 × $C^{2,6}$-$CH(CH_3)_A(CH_3)_B$, $(Idipp)_X$), 25.1 (s, 4C, 2 × $C^{2,6}$-$CH(CH_3)_A(CH_3)_B$, $(Idipp)_X$), 25.9 (s, 4C, 2 × $C^{2,6}$-$CH(CH_3)_A(CH_3)_B$, $(Idipp)_Y$),[7] 29.7 (s, 4C, 2 × $C^{2,6}$-$CH(CH_3)_2$, $(Idipp)_X$), 29.9 (s, 4C, 2 × $C^{2,6}$-$CH(CH_3)_2$, $(Idipp)_Y$), 118.4 (br m, 4C, $\Delta\nu_{½}$ = 14.5 Hz, 4 × C^4-H, BAr^F_4), 125.3 (s, 4C, 2 × $C^{3,5}$-H, C_6H_3, $(Idipp)_Y$), 125.4 (q, 8C, ^1J(F,C) = 272.2 Hz, 4 × $C^{3,5}$-CF_3, BAr^F_4), 126.1 (s, 4C, 2 × $C^{3,5}$-H, C_6H_3, $(Idipp)_X$), 127.4 (s, 4C, $C^{4,5}$-H, $(Idipp)_X$ + $C^{4,5}$-H, $(Idipp)_Y$), 130.0 (qq, 8C, ^2J(F,C) = 31.7 Hz, ^3J(C,^{11}B) = 2.8 Hz, 4 × $C^{3,5}$-CF_3, BAr^F_4), 131.5 (s, 2C, 2 × C^4-H, C_6H_3, $(Idipp)_Y$), 132.1 (s, 2C, 2 × C^4-H, C_6H_3, $(Idipp)_X$), 133.4 (s, 2C, 2 × C^1, C_6H_3, $(Idipp)_X$), 134.4 (s, 2C, 2 × C^1, C_6H_3, $(Idipp)_Y$) 135.4 (br s, 8C, $\Delta\nu_{½}$ = 10.6 Hz, 4 x $C^{2,6}$-H, BAr^F_4), 145.7 (s, 4C, 2 × $C^{2,6}$, C_6H_3, $(Idipp)_Y$), 145.8 (s, 4C, 2 × $C^{2,6}$, C_6H_3, $(Idipp)_X$), 161.8 (s, 1C, C^2-SiH-Si, $(Idipp)_X$), 163.0 (q, 4C, ^1J(C,^{11}B) = 49.3 Hz, ^1J(C,^{10}B) = 16.5 Hz, 4 × C^1, BAr^F_4) 174.5 (s, 1C, C^2-Si-SiH, $(Idipp)_Y$).

^{29}Si NMR (*Figure S8*, 59.63 MHz, THF-d_8, 213 K, ppm): δ = 69.4 (d, 1Si, ^1J(Si,H) = 204.2 Hz, H-*Si*-Si), 125.4 (d, 1Si, ^2J(Si,H) = 14.8 Hz, H-Si-*Si*).[8]

$^{19}F\{^1H\}$ NMR (282.4 MHz, THF-d_8, 298 K, ppm): δ = −63.3 (s, 24F, 4 × $C^{3,5}$-CF_3, BAr_4^F).

$^{11}B\{^1H\}$ NMR (96.29 MHz, THF-d_8, 298 K, ppm): δ = −6.5 (s, 1B, BAr^F_4).

---

[6] The Si-bonded C^2 signals of the Idipp substituents were not observed in the $^{13}C\{^1H\}$ NMR spectrum at 298 K.

[7] The signal at δ = 25.9 ppm overlaps with that of the deuterated solvent but was easily detected in the $^{13}C\{^1H\}$ DEPT135 experiment.

[8] No ^{29}Si NMR signals of **1H**[$B(Ar^F)_4$] could be detected at 298 and 333 K due to the dynamic process.

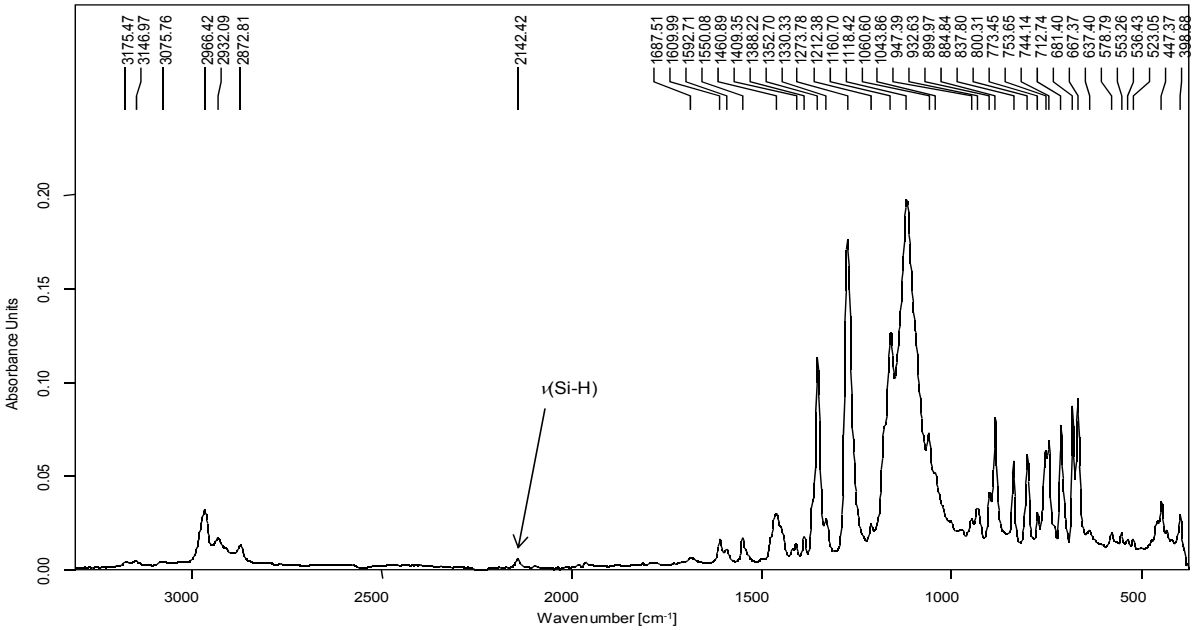

Figure S1. FT-IR spectrum of a solid state sample of **1H**[B(Ar^F)$_4$] at ambient temperature.

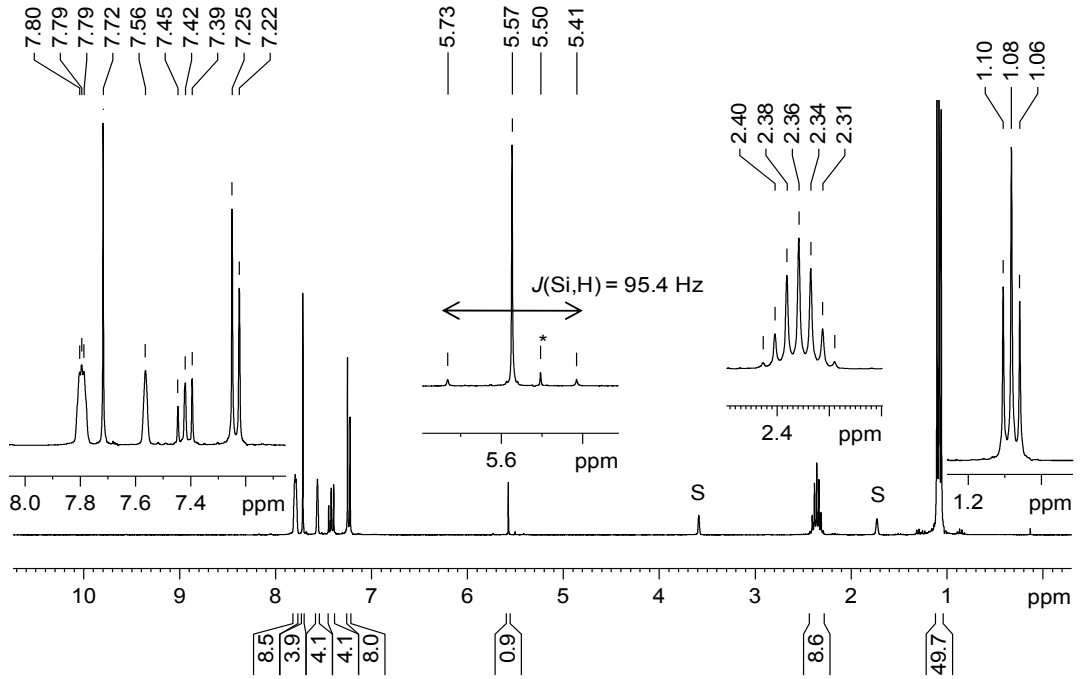

Figure S2. ^{1}H NMR (300.1 MHz) spectrum of **1H**[B(Ar^F)$_4$] in THF-d_8 at 333 K; the signals of the deuterated solvent are marked with the character S. Enlarged excerpts are shown in the insets.

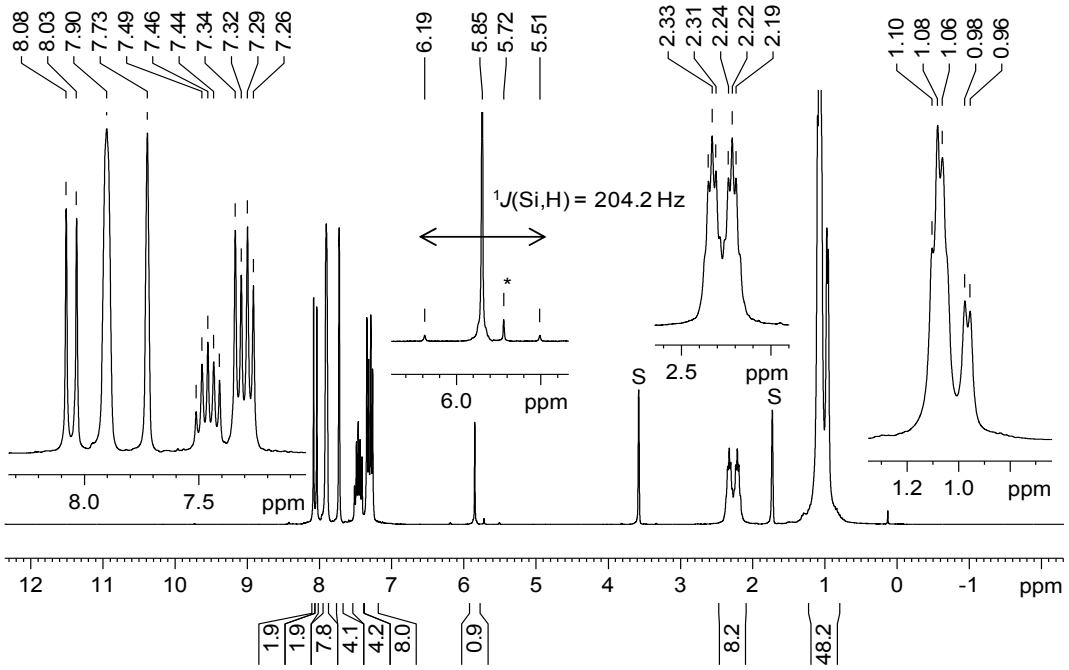

Figure S3. ^{1}H NMR (300.1 MHz) spectrum of **1H**[B(Ar^{F})$_4$] in THF-d_8 at 213 K; the signals of the deuterated solvent are marked with the character S. Enlarged excerpts are shown in the insets; the signal marked with an asterisk (*) originates from a tiny impurity.

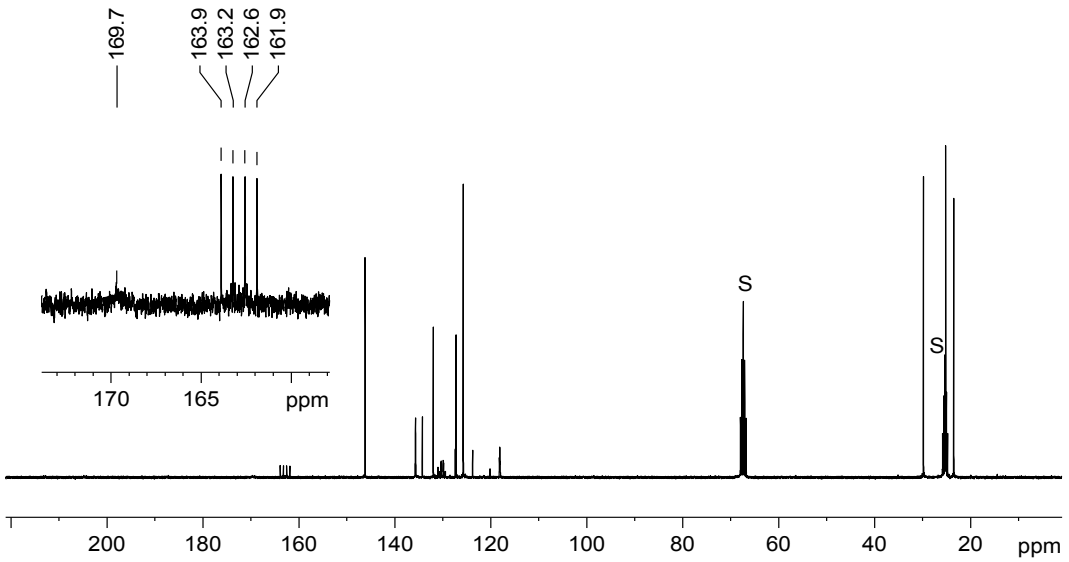

Figure S4. ^{13}C{^{1}H} NMR (75.47 MHz) spectrum of **1H**[B(Ar^{F})$_4$] in THF-d_8 at 333 K; the signals of the deuterated solvent are marked with the character S. An enlarged excerpt is shown in the inset.

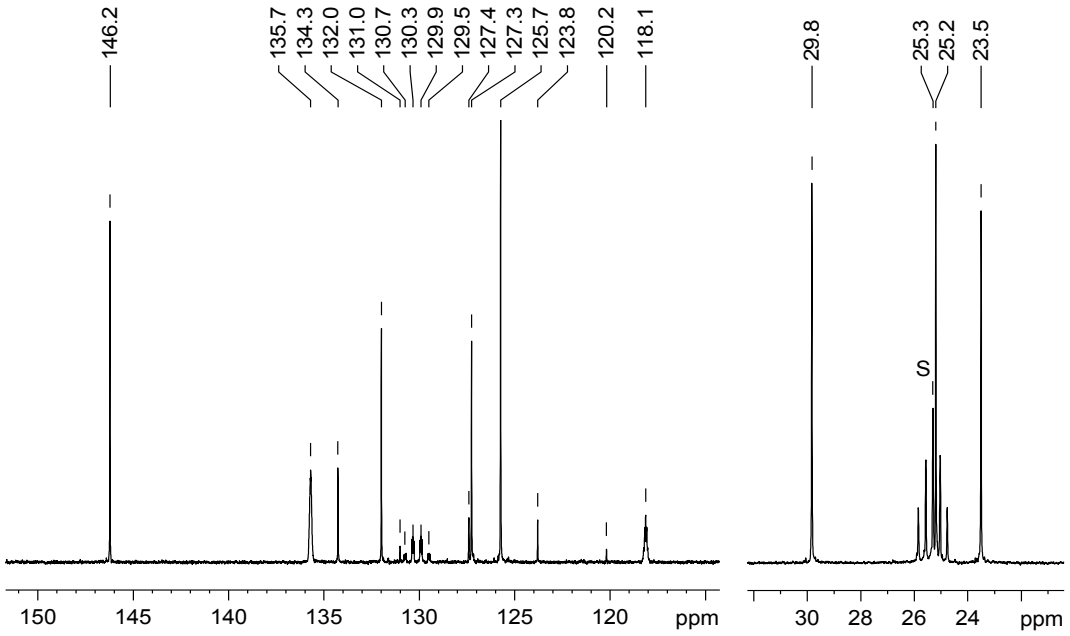

Figure S5. Excerpts of the $^{13}C\{^{1}H\}$ NMR (75.47 MHz) spectrum of **1H**[$B(Ar^F)_4$] in THF-d_8 at 333 K depicted in Figure S4; the signal of the deuterated solvent is marked with the character S.

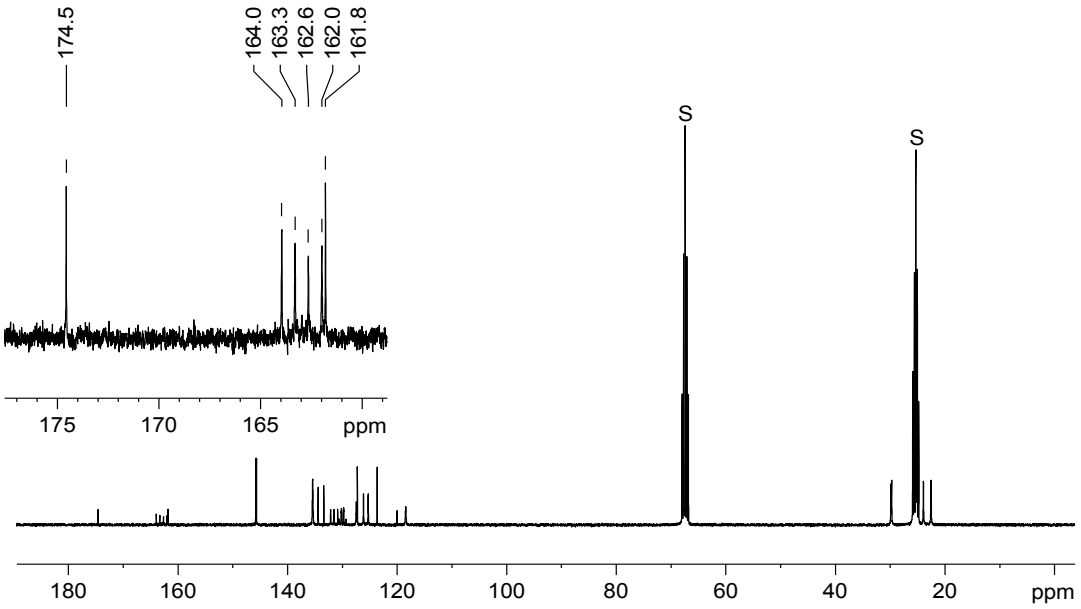

Figure S6. $^{13}C\{^{1}H\}$ NMR (75.47 MHz) spectrum of **1H**[$B(Ar^F)_4$] in THF-d_8 at 213 K; the signals of the deuterated solvent are marked with the character S. An enlarged excerpt is shown in the inset.

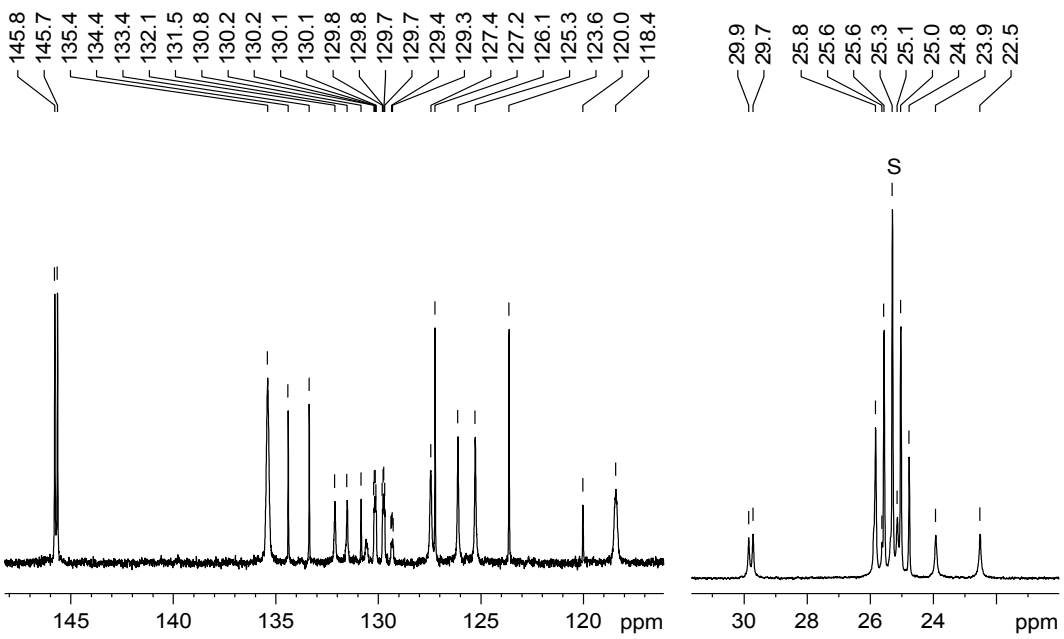

Figure S7. Excerpts of the $^{13}C\{^{1}H\}$ NMR (75.47 MHz) spectrum of **1H**[$B(Ar^F)_4$] in THF-d_8 at 213 K depicted in Figure S6; the signal of the deuterated solvent is marked with the character S.

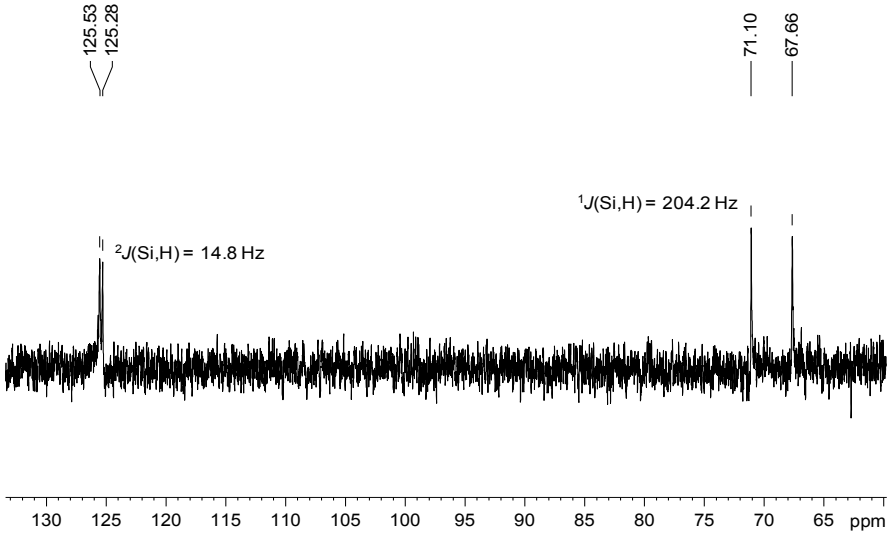

Figure S8. ^{29}Si NMR (59.63 MHz) spectrum of **1H**[$B(Ar^F)_4$] in THF-d_8 at 213 K.

2.2 Synthesis of $[Si_2(D)(Idipp)_2][B(Ar^F)_4]$ (**1D**$[B(Ar^F)_4]$)

The compound **1D**$[B(Ar^F)_4]$ was synthesized in 70 % yield from **1** and $[D(Et_2O)_2][B(Ar^F)_4]$ following the procedure described for **1H**$[B(Ar^F)_4]$ (chapter 2.1). The purity of **1D**$[B(Ar^F)_4]$ was confirmed by IR and ^{1}H NMR spectroscopy (Figures S9 – S11).

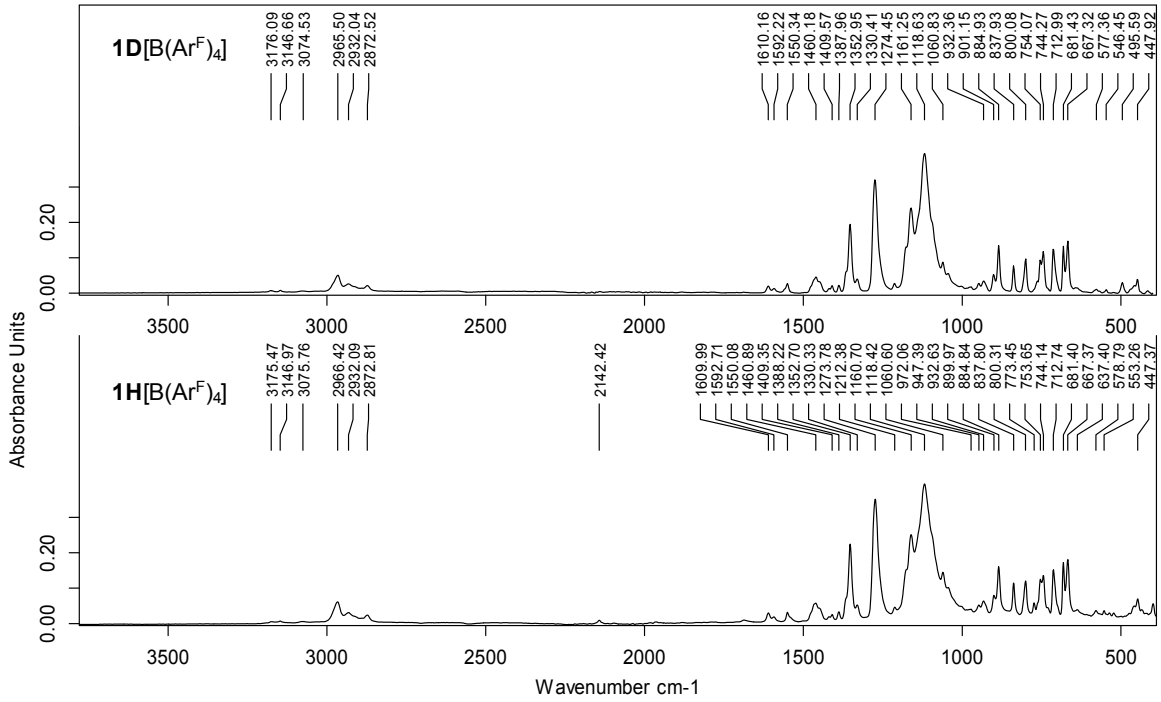

Figure S9. FT-IR spectra of solid state samples of **1D**$[B(Ar^F)_4]$ (top) and **1H**$[B(Ar^F)_4]$ (bottom) at ambient temperature.

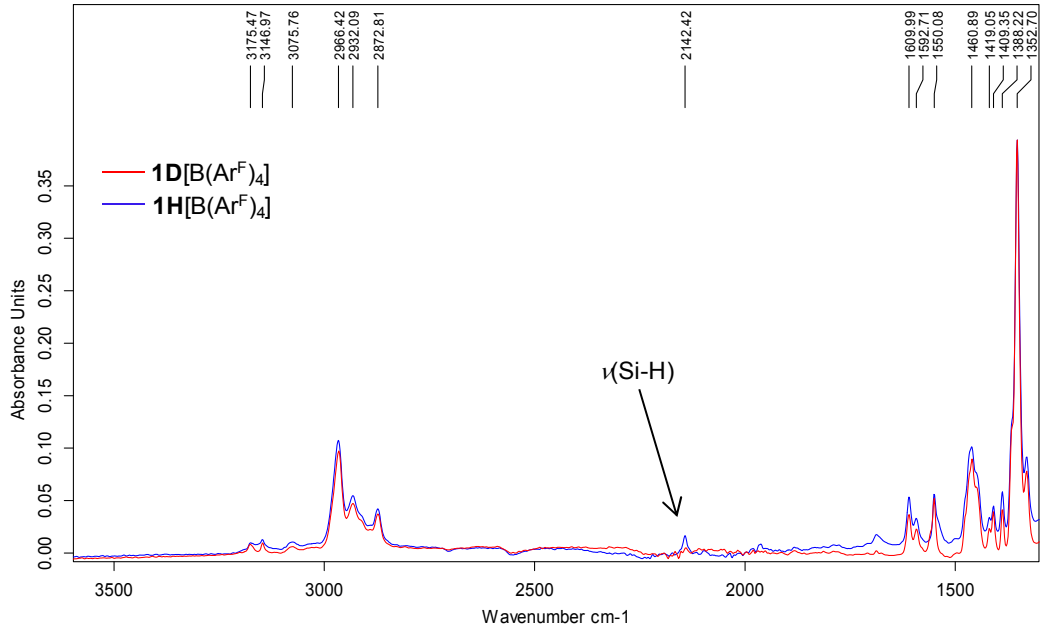

Figure S10. Excerpts of the FT-IR spectra (1300 – 3600 cm^{-1}) of solid state samples of **1D**$[B(Ar^F)_4]$ (red curve) and **1H**$[B(Ar^F)_4]$ (blue curve) shown in Figure S9 at ambient temperature. The position of the ν(Si-H) absorption band (blue curve) is pointed out with an arrow. This band is absent in the IR spectrum of **1D**$[B(Ar^F)_4]$ (red curve).

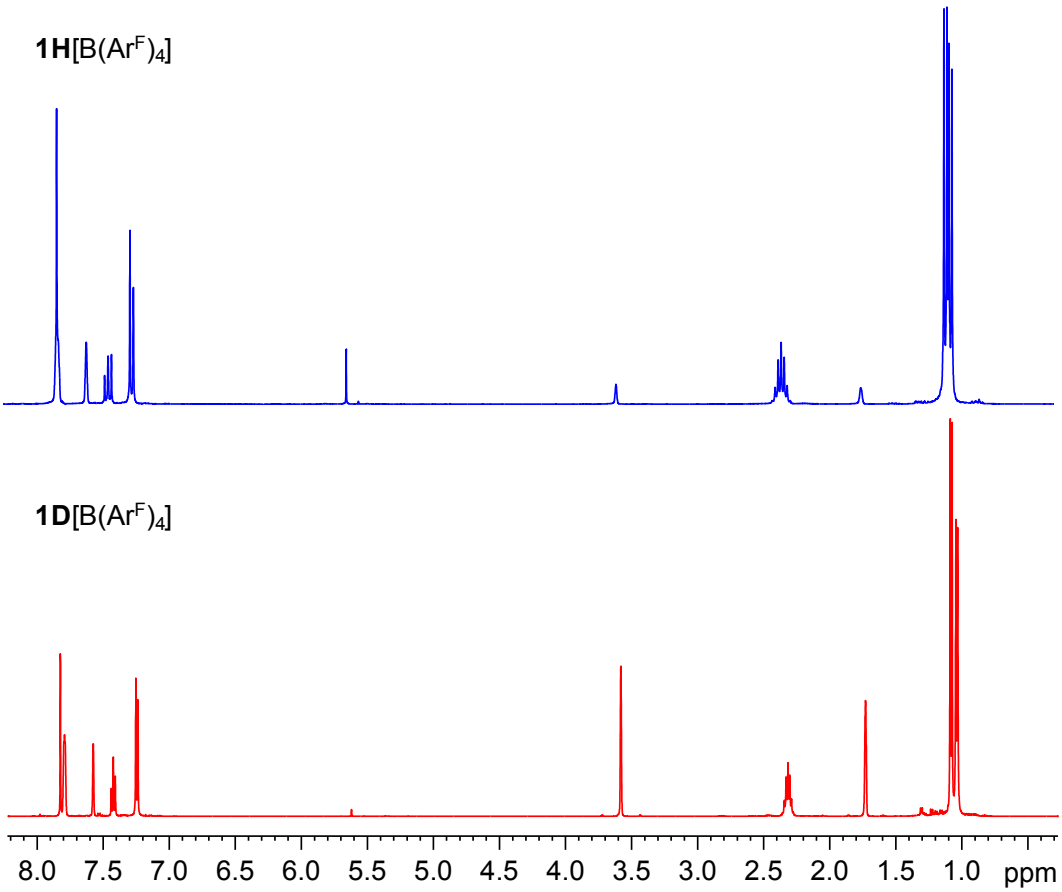

Figure S11. ^{1}H NMR spectra of **1D**[B(Ar^{F})$_4$] (500.2 MHz, red curve, bottom) and **1H**[B(Ar^{F})$_4$] (300.1 MHz, blue curve, top) in THF-d_8 at 298 K.

2.3 Synthesis of [Si$_2$(Me)(Idipp)$_2$][B(Ar^{F})$_4$] (1Me[B(Ar^{F})$_4$])

A suspension of **1** (150 mg, 0.18 mmol) and Na[B(Ar^{F})$_4$] (160 mg, 0.18 mmol) in 15 mL of C_6H_5F was cooled to −30 °C. 2.4 mL of a 0.076 M solution of iodomethane (0.18 mmol) in toluene were added. The colour changed from dark red to orange and a small amount of a colourless precipitate was formed (NaI). The suspension was stirred for 1 hour at −30 °C and for 1 hour at ambient temperature. The suspension was concentrated under vacuum to *ca.* 4 mL and filtered from the colourless precipitate. *n*-Hexane (6 mL) was added to the orange filtrate and an orange solid precipitated. The supernatant was decanted with a cannula and the solid was washed once with 2 mL of *n*-hexane. The solid was dissolved in a mixture of 4 mL of C_6H_5F and 3 mL of *n*-hexane, and the orange suspension was filtered from a small amount of an orange solid. Storage of the clear, orange filtrate at −30 °C for 14 days afforded orange crystals of **1Me**[B(Ar^{F})$_4$]. The crystals were separated from the supernatant with a cannula (Ø = 1 mm) at −30 °C and dried under vacuum ($5 \cdot 10^{-2}$ mbar) at −30 °C for 30 minutes and for 2 h at ambient temperature. Yield: 110 mg (0.064 mmol, 36 %). The obtained crystals were suitable for single crystal x-ray diffraction analysis. A red powder was obtained after grinding of the crystals. Compound **1Me**[B(Ar^{F})$_4$] gradually turns dark brown

above 198 °C and melts under decomposition at 213 °C.[9] Elemental analysis calcd (%) for $C_{87}H_{87}BF_{24}N_4Si_2$ (1711.60): C 61.05, H 5.12, N 3.27; found: C 61.05, H 5.21, N 3.21 %.

^{1}H NMR (*Figures S12 and S13*, 300.1 MHz, THF-d_8, 298 K, ppm): δ = 0.14 (s, 3H, ^2J(Si,H) = 10.0 Hz, Si-CH_3), 0.99 (d, 12H, ^3J(H,H) = 6.8 Hz, 2 × C^{2,6}-CH(CH_3)$_A$(CH$_3$)$_B$, (Idipp)$_X$), 1.07 (d, 12H, ^3J(H,H) = 6.8 Hz, 2 × C^{2,6}-CH(CH_3)$_A$(CH$_3$)$_B$, (Idipp)$_Y$), 1.08 (d, 12H, ^3J(H,H) = 6.8 Hz, 2 × C^{2,6}-CH(CH$_3$)$_A$(CH_3)$_B$, (Idipp)$_X$), 1.17 (d, 12H, ^3J(H,H) = 6.8 Hz, 2 × C^{2,6}-CH(CH$_3$)$_A$(CH_3)$_B$, (Idipp)$_Y$), 2.35 (sept, 4H, ^3J(H,H) = 6.8 Hz, 2 × C$^{2.6}$-CH(CH$_3$)$_2$, (Idipp)$_X$), 2.44 (sept, 4H, ^3J(H,H) = 6.8 Hz, 2 × C^{2,6}-CH(CH$_3$)$_2$, (Idipp)$_Y$), 7.25 (d, 4H, ^3J(H,H) = 7.7 Hz, 2 × C^{3,5}-*H*, C$_6$H$_3$, (Idipp)$_Y$), 7.26 (d, 4H, ^3J(H,H) = 7.7 Hz, 2 × C^{3,5}-*H*, C$_6$H$_3$, (Idipp)$_X$), 7.41 (t, 2H, ^3J(H,H) = 7.8 Hz, 2 × C^4-*H*, C$_6$H$_3$, (Idipp)$_Y$), 7.45 (t, 2H, ^3J(H,H) = 7.8 Hz, 2 × C^4-*H*, C$_6$H$_3$, (Idipp)$_X$), 7.58 (s, 4H, 4 × C^4-*H*, BAr$^F_4$), 7.74 (s, 2H, C^{4,5}-*H*, (Idipp)$_Y$), 7.77 (s, 2H, C^{4,5}-*H*, (Idipp)$_X$), 7.80 (br m, 8H, $\Delta\nu_{½}$ = 9.6 Hz, 4 × C^{2,6}-*H*, BAr$^F_4$).

^{13}C{^{1}H} NMR (*Figures S14 and S15*, 75.47 MHz, THF-d_8, 298 K, ppm): δ = 4.5 (s, 1C, Si-*C*H$_3$), 23.0 (s, 4C, 2 × C^{2,6}-CH(CH$_3$)$_A$(*C*H$_3$)$_B$, (Idipp)$_Y$), 23.4 (s, 4C, 2 × C^{2,6}-CH(*C*H$_3$)$_A$(CH$_3$)$_B$, (Idipp)$_X$), 25.3 (s, 4C, 2 × C^{2,6}-CH(CH$_3$)$_A$(*C*H$_3$)$_B$, (Idipp)$_X$),[10] 25.9 (s, 4C, 2 × C^{2,6}-CH(*C*H$_3$)$_A$(CH$_3$)$_B$, (Idipp)$_Y$), 29.8 (s, 8C, 2 × C^{2,6}-*C*H(CH$_3$)$_2$, (Idipp)$_X$ + 2 × C$^{2.6}$-*C*H(CH$_3$)$_2$, (Idipp)$_Y$), 118.2 (sept, 4C, ^3J(F,C) = 4.0 Hz, 4 × *C*^{4}-H, BAr$^F_4$), 125.4 (s, 4C, 2 × *C*^{3,5}-H, C$_6$H$_3$, (Idipp)$_Y$), 125.5 (q, 8C, ^1J(F,C) = 272.1 Hz, 4 × C^{3,5}-*C*F$_3$, BAr$^F_4$), 126.1 (s, 4C, 2 × *C*^{3,5}-H, C$_6$H$_3$, (Idipp)$_X$), 127.3 (s, 2C, *C*^{4,5}-H, (Idipp)$_Y$), 127.6 (s, 2C, *C*^{4,5}-H, (Idipp)$_X$), 130.1 (qq, 8C, ^2J(F,C) = 31.5 Hz, ^3J(C,^{11}B) = 3.0 Hz, 4 × *C*^{3,5}-CF$_3$, BAr$^F_4$), 131.4 (s, 2C, 2 × *C*^{4}-H, C$_6$H$_3$, (Idipp)$_Y$), 132.3 (s, 2C, 2 × *C*^{4}-H, C$_6$H$_3$, (Idipp)$_X$), 134.2 (s, 2C, 2 × *C*^{1}, C$_6$H$_3$, (Idipp)$_X$), 134.9 (s, 2C, 2 × *C*^{1}, C$_6$H$_3$, (Idipp)$_Y$), 135.6 (br s, 8C, $\Delta\nu_{½}$ = 10.7 Hz, 4 × *C*^{2,6}-H, BAr$^F_4$), 146.1 (s, 4C, 2 × *C*^{2,6}, C$_6$H$_3$, (Idipp)$_Y$), 146.3 (s, 4C, 2 × *C*^{2,6}, C$_6$H$_3$, (Idipp)$_X$), 162.8 (q, 4C, ^1J(C,^{11}B) = 49.8 Hz, ^1J(C,^{10}B) = 16.7 Hz, 4 × *C*^{1}, BAr$^F_4$), 162.9 (s, 1C, *C*^{2}-SiMe-Si, (Idipp)$_X$), 177.1 (s, 1C, *C*^{2}-Si-SiMe, (Idipp)$_Y$).

^{29}Si NMR (*Figure S16*, 59.63 MHz, THF-d_8, 298 K, ppm): δ = 102.8 (q, 1Si, ^2J(Si,H) = 10.0 Hz, Si-*Si*-CH$_3$), 115.2 (s, 1Si, *Si*-Si-CH$_3$).

---

[9] A ^{1}H NMR spectrum in THF-d_8 of the red residue obtained after cooling of the molten sample to room temperature revealed the unselective decomposition of **1Me**[B(Ar^F)$_4$].

[10] The signal at δ = 25.3 ppm overlaps with that of the deuterated solvent but was easily detected in the ^{13}C{^{1}H} DEPT135 experiment.

$^{19}F\{^{1}H\}$ NMR (282.4 MHz, THF-d_8, 298 K, ppm): δ = −63.3 (s, 24F, 4 x $C^{3,5}$-CF_3, BAr_4^F).

$^{11}B\{^{1}H\}$ NMR (96.29 MHz, THF-d_8, 298 K, ppm): δ = −6.5 (s, 1B, BAr$^F_4$).

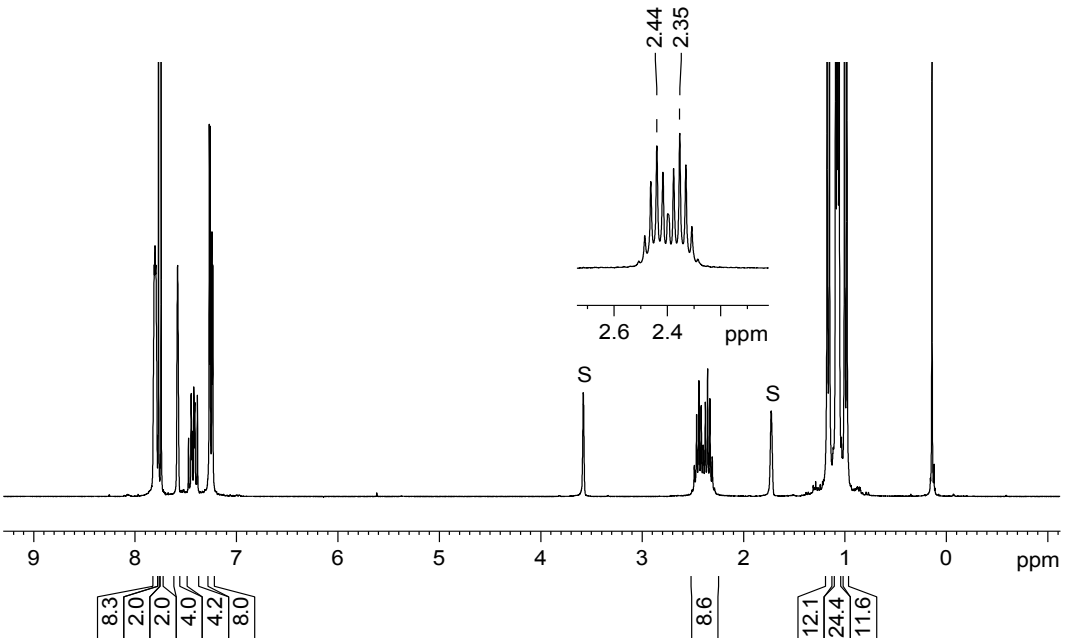

Figure S12. ^{1}H NMR (300.1 MHz) spectrum of **1Me**[B(Ar^F)$_4$] in THF-d_8 at 298 K; the signals of the deuterated solvent are marked with the character S. An enlarged excerpt displaying the methine resonances is shown in the inset.

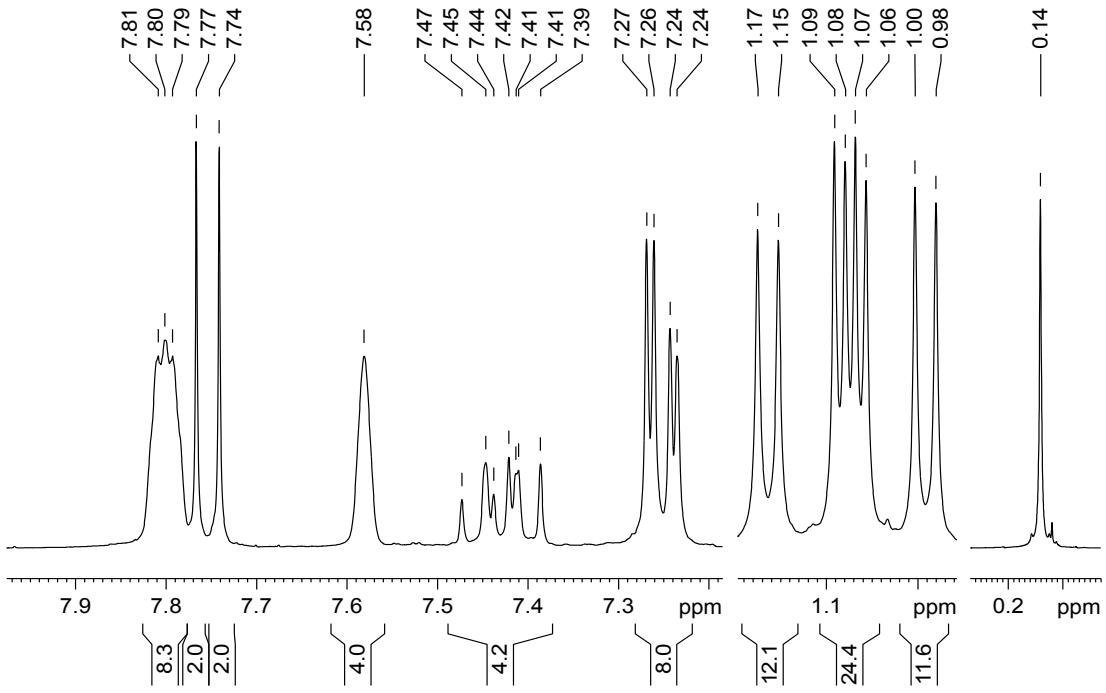

Figure S13. Excerpts of the ^{1}H NMR (300.1 MHz) spectrum of **1Me**[B(Ar^F)$_4$] in THF-d_8 at 298 K depicted in Figure S12.

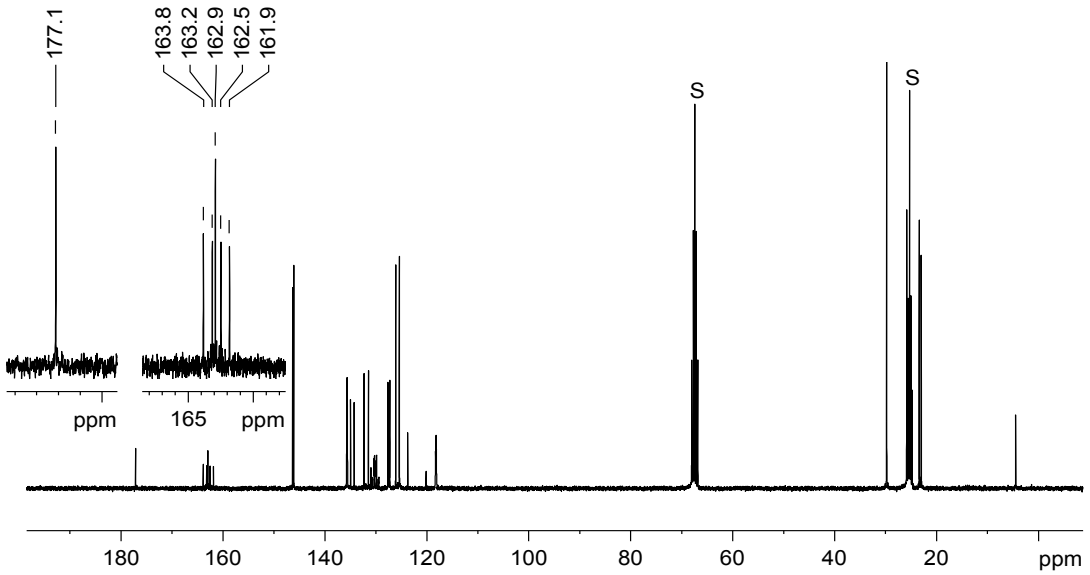

Figure S14. $^{13}C\{^{1}H\}$ NMR (75.47 MHz) spectrum of **1Me**[$B(Ar^F)_4$] in THF-d_8 at 298 K; the signals of the deuterated solvent are marked with the character S. Enlarged excerpts are shown in the insets.

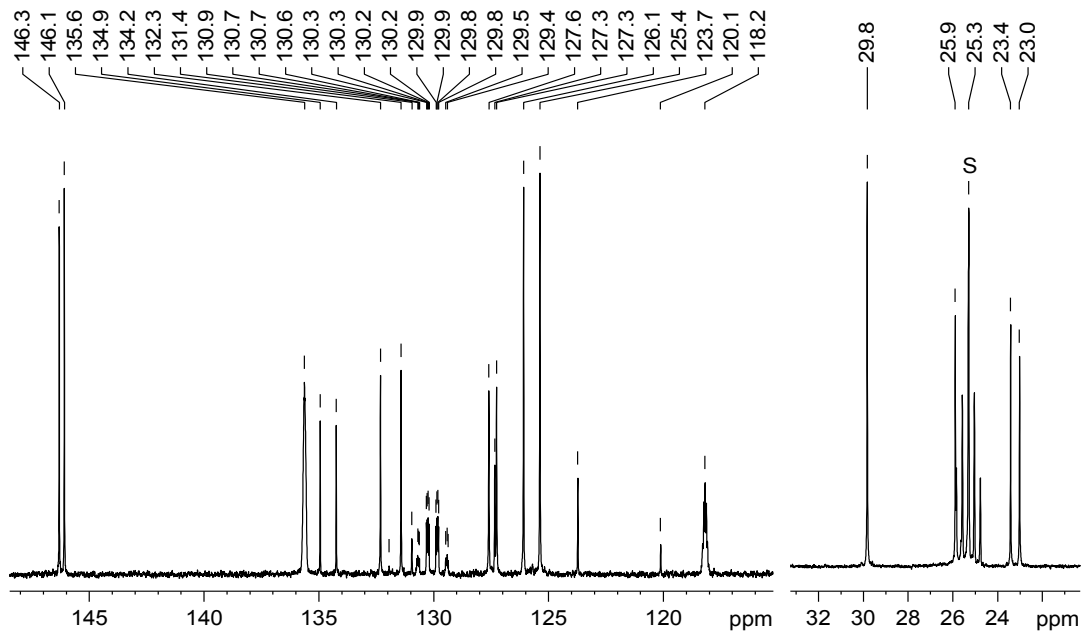

Figure S15. Excerpts of the $^{13}C\{^{1}H\}$ NMR (75.47 MHz) spectrum of **1Me**[$B(Ar^F)_4$] in THF-d_8 at 298 K depicted in Figure S14; the signal of the deuterated solvent is marked with the character S.

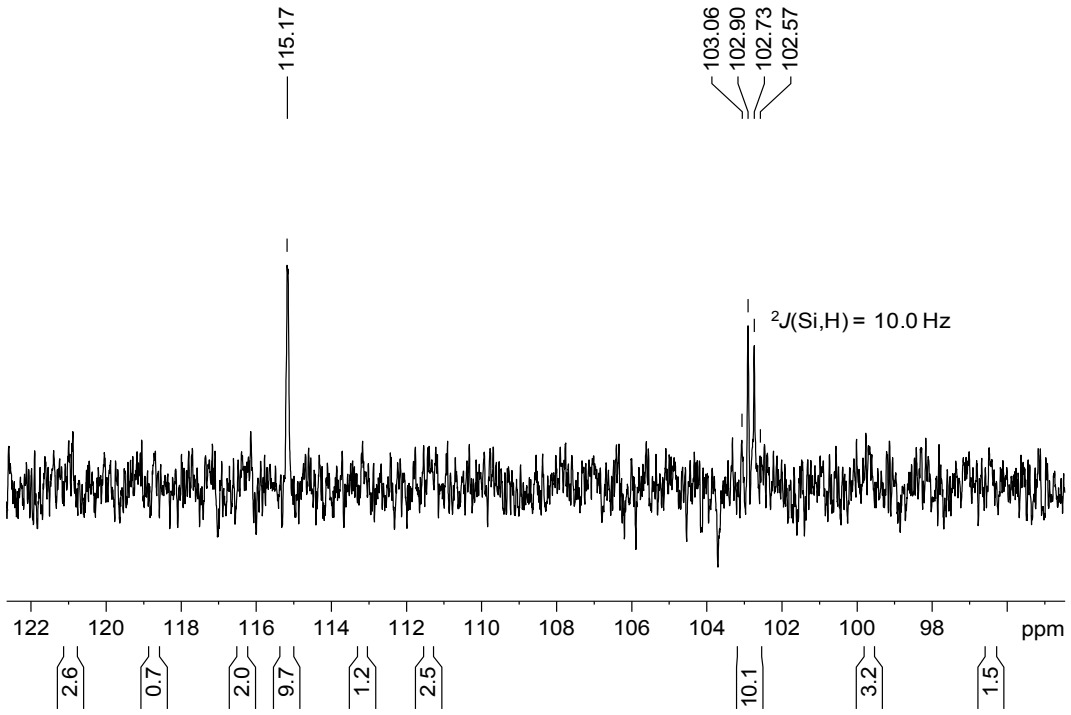

Figure S16. ^{29}Si NMR (59.63 MHz) spectrum of **1Me**[B(Ar^F)$_4$] in THF-d_8 at 298 K.

2.4 Synthesis of [Si$_2$(Et)(Idipp)$_2$][B(Ar^F)$_4$] (1Et[B(Ar^F)$_4$])

A solution of **1** (150 mg, 0.18 mmol) and Na[B(Ar^F)$_4$] (160 mg, 0.18 mmol) in 8 mL of C_6H_5F was cooled to −30 °C and 0.62 mL of a 0.289 M solution of iodoethane (0.18 mmol) in C_6H_5F was added with a syringe. After *ca.* 30 minutes of stirring at −30 °C, the reaction mixture turned orange and precipitation of a colorless solid was observed (NaI). The mixture was warmed to ambient temperature, stirred for 30 minutes and concentrated under vacuum to *ca.* 6 mL. *n*-Hexane (8 mL) was added, and the suspension was stirred for 5 minutes and filtered. The clear red-orange filtrate was stored at −30 °C for 14 days, whereupon red-orange crystals of **1Et**[B(Ar^F)$_4$] were formed. The supernatant was removed by decantation with a cannula (Ø = 1 mm) at −30 °C and the crystals were dried for 1 h under vacuum ($5 \cdot 10^{-2}$ mbar) at ambient temperature. Yield: 154 mg (0.089 mmol, 50 %). The crystals were suitable for X-ray diffraction analysis. A red powder was obtained after grinding of the crystals. Compound **1Et**[B(Ar^F)$_4$] gradually turns dark brown above 193 °C and melts under decomposition at 209 °C. Elemental analysis calcd (%) for $C_{88}H_{89}BF_{24}N_4Si_2$ (1725.62): C 61.25, H 5.20, N 3.25; found: C 60.90, H 5.08, N 3.19 %.

^{1}H NMR (*Figures S17 – S19*, 300.1 MHz, THF-d_8, 298 K, ppm): δ = 0.62 – 0.72 (m, 2H, Si-CH_2CH$_3$), 0.74 – 0.81 (m, 3H, Si-CH$_2$CH_3),[11] 1.03 – 1.12 (overlapping doublets, 48H, 2 × C^{2,6}-CH(CH_3)$_A$(CH$_3$)$_B$, (Idipp)$_X$ + 2 × C^{2,6}-CH(CH$_3$)$_A$(CH_3)$_B$, (Idipp)$_X$ + 2 × C^{2,6}-CH(CH_3)$_A$(CH$_3$)$_B$, (Idipp)$_Y$ + 2 × C^{2,6}-CH(CH$_3$)$_A$(CH_3)$_B$, (Idipp)$_Y$), 2.40 – 2.50 (two overlapping septets, 8H, 2 × C^{2,6}-CH(CH$_3$)$_2$, (Idipp)$_X$ + 2 × C^{2,6}-CH(CH$_3$)$_2$, (Idipp)$_Y$), 7.22 (d, 4H, ^{3}J(H,H) = 7.8 Hz, 2 × C^{3,5}-*H*, (Idipp)$_X$), 7.25 (d, 4H, ^{3}J(H,H) = 7.8 Hz, 2 × C^{3,5}-*H*, (Idipp)$_Y$), 7.46 (t, 4H, ^{3}J(H,H) = 7.8 Hz, 2 × C^{4}-*H*, C$_6$H$_3$, (Idipp)$_X$ + 2 × C^{4}-*H*, C$_6$H$_3$, (Idipp)$_Y$), 7.57 (s, 4H, 4 × C^{4}-*H*, BAr$^{F}_4$), 7.72 (s, 2H, C^{4,5}-*H*, (Idipp)$_Y$), 7.79 (br m, 8H, $\Delta\nu_{½}$ = 10.0 Hz, 4 × C^{2,6}-*H*, BAr$^{F}_4$), 7.85 (s, 2H, C^{4,5}-*H*, (Idipp)$_X$).

^{13}C{^{1}H} NMR (*Figures S20 and S21*, 75.47 MHz, THF-d_8, 298 K, ppm): δ = 13.1 (s, 1C, Si-CH$_2$*C*H$_3$), 15.5 (s, 1C, Si-*C*H$_2$CH$_3$), 23.0, 23.1 (s each, 4C each, 2 × C^{2,6}-CH(*C*H$_3$)$_A$(CH$_3$)$_B$, (Idipp)$_X$ + 2 × C^{2,6}-CH(*C*H$_3$)$_A$(CH$_3$)$_B$, (Idipp)$_Y$), 25.7, 25.9 (s each, 4C each, 2 × C^{2,6}-CH(CH$_3$)$_A$(*C*H$_3$)$_B$, (Idipp)$_X$ + 2 × C^{2,6}-CH(CH$_3$)$_A$(*C*H$_3$)$_B$, (Idipp)$_Y$), 29.8 (s, 8C, 2 × C^{2,6}-*C*H(CH$_3$)$_2$, (Idipp)$_X$ + 2 × C^{2,6}-*C*H(CH$_3$)$_2$, (Idipp)$_Y$), 118.2 (sept, 4C, ^{3}J(F,C) = 4.1 Hz, 4 × *C*^{4}-H, BAr$^{F}_4$), 125.4, 125.6 (s each, 4C each, 2 × *C*^{3,5}-H, C$_6$H$_3$, (Idipp)$_X$ + 2 × *C*^{3,5}-H, C$_6$H$_3$, (Idipp)$_Y$), 125.5 (q, 8C, ^{1}J(F,C) = 272.3 Hz, 4 × C^{3,5}-*C*F$_3$, BAr$^{F}_4$), 127.4 (s, 2C, *C*^{4,5}-H, (Idipp)$_Y$), 127.8 (s, 2C, *C*^{4,5}-H, (Idipp)$_X$), 130.0 (qq, 8C, ^{3}J(F,C) = 31.5 Hz, ^{3}J(C,^{11}B) = 2.9 Hz, 4 × *C*^{3,5}-CF$_3$, BAr$^{F}_4$), 131.5, 132.2 (s each, 2C each, 2 × *C*^{4}-H, C$_6$H$_3$, (Idipp)$_X$ + 2 × *C*^{4}-H, C$_6$H$_3$, (Idipp)$_Y$), 134.2 (s, 2C, 2 × *C*^{1}, C$_6$H$_3$, (Idipp)$_X$), 135.2 (s, 2C, 2 × *C*^{1}, C$_6$H$_3$, (Idipp)$_Y$), 135.6 (br s, 8C, $\Delta\nu_{½}$ = 10.0 Hz, 4 × *C*^{2,6}-H, BAr$^{F}_4$), 146.1, 146.2 (s each, 4C each, 2 × *C*^{2,6}, (Idipp)$_X$ + 2 × *C*^{2,6}, (Idipp)$_Y$) 162.8 (q, 4C, ^{1}J(C,^{11}B) = 49.8 Hz, ^{1}J(C,^{10}B) = 16.8 Hz, 4 × *C*^{1}, BAr$^{F}_4$), 164.2 (s, 1C, *C*^{2}-SiEt-Si, (Idipp)$_X$), 176.1 (s, 1C, *C*^{2}-Si-SiEt, (Idipp)$_Y$).

^{29}Si NMR (*Figure S22*, 59.63 MHz, THF-d_8, 298 K, ppm): δ = 87.2 (s, 1Si, *Si*-Si-Et), 111.6 (t, 1Si, ^{2}J(Si,H) = 8.4 Hz, Si-*Si*-Et).

^{19}F{^{1}H} NMR (282.4 MHz, THF-d_8, 298 K, ppm): δ = −63.4 (s, 24F, 4 × C^{3,5}-C*F*$_3$, BAr$^{F}_4$).

^{11}B{^{1}H} NMR (96.29 MHz, THF-d_8, 298 K, ppm): δ = −6.5 (s, 1B, *B*Ar$^{F}_4$).

---

[11] The ^{1}H NMR signals of the ethyl group of **1Et**[B(Ar^{F})$_4$] show the multiplicity pattern of an A$_2$B$_3$ type spin system. The signals could be well simulated with the NMR simulation program g*NMR* (Figure S19, ref. [S5]), leading to the following values: Si-CH_2CH$_3$: δ = 0.68 ppm, ^{3}J(H,H) = 7.84 Hz, $\Delta\nu_{½}$ = 1.7 Hz; Si-CH$_2$CH_3: δ = 0.77 ppm, ^{3}J(H,H) = 7.84 Hz, $\Delta\nu_{½}$ = 1.7 Hz. For other A$_2$B$_3$ type spin systems found in ethylsilanes see: a) B. R. McGarvey, G. Slomp, *J. Chem. Phys.* **1959**, *30*, 1586; b) H. Schmidbaur, F. Schindler, *J. Organomet. Chem.* **1964**, *2*, 466.

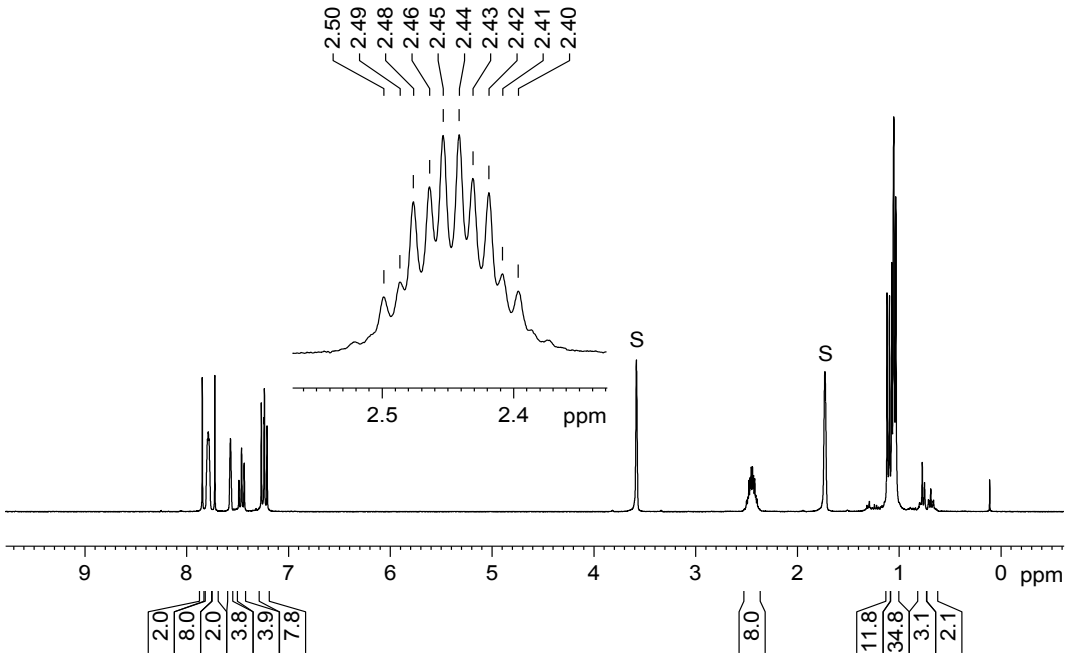

Figure S17. ^{1}H NMR (300.1 MHz) spectrum of **1Et**[B(Ar^{F})$_4$] in THF-d_8 at 298 K; the signals of the deuterated solvent are marked with the character S. An enlarged excerpt with the methine resonances is shown in the inset.

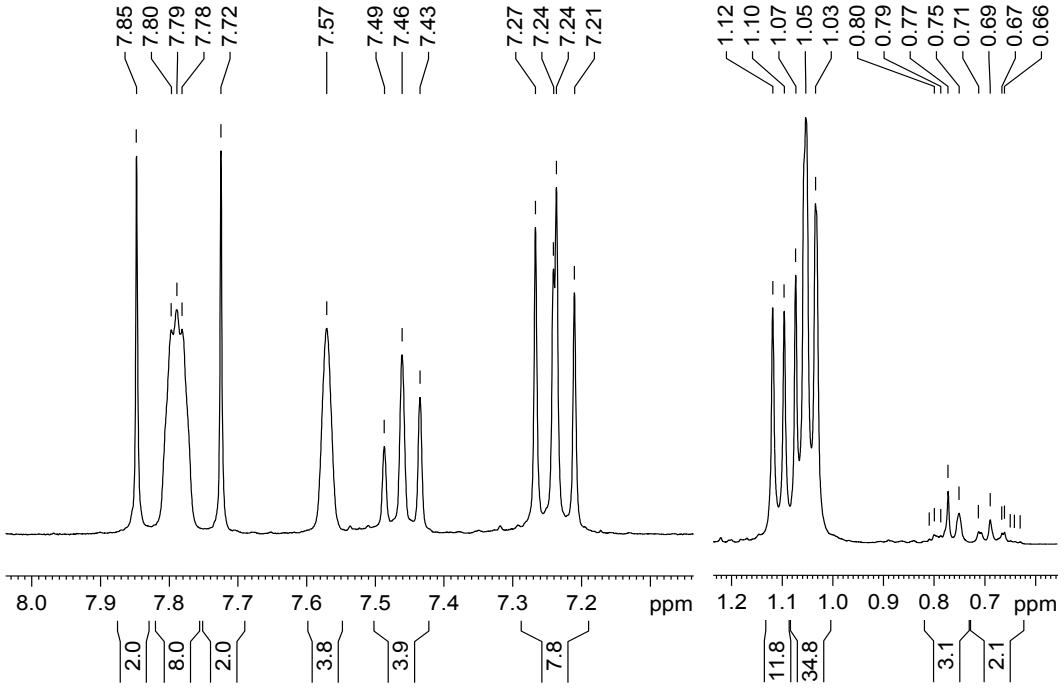

Figure S18. Excerpts of the ^{1}H NMR (300.1 MHz) spectrum of **1Et**[B(Ar^{F})$_4$] in THF-d_8 at 298 K depicted in Figure S17.

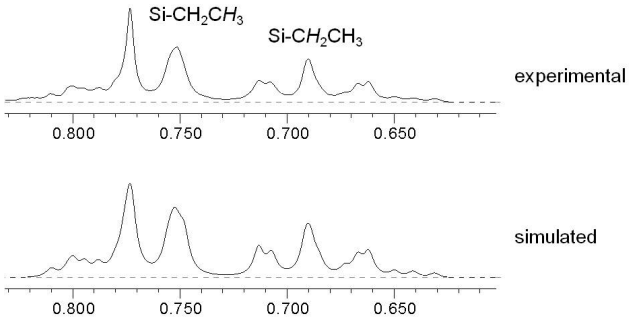

Figure S19. Experimental and simulated ^{1}H NMR spectrum of the A_2B_3 spin system of the ethyl group in **1Et**[B(Ar^{F})$_4$]. The NMR simulation was performed with the program g*NMR*.[S5]

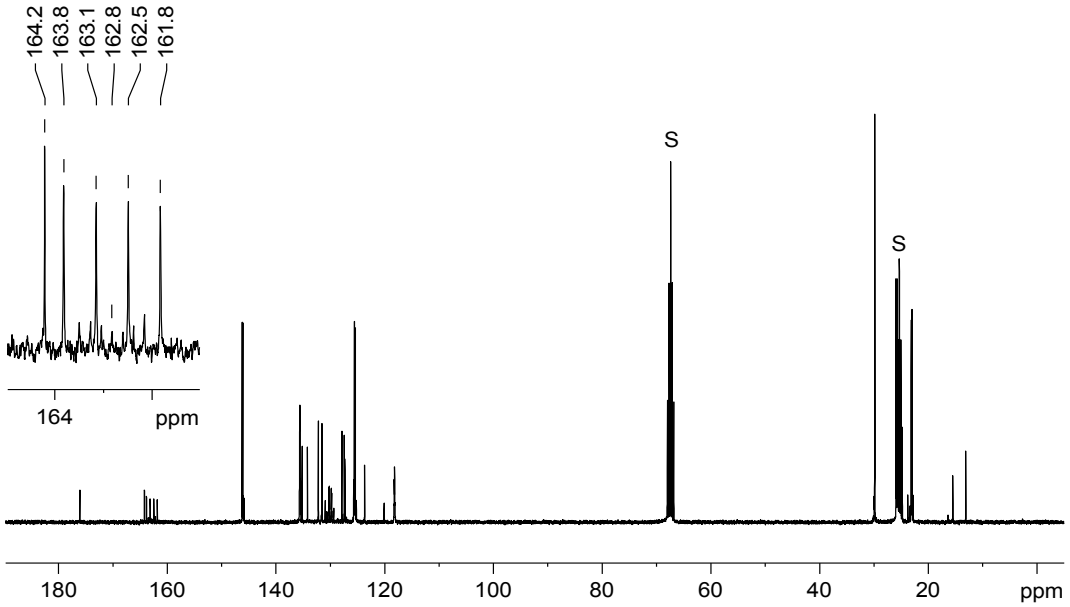

Figure S20. ^{13}C{^{1}H} NMR (75.47 MHz) spectrum of **1Et**[B(Ar^{F})$_4$] in THF-d_8 at 298 K; the signals of the deuterated solvent are marked with the character S. An enlarged excerpt is shown in the inset.

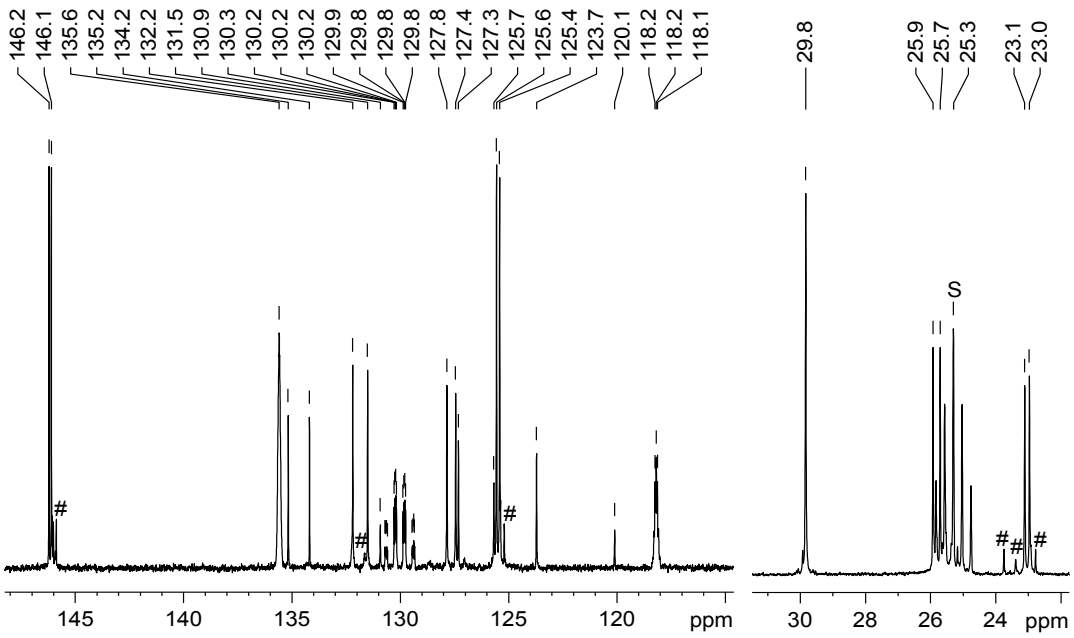

Figure S21. Excerpts of the $^{13}C\{^{1}H\}$ NMR (75.47 MHz) spectrum of **1Et**[$B(Ar^F)_4$] in THF-d_8 at 298 K depicted in Figure S20; the signal of the deuterated solvent is marked with the character S and the signals of a tiny impurity are marked with #.

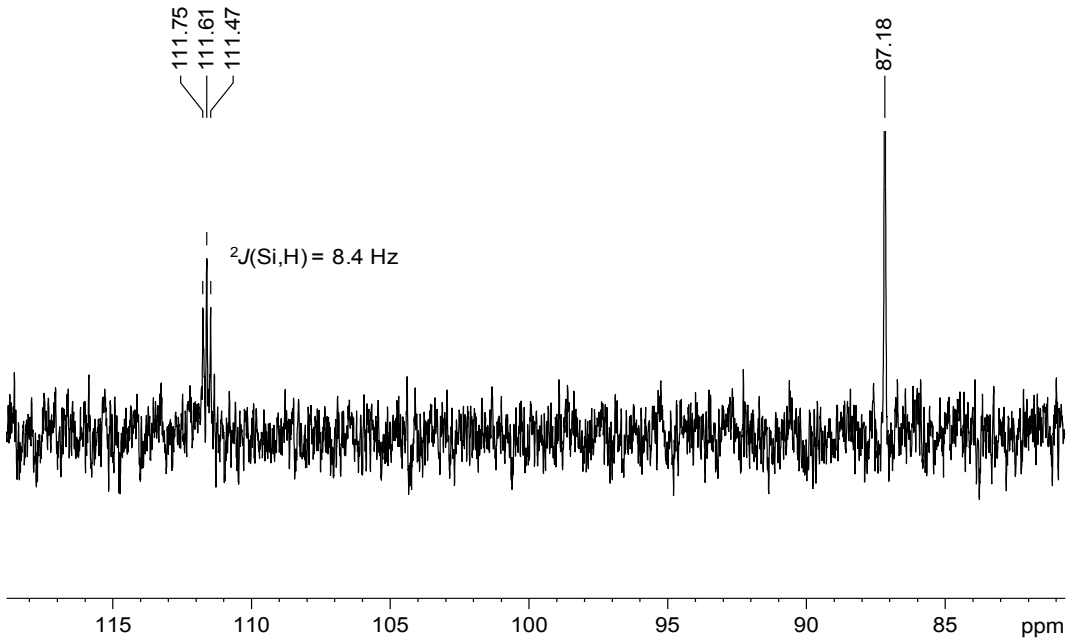

Figure S22. ^{29}Si NMR (59.63 MHz) spectrum of **1Et**[$B(Ar^F)_4$] in THF-d_8 at 298 K.

2.5 Synthesis of $[Si_2(Li)(Idipp)_2][B(C_6F_5)_4]$ (1Li[$B(C_6F_5)_4$])

Fluorobenzene (6 mL) was added to a mixture of **1** (200 mg, 0.24 mmol) and $[Li(Et_2O)_{2.5}][B(C_6F_5)_4]$ (209 mg, 0.24 mmol), whereupon a yellowish dark red suspension was obtained containing a red solid. After 10 minutes of stirring the solvent was removed under vacuum, and the dark-brown residue was dried for 2 h at 60 °C. The solid was digested in 4 mL of fluorobenzene, and 2 mL of *n*-hexane were added to afford a yellowish-brown suspension. The suspension was filtered from a small amount of a brown solid, and the yellowish brown filtrate was overlaid with 4 mL of *n*-hexane. After 20 h of storage dark-brownish black, needle-shaped crystals were formed, which were separated from the supernatant and dried under vacuum ($5 \cdot 10^{-2}$ mbar) for 2 h at ambient temperature. Yield: 158 mg (0.104 mmol, 43 %). The obtained crystals were shown by single crystal x-ray diffraction analysis and ^{1}H and ^{13}C NMR spectroscopy to be the *n*-hexane monosolvate of **1Li**[$B(C_6F_5)_4$]. A brown powder was obtained after fine grinding of the crystals and drying under vacuum.[12] Compound **1Li**[$B(C_6F_5)_4$] turns dark red at 192 – 193 °C and melts to a dark red mass under decomposition at 202 °C. Elemental analysis calcd (%) for $C_{78}H_{72}BF_{20}LiN_4Si_2$ (1519.32): C 61.66, H 4.78, N 3.69; found: C 61.43, H 5.07, N 3.67 %.

^{1}H NMR (*Figure S23*, 300.1 MHz, C_6D_5Cl, 298 K, ppm): δ = 0.86 (t, 6H, ^3J(H,H) = 6.2 Hz, 2 × CH_3, *n*-C_6H_{14}), 0.95 (d, 24H, ^3J(H,H) = 6.8 Hz, 4 × $C^{2,6}$-CH(CH_3)$_A$(CH_3)$_B$), 0.96 (d, 24H, ^3J(H,H) = 6.8 Hz, 4 × $C^{2,6}$-CH(CH_3)$_A$(CH_3)$_B$), 1.20 (m, 8H, 4 × CH_2, *n*-C_6H_{14}), 2.63 (sept, 8H, ^3J(H,H) = 6.8 Hz, 4 × $C^{2,6}$-C*H*(CH_3)$_2$), 6.99 (d, 8H, ^3J(H,H) = 7.7 Hz, 4 × $C^{3,5}$-*H*, C_6H_3), 7.00 (s, 4H, 2 × $C^{4,5}$-*H*), 7.29 (t, 4H, ^3J(H,H) = 7.7 Hz, 4 × C^4-*H*, C_6H_3).

^{13}C{^{1}H} NMR (*Figures S24 and S25*, 75.47 MHz, C_6D_5Cl, 298 K, ppm): δ = 14.3 (s, 2C, 2 × *C*H_3, *n*-C_6H_{14}), 22.0 (s, 8C, 4 × $C^{2,6}$-CH(*C*H_3)$_A$(CH_3)$_B$), 23.0 (s, 2C, 2 × *C*H_2, *n*-C_6H_{14}), 25.3 (s, 8C, 4 × $C^{2,6}$-CH(CH_3)$_A$(*C*H_3)$_B$), 29.2 (s, 8C, 4 × $C^{2,6}$-*C*H(CH_3)$_2$), 31.9 (s, 2C, 2 × *C*H_2, *n*-C_6H_{14}), 124.1 (s, 4C, 2 × *C*^{4,5}-H), 124.4 (s, 8C, 4 × *C*^{3,5}-H, C_6H_3), 131.1 (s, 4C, 4 × *C*^{4}-H, C_6H_3), 134.7 (s, 4C, 4 × *C*^{1}, C_6H_3), 136.8 (dm, 8C, ^1J(F,C) = 250.7 Hz, 4 × *C*^{3,5}-F, C_6F_5),[13] 138.7 (dm, 4C, ^1J(F,C) = 247.4 Hz, 4 × *C*^{4}-F, C_6F_5),[13] 147.0 (s, 8C, 4 × *C*^{2,6}, C_6H_3), 149.0 (dm, 8C, ^1J(F,C) = 249.6 Hz, 4 × *C*^{2,6}-F, C_6F_5),[13] 188.8 (s, 2C, 2 × *C*^{2}-Si).

[12] The brown powder obtained after fine-grinding of the crystals and prolonged drying under vacuum did not contain *n*-hexane according to the elemental analysis.

[13] The ^{13}C and ^{19}F NMR signals of the $C^{3,5}$-F and $C^{2,6}$-F groups were assigned tentatively as in ref. [S3].

^{29}Si{^{1}H} NMR (*Figure S26*, 59.63 MHz, C_6D_5Cl, 298 K, ppm): δ = 301.1 (br m, 2Si, $\Delta\nu_{½}$ = 30.7 Hz, $\Delta\nu$ = 56 Hz).[14,15]

^{7}Li NMR (116.6 MHz, C_6D_5Cl, 298 K, ppm): δ = −6.7 (s, 1Li).

^{19}F{^{1}H} NMR (282.4 MHz, C_6D_5Cl, ppm): δ = −166.8 (m, 8F, 4 × $C^{3,5}$-*F*, C_6F_5), −163.1 (t, ^{3}J(F,F) = 20.8 Hz, 4F, 4 × C^{4}-*F*, C_6F_5), −132.3 (m, 8F, 4 × $C^{2,6}$-*F*, C_6F_5).[13]

^{11}B{^{1}H} NMR (96.29 MHz, C_6D_5Cl, 298 K, ppm): δ = −16.5 (s, 1B).

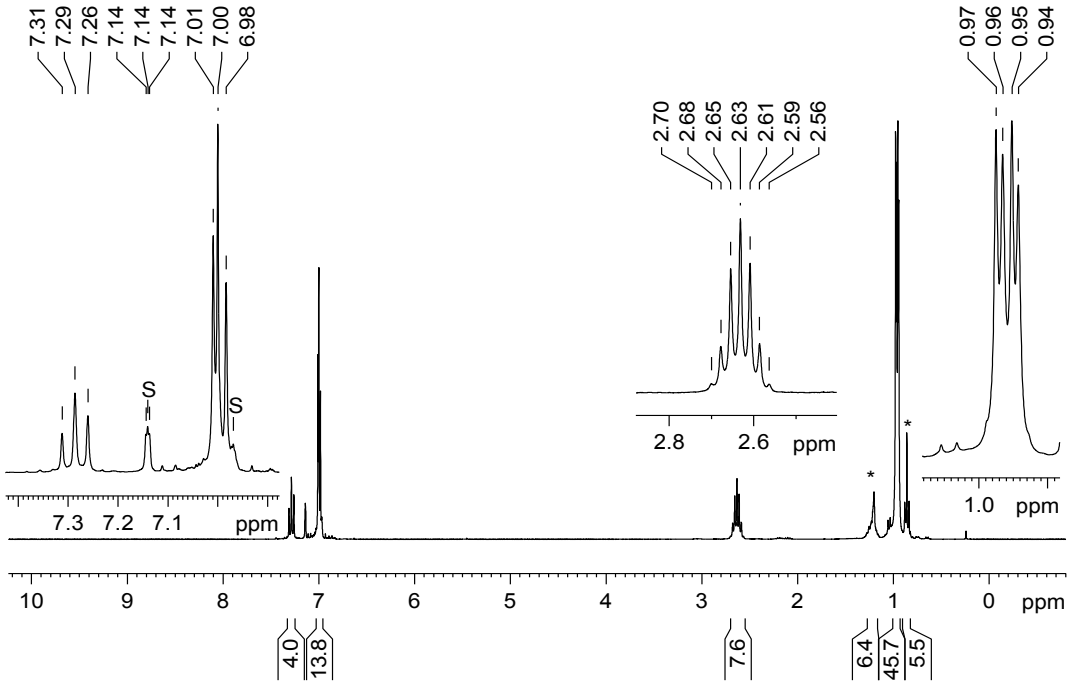

Figure S23. ^{1}H NMR (300.1 MHz) spectrum of **1Li**[$B(C_6F_5)_4$]·(*n*-C_6H_{14}) in C_6D_5Cl at 298 K; the signals of the deuterated solvent are marked with the character S and the signals of *n*-hexane with an asterisk (*). Enlarged excerpts are shown in the insets.

[14] $\Delta\nu$ denotes the width of the ^{29}Si{^{1}H} NMR signal of **1Li**[$B(C_6F_5)_4$].

[15] In order to determine the $J(^{29}Si,^{7}Li)$ coupling constant, attempts were undertaken to obtain a better resolved ^{29}Si NMR signal of **1Li**[$B(C_6F_5)_4$] either by increasing the number of scans, recording the ^{29}Si NMR spectrum on a higher field (500 MHz) spectrometer or repeating the measurement at 243 K. All these attempts failed.

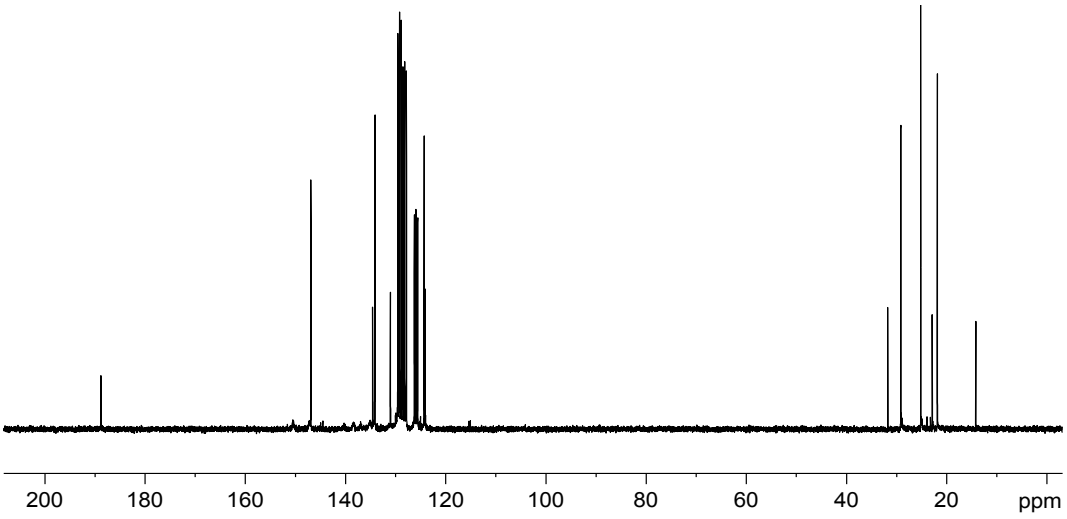

Figure S24. $^{13}C\{^{1}H\}$ NMR (75.47 MHz) spectrum of **1Li**$[B(C_6F_5)_4]\cdot(n\text{-}C_6H_{14})$ in C_6D_5Cl at 298 K.

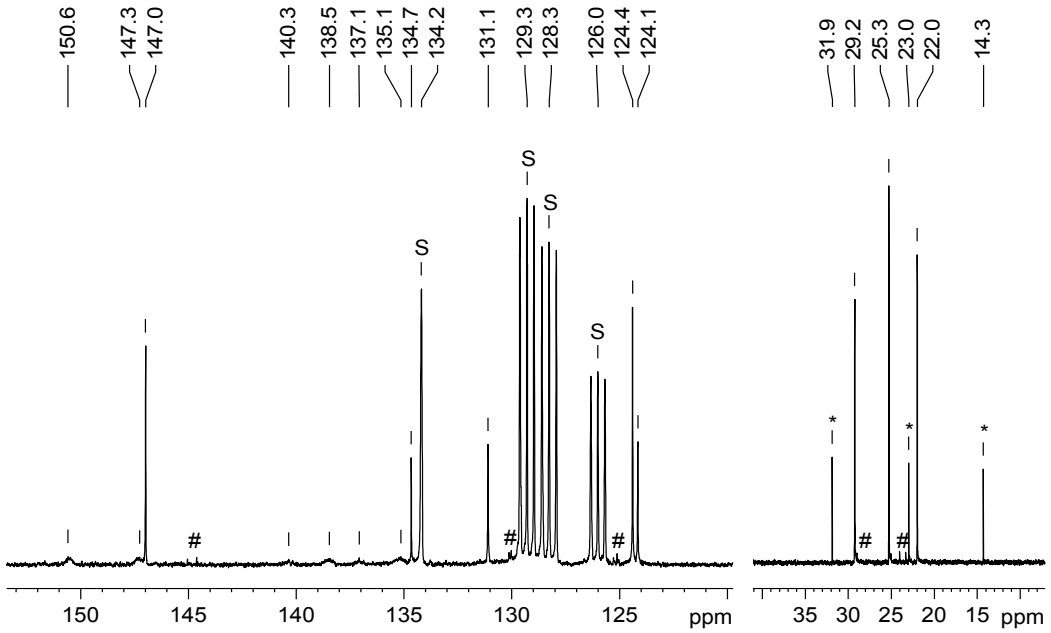

Figure S25. Excerpts of the $^{13}C\{^{1}H\}$ NMR (75.47 MHz) spectrum of **1Li**$[B(C_6F_5)_4]\cdot(n\text{-}C_6H_{14})$ in C_6D_5Cl at 298 K depicted in Figure S24; the signals of the deuterated solvent are marked with the character S, the signals of *n*-hexane with an asterisk (*) and the signals of a tiny impurity with **#**.

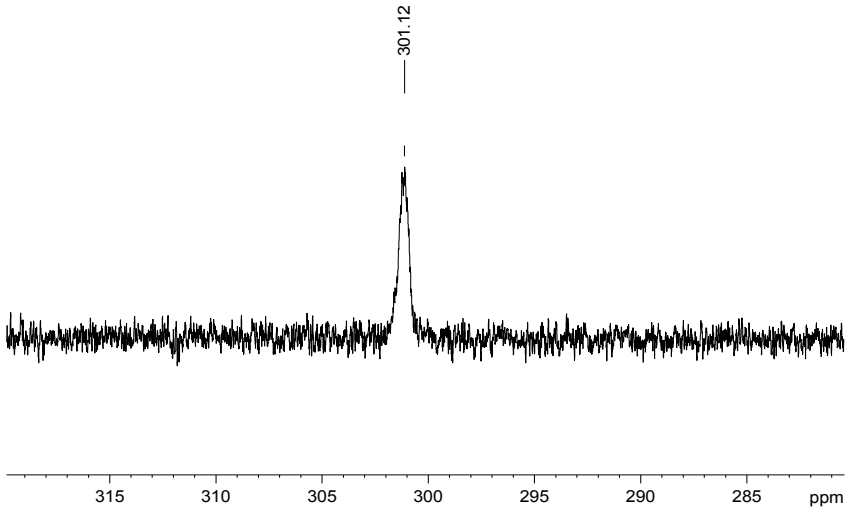

Figure S26. $^{29}Si\{^{1}H\}$ NMR (59.63 MHz) spectrum of **1Li**$[B(C_6F_5)_4]\cdot(n\text{-}C_6H_{14})$ in C_6D_5Cl at 298 K (number of scans: 10240).

2.6 Synthesis of $[Si_2(Na)(Idipp)_2][B(Ar^F)_4]$ (1Na$[B(Ar^F)_4]$)

Fluorobenzene (4 mL) was added to a mixture of **1** (200 mg, 0.24 mmol) and $Na[B(Ar^F)_4]$ (213 mg, 0.24 mmol), whereupon a yellowish-brown solution was obtained. After 2 h of stirring at ambient temperature, 2 mL of *n*-hexane were added, and the mixture was filtered from a small amount of a brown solid. *n*-Hexane (2 mL) was added to the yellowish-brown filtrate, and the biphasic mixture was mixed upon shaking the tube to obtain a clear yellowish-brown solution. Storage of the solution at −30 °C for 5 days afforded a dark-brown, crystalline solid, which was separated from the supernatant with a cannula (Ø = 1 mm) at −30 °C and dried for 2 h under vacuum ($5 \cdot 10^{-2}$ mbar) at room temperature. Yield: 288 mg (0.167 mmol, 70 %). After grinding of the crystalline solid a brown powder was obtained. Compound **1Na**$[B(Ar^F)_4]$ turns dark red at 207 °C and melts to a dark red mass under decomposition at 211 – 212 °C. Elemental analysis calcd (%) for $C_{86}H_{84}BF_{24}N_4NaSi_2$ (1719.55): C 60.07, H 4.92, N 3.26; found: C 60.02, H 5.03, N 3.21 %.

^{1}H NMR (*Figure S27*, 300.1 MHz, C_6D_5Cl, 298 K, ppm): δ = 0.95 (d, 24H, ^{3}J(H,H) = 6.9 Hz, 4 × $C^{2,6}$-$CH(CH_3)_A(CH_3)_B$), 0.96 (d, 24H, ^{3}J(H,H) = 6.9 Hz, 4 × $C^{2,6}$-$CH(CH_3)_A(CH_3)_B$), 2.66 (sept, 8H, ^{3}J(H,H) = 6.9 Hz, 4 × $C^{2,6}$-$CH(CH_3)_2$), 6.94 (s, 4H, 2 × $C^{4,5}$-*H*), 6.98 (d, 8H, ^{3}J(H,H) = 7.4 Hz, 4 × $C^{3,5}$-*H*, C_6H_3), 7.25 (t, 4H, ^{3}J(H,H) = 7.4 Hz, 4 × C^{4}-*H*, C_6H_3), 7.62 (s, 4H, 4 × C^{4}-*H*, BAr^F_4), 8.26 (br m, 8H, $\Delta\nu_{½}$ = 10.4 Hz, 4 × $C^{2,6}$-*H*, BAr^F_4).

$^{13}C\{^{1}H\}$ NMR (*Figures S28 and S29*, 75.47 MHz, C_6D_5Cl, 298 K, ppm): δ = 22.3 (s, 8C, 4 × $C^{2,6}$-$CH(CH_3)_A(CH_3)_B$), 25.1 (s, 8C, 4 × $C^{2,6}$-$CH(CH_3)_A(CH_3)_B$), 29.1 (s, 8C, 4 × $C^{2,6}$-$CH(CH_3)_2$), 117.8 (sept, 4C, ^{3}J(F,C) = 4.2 Hz, 4 × C^{4}-H, BAr^F_4), 124.2 (s, 8C, 4 × $C^{3,5}$-H, C_6H_3), 124.3 (s, 4C, 2 × $C^{4,5}$-H), 125.0 (q, 8C, ^{1}J(F,C) = 272 Hz, 4 × $C^{3,5}$-CF_3, BAr^F_4), 129.2 (qq, 8C, ^{2}J(F,C) =

31.8 Hz, ^{3}J(C,^{11}B) = 2.8 Hz, 4 × $C^{3,5}$-CF_3, BAr^F_4), 130.4 (s, 4C, 4 × C^4-H, C_6H_3), 135.1 (s, 4C, 4 × C^1, C_6H_3), 135.3 (br s, 8C, $\Delta\nu_{½}$ = 10.4 Hz, 4 × $C^{2,6}$-H, BAr^F_4), 147.2 (s, 8C, 4 × $C^{2,6}$, C_6H_3), 162.4 (q, 4C, ^{1}J(C,^{11}B) = 49.6 Hz, ^{1}J(C,^{10}B) = 16.6 Hz, 4 × C^1, BAr^F_4), 189.1 (s, 2C, 2 × C^2-Si).

^{29}Si{^{1}H} NMR (*Figure S30*, 59.63 MHz, C_6D_5Cl, 298 K, ppm): δ = 288.8 (s, 2Si).

^{19}F{^{1}H} NMR (282.4 MHz, C_6D_5Cl, 298 K, ppm): δ = −62.6 (s, 24F, 4 × $C^{3,5}$-CF_3, BAr^F_4).

^{11}B{^{1}H} NMR (96.29 MHz, C_6D_5Cl, 298 K, ppm): δ = −6.5 (s, 1B, BAr^F_4).

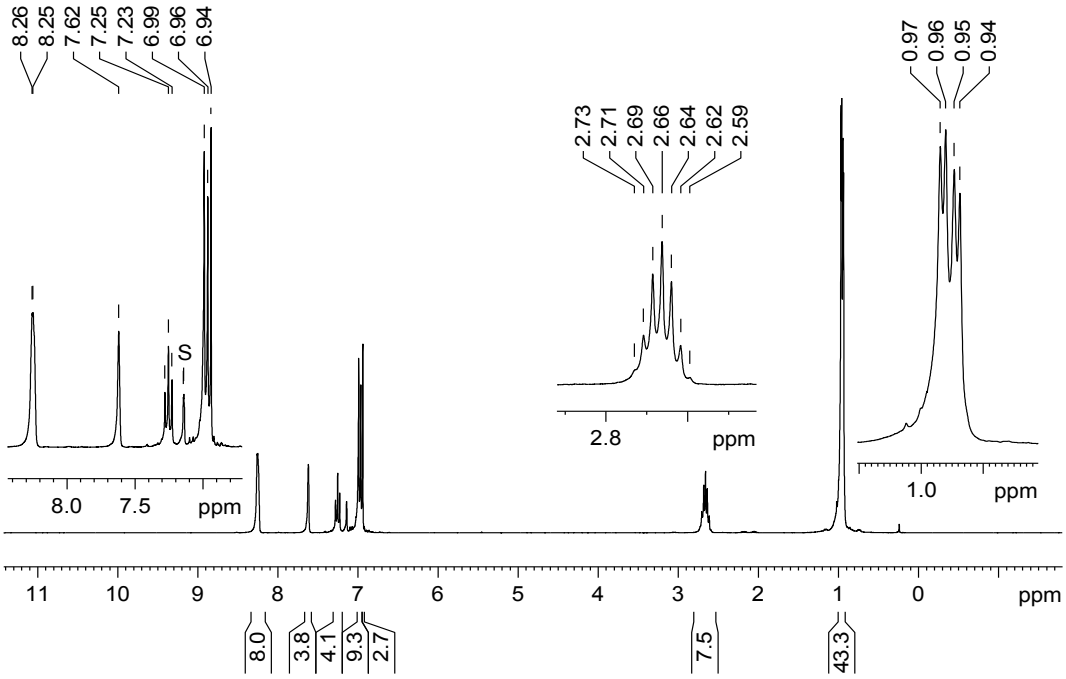

Figure S27. ^{1}H NMR (300.1 MHz) NMR spectrum of **1Na**[$B(Ar^F)_4$] in C_6D_5Cl at 298 K; the signal of the deuterated solvent is marked with the character S. Enlarged excerpts are shown in the insets.

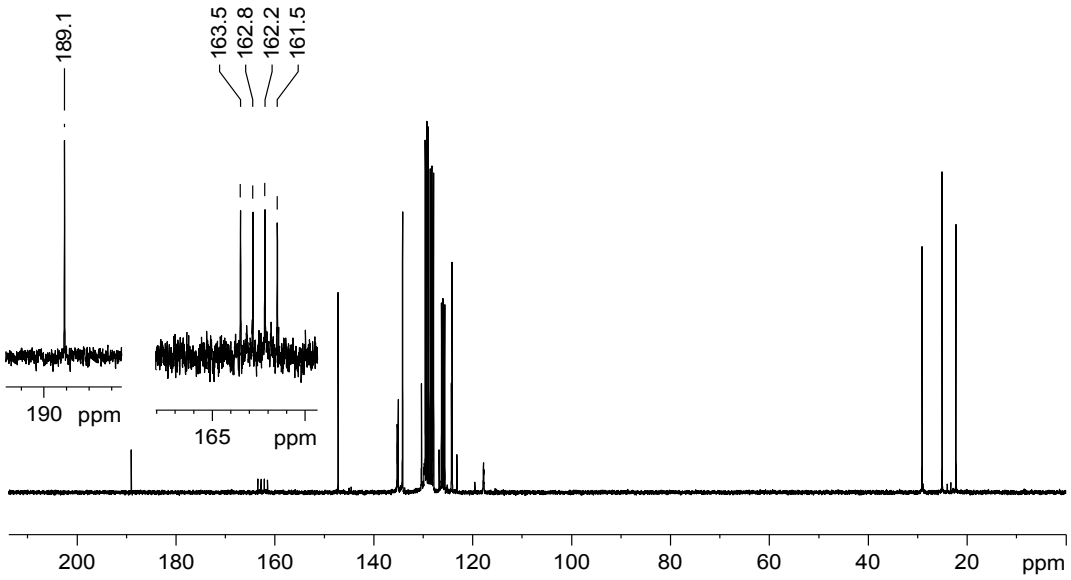

Figure S28. $^{13}C\{^{1}H\}$ NMR (75.47 MHz) spectrum of **1Na**[$B(Ar^F)_4$] in C_6D_5Cl at 298 K. Enlarged excerpts are shown in the insets.

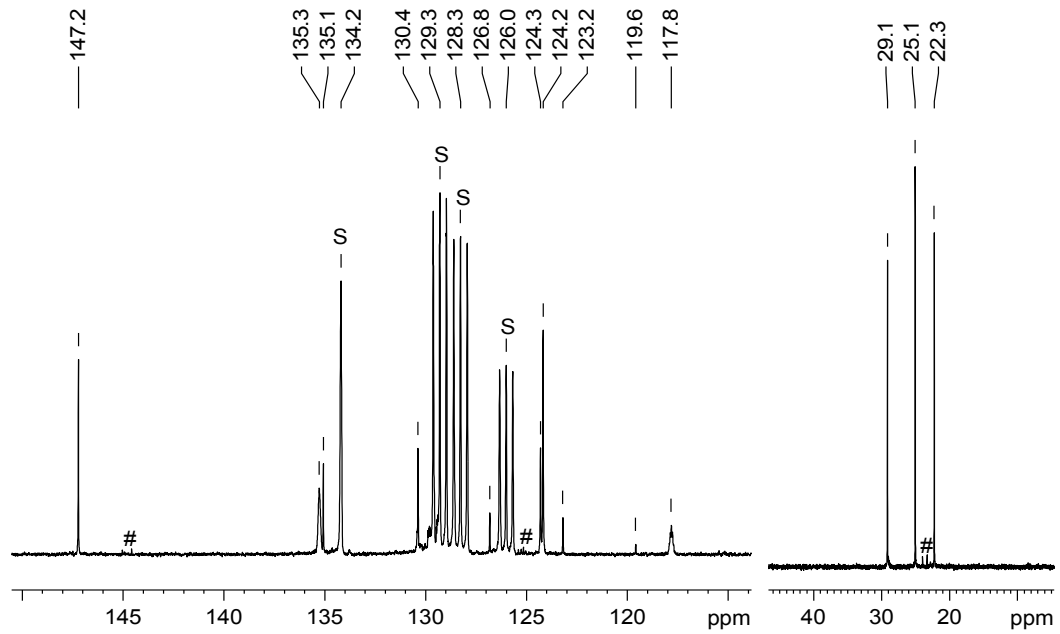

Figure S29. Excerpts of the $^{13}C\{^{1}H\}$ NMR (75.47 MHz) spectrum of **1Na**[$B(Ar^F)_4$] in C_6D_5Cl at 298 K depicted in Figure S28; the signals of the deuterated solvent are marked with the character S and the signals of a tiny impurity with #.

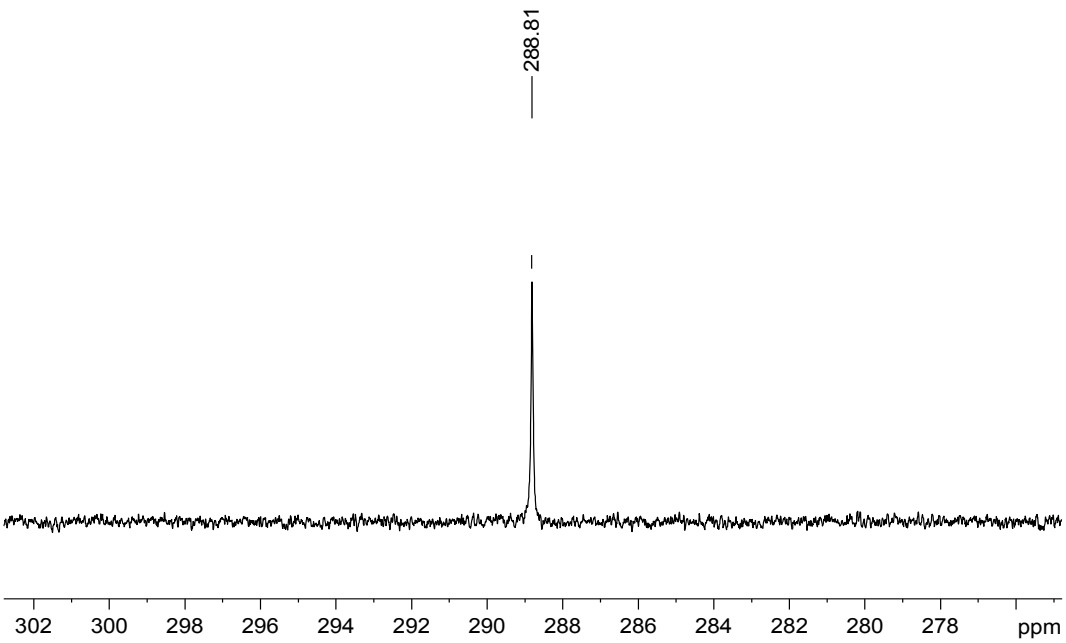

Figure S30. $^{29}Si\{^{1}H\}$ NMR (59.63 MHz) spectrum of **1Na**[$B(Ar^F)_4$] in C_6D_5Cl at 298 K.

3. Determination of the standard Gibbs energy of activation for 1H[B(Ar^F)$_4$]

The thermodynamic values ($\Delta G^{\neq}$, $\Delta H^{\neq}$, $\Delta S^{\neq}$, E_a) of the dynamic process of **1H**[B(Ar^F)$_4$] were determined with variable temperature ^{1}H NMR spectroscopy from 213 K to 273 K (Figure S31).

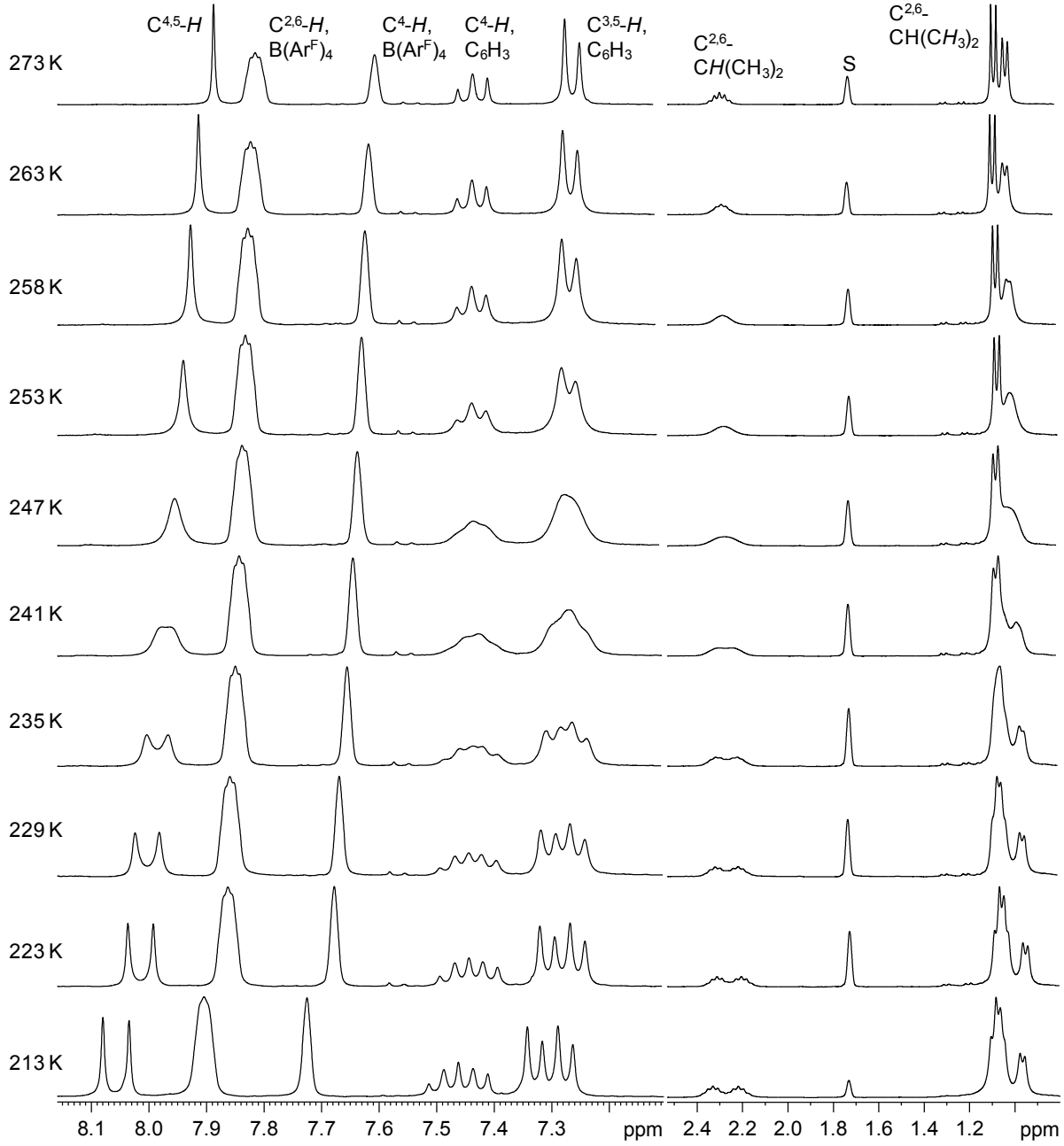

Figure S31. Excerpts of the variable temperature ^{1}H NMR (300.1 MHz) spectra of **1H**[B(Ar^F)$_4$] in THF-d_8 from 213 – 273 K showing the dynamic behaviour. The signal marked with S corresponds to the residual proton resonance of the deuterated solvent.[16]

[16] The ^{1}H NMR spectrum at 213 K was used for ^{13}C and ^{29}Si NMR spectroscopy and recorded at a higher concentration of **1H**[B(Ar^F)$_4$].

The rate constants (k) and errors of the rate constants ($\sigma(k)$) were obtained from a full line-shape analysis of the $C^{4,5}$-*H* signals using the NMR simulation program g*NMR*.[S5] The calculations were performed using standard methods of dynamic NMR spectroscopy.[S6] The error of the temperature ($\sigma(T)$) was estimated to $\sigma(T)$ = 2 K.

The free Gibbs energy of activation ($\Delta G^{\neq}$) at the temperature of coalescence (T_c) can be calculated using the equation (1), where $\Delta\nu$ is the peak separation of the signals in Hz in the low temperature limit spectrum.

$$\Delta G^{\neq} = 0.0191 \cdot T_c \cdot \left[9.97 + \lg\left(\frac{T_c}{\Delta\nu}\right)\right] \text{ [kJ mol}^{-1}\text{]} \qquad (1)$$

Using the values T_c = 241 K and $\Delta\nu$ = 13.7 Hz (at 213 K) the free Gibbs energy of activation $\Delta G^{\neq}$ was calculated to 51.6 kJ mol^{-1} at 241 K.

The $\Delta G^{\neq}$ values can be calculated at each temperature from the rate constants k using equation (2).

$$\Delta G^{\neq} = 0.0191 \cdot T \cdot \left[10.319 + \lg\left(\frac{T}{k}\right)\right] \text{ [kJ mol}^{-1}\text{]} \qquad (2)$$

The rate constants (k) and errors of the rate constants ($\sigma(k)$) obtained from simulation and the corresponding $\Delta G^{\neq}$ values calculated from equation (2) are given in Table S1.

Table S1: Determined rate constants and $\Delta G^{\neq}$ values from 213 – 273 K.

T [K]	k [Hz]	$\sigma(k)$ [Hz]	$\Delta G^{\neq}$ [kJ mol^{-1}]	T [K]	k [Hz]	$\sigma(k)$ [Hz]	$\Delta G^{\neq}$ [kJ mol^{-1}]
213	2.98	1.24	49.5	244	40.1	1.25	51.7
223	6.04	3.03	50.6	247	52.3	1.31	51.9
226	8.05	2.65	50.8	250	66.9	2.21	52.0
229	10.4	1.94	51.0	253	86.4	4.40	52.1
232	14.3	2.09	51.1	258	117	1.07	52.5
235	18.1	2.41	51.3	263	187	1.03	52.6
238	24.4	2.78	51.4	268	259	1.16	52.9
241	31.4	1.24	51.6	273	400	2.56	52.9

The $\Delta G^{\neq}$ values range from 49.5 to 52.9 kJ mol^{-1} in the temperature range of 213 – 273 K. The standard deviation $\sigma(\Delta G^{\neq})$ was calculated from the root of the variance of $\Delta G^{\neq}$ to 0.9 kJ mol^{-1}.

An Arrhenius plot of ln(k) versus 1/T gave a linear fit with R^2 = 0.9949 (Figure S32). Using the Arrhenius equation (3), the energy of activation (E_a) was determined from the slope using the equation E_a = −slope · R (R = 8.314462 J K^{-1} mol^{-1}) and found to be 40.7 kJ mol^{-1}.

The error of the energy of activation ($\sigma(E_a)$) was calculated using equation (4),[S7] where T is the average temperature of the measurements (T = 243.31 K), ΔT = T_{max} – T_{min} = 60 K,

$\Delta(ln\ k)$ = ln(k_{max}) – ln(k_{min}) = 4.90, $\sigma(T)/T$ is the average value of the relative errors for each temperature $\sigma(T)/T_i$ from 213 – 273 K, and $\sigma(k)/k$ is the average value of the relative errors for each rate constant $\sigma(k_i)/k_i$ from 213 – 273 K. Thereby $\sigma(E_a)$ was calculated to 2.4 kJ mol^{-1}.

$$k = A \cdot e^{-E_a/RT} \qquad (3)$$

$$\left(\frac{\sigma(E_a)}{E_a}\right)^2 \approx \frac{2T^2}{(\Delta T)^2}\left(\frac{\sigma(T)}{T}\right)^2 + 2\left(\frac{1}{\Delta(ln(k))}\right)^2\left(\frac{\sigma(k)}{k}\right)^2 \qquad (4)$$

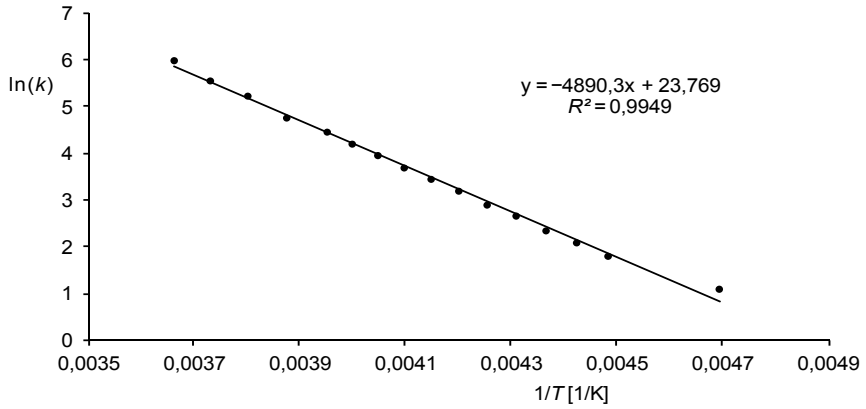

Figure S32. Arrhenius plot of ln(k) versus 1/T for **1H**[B(Ar^F)$_4$].

The enthalpy of activation ($\Delta H^{\neq}$) can be calculated using the equation $\Delta H^{\neq} = E_a - RT$, with $T = T_c$ = 241 K, to yield $\Delta H^{\neq}$ = 38.7 kJ mol^{-1}.

The error of the enthalpy of activation ($\sigma(\Delta H^{\neq})$) was calculated using the equation $\sigma(\Delta H^{\neq}) = \sigma(E_a) - R \cdot \sigma(T)$, with $\sigma(E_a)$ = 2.4 kJ mol^{-1} and $\sigma(T)$ = 2 K, to yield $\sigma(\Delta H^{\neq})$ = 2.4 kJ mol^{-1}.

The entropy of activation was calculated using the equation (5), with $\Delta G^{\neq}$(241 K) = 51.6 kJ mol^{-1}, E_a = 40.7 kJ mol^{-1} and $T = T_c$ = 241 K, to yield $\Delta S^{\neq}$ = −53.8 J K^{-1} mol^{-1}.

$$\Delta S^{\neq} = \frac{\left[(E_a - RT) - \Delta G^{\neq}\right]}{T} \qquad (5)$$

The error of the entropy of activation ($\sigma(\Delta S^{\neq})$) was calculated using equation (6), with $T = T_c$ = 241 K, $\sigma(\Delta H^{\neq})$ = 2.4 kJ mol^{-1}, $\sigma(\Delta G^{\neq})$ = 0.9 kJ mol^{-1}, $\Delta H^{\neq}$ = 38.7 kJ mol^{-1}, $\Delta G^{\neq}$ = 51.6 kJ mol^{-1} and $\sigma(T)$ = 2 K, to yield $\sigma(\Delta S^{\neq})$ = 6.6 J K^{-1} mol^{-1}.

$$\sigma\left(\Delta S^{\neq}\right)= \frac{\sigma(\Delta H^{\neq})}{T} - \frac{\sigma(\Delta G^{\neq})}{T} - \sigma(T)\left(\frac{\Delta H^{\neq} - \Delta G^{\neq}}{T^2}\right) \quad (6)$$

The Eyring plot of ln(k/T) versus 1/T gave a linear fit with R^2 = 0.9957 (Figure S33). Determination of the thermodynamic values from the Eyring plot using the modified Eyring equation (7) and the equations $\Delta H^{\neq}$ = −slope · R, $\Delta S^{\neq} = R \cdot$ (intercept – ln(k_B/h)), with ln(k_B/h) = 23.760 and $\Delta G^{\neq} = \Delta H^{\neq} - T \cdot \Delta S^{\neq}$, led to $\Delta H^{\neq}$ = 38.5 kJ mol^{-1}, $\Delta S^{\neq}$ = −54.3 J K^{-1} mol^{-1} and $\Delta G^{\neq}$(241 K) = 51.6 kJ mol^{-1}.

$$\ln\left(\frac{k}{T}\right) = \ln\left(\frac{k_B}{h}\right) + \frac{\Delta S^{\neq}}{R} - \frac{\Delta H^{\neq}}{R}\left(\frac{1}{T}\right) \quad (7)$$

The error of the enthalpy of activation ($\sigma(\Delta H^{\neq})$) and the error of the entropy of activation ($\sigma(\Delta S^{\neq})$) were calculated using equations (8) and (9), respectively. Equations (8) and (9) were derived from the Eyring equation by error propagation,[S8] where $\Delta T = T_{max} - T_{min}$ = 60 K and ΔL = (ln(k_{max}/T_{max}) – ln(k_{min}/T_{min})) = 4.65. The relative errors $\sigma(T)/T$ and $\sigma(k)/k$ were used as the average values from 213 – 273 K as for the Arrhenius plot. The calculations yielded $\sigma(\Delta H^{\neq})$ = 2.4 kJ mol^{-1} and $\sigma(\Delta S^{\neq})$ = 7.7 J K^{-1} mol^{-1}. The error of the Gibbs free energy of activation ($\sigma(\Delta G^{\neq})$) was calculated to 0.6 kJ mol^{-1} using the equation $\sigma(\Delta G^{\neq}) = \sigma(\Delta H^{\neq}) - T \cdot \sigma(\Delta S^{\neq}) - \Delta S^{\neq} \cdot \sigma(T)$, with $\sigma(\Delta H^{\neq})$ = 2.4 kJ mol^{-1}, $T = T_c$ = 241 K, $\Delta S^{\neq}$ = −54.3 J K^{-1} mol^{-1}, $\sigma(\Delta S^{\neq})$ = 7.7 J K^{-1} mol^{-1} and $\sigma(T)$ = 2 K.

$$(\sigma(\Delta H^{\neq}))^2 = \frac{R^2 T_{max}^{\,2} T_{min}^{\,2}}{\Delta T^2}\left\{\left(\frac{\sigma(T)}{T}\right)^2\left[\left(1 + T_{min}\frac{\Delta L}{\Delta T}\right)^2 + \left(1 + T_{max}\frac{\Delta L}{\Delta T}\right)^2\right] + 2\left(\frac{\sigma(k)}{k}\right)^2\right\} \quad (8)$$

$$\left(\sigma\left(\Delta S^{\neq}\right)\right)^2 = \frac{R^2}{\Delta T^2}\left\{\left(\frac{\sigma(T)}{T}\right)^2\left[T_{max}^{\,2}\left(1 + T_{min}\frac{\Delta L}{\Delta T}\right)^2 + T_{min}^{\,2}\left(1 + T_{max}\frac{\Delta L}{\Delta T}\right)^2\right] + \left(\frac{\sigma(k)}{k}\right)^2 (T_{max}^{\,2} + T_{min}^{\,2})\right\} \quad (9)$$

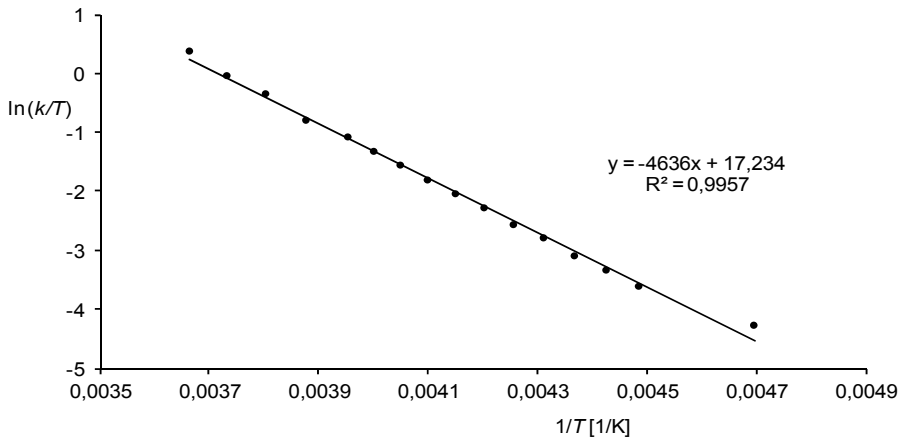

Figure S33. Eyring plot of ln(*k*/*T*) versus 1/*T* for **1H**[B(Ar^F)$_4$].

The results of the dynamic NMR spectroscopic analysis are summarized in Table S2 and show a good agreement of the values of $\Delta H^{\neq}$, $\Delta S^{\neq}$ and $\Delta G^{\neq}$ obtained from the Arrhenius or the Eyring plot. In the main text, only the values derived from the Eyring plot are discussed.

Table S2: Summary of the dynamic NMR spectroscopic analysis of **1H**[B(Ar^F)$_4$].

Estimation[a]	Arrhenius plot[b]	Eyring plot
$\Delta G^{\neq}$(241 K) = 51.6 kJ mol^{-1}	$\Delta G^{\neq}$(241 K) = 51.6 ± 0.9 kJ mol^{-1}	$\Delta G^{\neq}$(241 K) = 51.6 ± 0.6 kJ mol^{-1}
	$\Delta H^{\neq}$ = 38.7 ± 2.4 kJ mol^{-1}	$\Delta H^{\neq}$ = 38.5 ± 2.4 kJ mol^{-1}
	$\Delta S^{\neq}$ = −53.8 ± 6.6 J K^{-1} mol^{-1}	$\Delta S^{\neq}$ = −54.3 ± 7.7 J K^{-1} mol^{-1}
	E_a = 40.7 ± 2.4 kJ mol^{-1}	

[a]: The estimation was carried out using equation (1). [b]: $\Delta G^{\neq}$ was determined using equation (2).

4. Crystal structure determination

Orange-red plates of **1H**[B(Ar^F)$_4$] for single-crystal X-ray diffraction were obtained upon crystallization from a C_6H_5F / *n*-hexane (1:1) mixture at −30 °C. Red blocks of **1Me**[B(Ar^F)$_4$] were obtained upon crystallization from a C_6H_5F / *n*-hexane (4:3) mixture at −30 °C. Red plates of **1Et**[B(Ar^F)$_4$] were obtained upon crystallization from a C_6H_5F / *n*-hexane (3:4) mixture at −30 °C. In each case, the solvent was decanted from the crystals with a cannula at −30 °C and the crystals were dried under vacuum. Yellow-orange rods of **1Li**[B(C_6F_5)$_4$]·(*n*-C_6H_{14}) were obtained upon diffusion of *n*-hexane into a saturated solution of **1Li**[B(C_6F_5)$_4$] in fluorobenzene at room temperature.[17] Clear red blocks of **1Na**[B(Ar^F)$_4$] were obtained by complete evaporation of the solvent of a C_6D_5Cl / *n*-hexane solution at room temperature. DIAMOND[S9] plots of the molecular structures of **1Et**[B(Ar^F)$_4$] and **1Na**[B(Ar^F)$_4$] are depicted in Figures S34 and S35, respectively.

The data collection for **1H**[B(Ar^F)$_4$], **1Me**[B(Ar^F)$_4$], **1Et**[B(Ar^F)$_4$], **1Li**[B(C_6F_5)$_4$]·(*n*-C_6H_{14}) and **1Na**[B(Ar^F)$_4$] was performed on a STOE IPDS2T diffractometer (area detector) using graphite monochromated Mo-$K\alpha$ irradiation (λ = 0.71073 Å). The diffractometer was equipped with a low-temperature device (Oxford Cryostream 700er series, Oxford Cryosystems, 123(2) K). Intensities were measured by fine-slicing ω and φ-scans and corrected for background, polarization and Lorentz effects. A numerical absorption correction was applied for compound **1H**[B(Ar^F)$_4$]. The absorption corrections for **1Me**[B(Ar^F)$_4$], **1Et**[B(Ar^F)$_4$], **1Li**[B(C_6F_5)$_4$]·(*n*-C_6H_{14}) and **1Na**[B(Ar^F)$_4$] were performed by integration. The structures were solved by direct methods and refined anisotropically by the least-square procedure implemented in the SHELX program system.[S10] Hydrogen atoms were included using the riding model on the bound carbon atoms, except the Si1-bonded H85 atom of **1H**[B(Ar^F)$_4$], which was located in the difference density map and refined isotropically.

1Na[B(Ar^F)$_4$] turned out to be non-merohedrally twinned. Inspection of the reciprocal lattice revealed a second orientation matrix of the twinned component. Twin integration yielded a refined twin law of (−0.967 −0.205 −0.139 −0.336 −0.947 −0.173 −0.069 −0.170 0.990) and a BASF factor of 0.291(7). Structure refinement was performed on the basis of the HKLF5 data obtained by the twin integration procedure.

[17] The colors of the crystals of **1Li**[B(C_6F_5)$_4$]·(*n*-C_6H_{14}) and **1Na**[B(Ar^F)$_4$] observed under the microscope differ from those of the macroscopic crystalline samples, which are given in the experimental part (cf. chapters 2.5 and 2.6).

CCDC numbers CCDC-1448827 (**1H**[B(Ar^F)$_4$]), CCDC-1448828 (**1Me**[B(Ar^F)$_4$]), CCDC-1448829 (**1Et**[B(Ar^F)$_4$]), CCDC-1448830 (**1Li**[B(C$_6$F$_5$)$_4$]·(*n*-C$_6$H$_{14}$)) and CCDC-1448831 (**1Na**[B(Ar^F)$_4$]) contain the supplementary crystallographic data for this paper, which can be obtained free of charge from the Cambridge Crystallographic Data Centre via www.ccdc.cam.ac.uk/data_request/cif.

Table S3: Crystal data and refinement.

	1H[B(Ar^F)$_4$]	**1Me**[B(Ar^F)$_4$]	**1Et**[B(Ar^F)$_4$]	**1Li**[B(C$_6$F$_5$)$_4$]·(*n*-C$_6$H$_{14}$)	**1Na**[B(Ar^F)$_4$]
Empirical formula	$C_{86}H_{85}BF_{24}N_4Si_2$	$C_{87}H_{87}BF_{24}N_4Si_2$	$C_{88}H_{89}BF_{24}N_4Si_2$	$C_{84}H_{86}BF_{20}LiN_4Si_2$	$C_{86}H_{84}BF_{24}N_4NaSi_2$
Moiety formula	$C_{54}H_{73}N_4Si_2$, $C_{32}H_{12}BF_{24}$	$C_{55}H_{75}N_4Si_2$, $C_{32}H_{12}BF_{24}$	$C_{56}H_{77}N_4Si_2$, $C_{32}H_{12}BF_{24}$	$C_{54}H_{72}LiN_4Si_2$, $C_{24}BF_{20}$, C_6H_{14}	$C_{54}H_{72}N_4NaSi_2$, $C_{32}H_{12}BF_{24}$
Formula weight	1697.57 gmol^{-1}	1711.60 gmol^{-1}	1725.62 gmol^{-1}	1605.50 gmol^{-1}	1719.55
Temperature	123(2) K	123(2) K	123(2) K	123(2)	123(2)
Wavelength	0.71073 Å	0.71073 Å	0.71073 Å	0.71073 Å	0.71073 Å
Crystal system, space group	triclinic, *P-1*	triclinic, *P-1*	triclinic, *P-1*	orthorombic, *aba2*	monoclinic, *I2/a*
Unit cell dimensions	*a* = 12.6179(4) Å	*a* = 12.5317(4) Å	*a* = 12.6984(4) Å	*a* = 21.7127(5) Å	*a* = 17.9849(6) Å
	b = 16.9418(6) Å	*b* = 16.8752(5) Å	*b* = 16.1030(5) Å	*b* = 29.2279(8) Å	*b* = 22.4945(10) Å
	c = 21.2119(7) Å	*c* = 21.5506(7) Å	*c* = 21.2179(7) Å	*c* = 26.0364(5) Å	*c* = 21.3530(7) Å
	α = 80.997(3)°	α = 81.388(3)°	α = 86.027(3)°	α = 90°	α = 90°
	β = 74.486(3)°	β = 74.544(2)°	β = 88.262(2)°	β = 90°	β = 95.132(3)°
	γ = 87.144(3)°	γ = 87.162(2)°	γ = 89.457(3)°	γ = 90°	γ = 90°
Volume	4315.3(2) Å^3	4342.8(2) Å^3	4326.2(2) Å^3	16523.1(7) Å^3	8604.0(6) Å^3
Z, Calculated density	2, 1.306 mg m^{-3}	2, 1.309 mg m^{-3}	2, 1.325 mg m^{-3}	8, 1.291 mg m^{-3}	4, 1.327 mg m^{-3}
Absorption coefficient	0.138 mm^{-1}	0.138 mm^{-1}	0.139 mm^{-1}	0.133 mm^{-1}	0.144 mm^{-1}
F(000)	1756	1772	1788	6672	3552.0
Crystal size	0.50 × 0.08 × 0.04 mm	0.25 × 0.20 × 0.18 mm	0.24 × 0.15 × 0.06 mm	0.50 × 0.09 × 0.06 mm	0.24 × 0.18 × 0.15
θ-range for data collection	2.92 – 28.00°	2.85 – 28.00°	2.89 – 28.00°	2.62 – 28.00°	2.55 – 26.18°
Limiting indices	−16 ≤ *h* ≤ 16	−16 ≤ *h* ≤ 16	−16 ≤ *h* ≤ 16	−24 ≤ *h* ≤ 28	−21 ≤ *h* ≤ 21
	−22 ≤ *k* ≤ 22	−22 ≤ *k* ≤ 20	−18 ≤ *k* ≤ 21	−37 ≤ *k* ≤ 38	−26 ≤ *k* ≤ 26
	−28 ≤ *l* ≤ 25	−27 ≤ *l* ≤ 28	−27 ≤ *l* ≤ 28	−34 ≤ *l* ≤ 22	−25 ≤ *l* ≤ 25
Reflections collected / unique	45959 / 20063 [R_{int} = 0.0472]	45709 / 20744 [R_{int} = 0.0519]	40688 / 20634 [R_{int} = 0.0402]	35881 / 16366 [R_{int} = 0.0611]	44493 / 16344 [R_{int} = 0.048]
Completeness to θ_{max}	96.2 %	98.9	98.8 %	99.3 %	99.8 %
Absorption correction	Numerical	Integration	Integration	Integration	Integration
Max. / min. transmission	0.9945 and 0.9341	0.9756 / 0.9663	0.9917 / 0.9674	0.9920 and 0.9363	0.9897 and 0.9580
Refinement method	Full-matrix least squares on F^2	Full-matrix least squares on F^2	Full-matrix least squares on F^2	Full-matrix least squares on F^2	Full-matrix least squares on F^2
Data / restraints / parameters	20063 / 162 / 1200	20744 / 511 / 1203	20634 / 347 / 1219	16366 / 128 / 1048	16344 / 116 / 655
Goodness-of-fit on F^2	0.945	1.050	0.922	0.915	0.698
Final *R* indices [$I > \sigma(I)$]	R_1 = 0.0456, wR_2 = 0.1047	R_1 = 0.0531, wR_2 = 0.1397	R_1 = 0.0497, wR_2 = 0.1177	R_1 = 0.0490, wR_2 = 0.1035	R_1 = 0.0452, wR_2 = 0.0989
R indices (all data)	R_1 = 0.0778, wR_2 = 0.1142	R_1 = 0.0797, wR_2 = 0.1515	R_1 = 0.0878, wR_2 = 0.1277	R_1 = 0.0745, wR_2 = 0.1116	R_1 = 0.1439, wR_2 = 0.1331
Largest diff. peak / hole	0.559 / −0.696 e Å^{-3}	0.59 / −0.47 e Å^{-3}	1.17 / −0.68 e Å^{-3}	0.54 / −0.63 e Å^{-3}	0.32 / −0.29 e Å^{-3}
CCDC number	CCDC-1448827	CCDC-1448828	CCDC-1448829	CCDC-1448830	CCDC-1448831

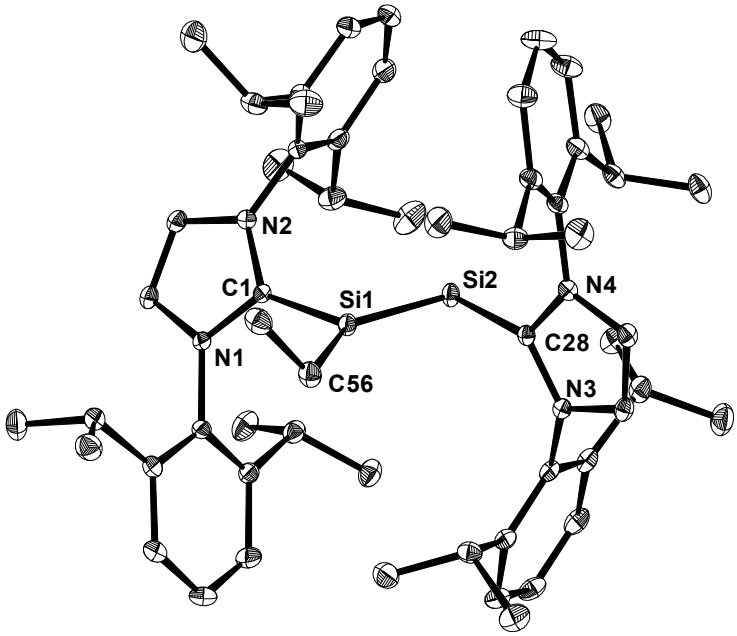

Figure S34. DIAMOND plot of the molecular structure of the cation **1Et**$^{+}$ in the crystal lattice of **1Et**[B(Ar^{F})$_4$] at 123(2) K. Thermal ellipsoids are set at 30 % propability. Hydrogen atoms were omitted for clarity. Selected bond lengths [Å], bond angles [°] and torsion angles [°]:Si1–Si2 2.1726(9), Si1–C1 1.912(2), Si2–C28 1.941(2), Si1–C56 1.893(2); C1-Si1-Si2 108.36(7), C1-Si1-C56 108.2(1), Si2-Si1-C56 143.36(9), C28-Si2-Si1 100.08(7); C1-Si1-Si2-C28 −178.16(9).

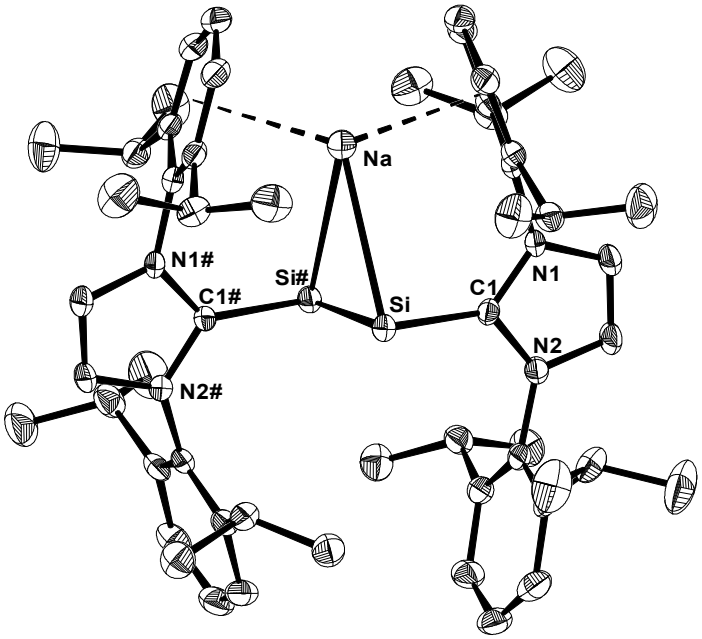

Figure S35. DIAMOND plot of the molecular structure of the cation **1Na**$^{+}$ in the crystal lattice of **1Na**[B(Ar^{F})$_4$] at 123(2) K. Thermal ellipsoids are set at 30 % propability. The hydrogen atoms were omitted for clarity. Selected bond lengths [Å], bond angles [°] and torsion angles: Si–Si# 2.248(2), Si–Na 3.096(3), Si–C1 1.948(4); Si#-Si-Na 68.71(3), Si-Na-Si# 42.58(5), C1-Si-Si# 95.4(1), C1-Si-Na 92.6(1); C1-Si-Si#-C1# 178.5(3).

5. Electronic structure calculations

Structure optimizations were performed without any symmetry restraints using the ORCA 3.0.0 programm package.[S11] The B97-D3[S12] functionals, including the conductor-like screening model (COSMO) for THF[S13] and RI-JCOSX approximations[S14] were employed in combination with the def2-TZVP basis set for the Si, N, Li and carbene C atoms as well as for the Si attached CH_3–group and Si-attached H-atom. The def2-SVP basis sets were used for all peripherical carbon and all other hydrogen atoms.[S15] This level of theory is abbreviated with B97-D3/**I**. The optimized geometries were verified as minima on the potential energy surface by two-sided numerical differentiation of the analytical gradients to obtain harmonic frequencies, which were also used to calculate the zero point vibrational energies (ZPVE). The thermodynamic energies and Gibbs energies at 298.15 K and 1 bar ($\Delta G°$) were calculated using standard procedures.[S16] NBO and NRT analyses were performed using NBO6.0.[S17] The cartesian coordinates of the solid state structures of **1**,[S1] **1H**[$B(Ar^F)_4$], **1Me**[$B(Ar^F)_4$] and **1Li**[$B(C_6F_5)_4$]·(n-C_6H_{14}) were used as a starting point for the structure optimizations.

In order to obtain a starting point for the localization of the transition state and the other minimum structure **(1H$^+$)'$_{calc}$** ("π-bonded isomer") of $[Si_2(H)(Idipp)_2]^+$, a relaxed potential energy surface scan of **1H$^+_{calc}$** was performed involving a decrease of the Si2–H distance from 345 to 125 pm in eleven steps. A similar relaxed potential energy surface scan was performed for **1Me$^+_{calc}$**, involving a decrease of the Si2–Me distance from 377 to 137 pm in twelve steps. Analyses of the harmonic frequencies at the energy maxima of these scans, with the aim to verify the correct trajectories of the selected vibrations for further transition state optimizations, revealed one imaginary frequency for $[Si_2(H)(Idipp)_2]^+$ and $[Si_2(Me)(Idipp)_2]^+$ at −440 cm^{-1} and –177 cm^{-1}, respectively. Both vibrations correspond to a rocking vibration of the H atom or the Me group interconverting the structures **1H$^+_{calc}$** and **1Me$^+_{calc}$** and the "π-bonded" isomers **(1H$^+$)'$_{calc}$** and **(1Me$^+$)'$_{calc}$**, respectively. Further geometrical transition state optimization at this point for $[Si_2(H)(Idipp)_2]^+$ led to a transition state **(1H$^+$)$^{TS}_{calc}$**, which shows one rocking vibration at ν = –505 cm^{-1}. In case of $[Si_2(Me)(Idipp)_2]^+$, the geometrical transition state optimization did not furnish the expected transition state **(1Me$^+$)$^{TS}_{calc}$**. Instead, the geometrical optimization of the energy maximum of $[Si_2(Me)(Idipp)_2]^+$ derived by the relaxed potential energy surface scan, which lies 97 kJ mol^{-1} above the minimum structure **1Me$^+_{calc}$**, led only to the minimum structures **1Me$^+_{calc}$** or **(1Me$^+$)'$_{calc}$**, suggesting a very flat progression of the potential energy surface upon the interconversion of **(1Me$^+$)'$_{calc}$** into **1Me$^+_{calc}$**.

5.1 Comparison of selected bonding parameters of 1H[B(Ar^F)$_4$], 1H$^+_{calc}$, (1H$^+$)$^{TS}_{calc}$, (1H$^+$)'$_{calc}$, 1Me$^+_{calc}$, (1Me$^+$)$^{TS}_{calc}$, (1Me$^+$)'$_{calc}$ and 1Li$^+_{calc}$

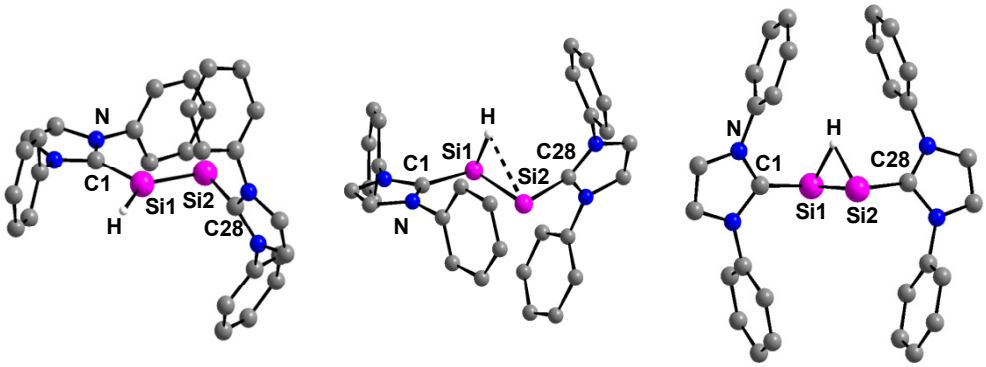

1H$^+_{calc}$, 0.0 kJ mol^{-1} **(1H$^+$)$^{TS}_{calc}$**, 42.9 kJ mol^{-1} **(1H$^+$)'$_{calc}$**, 30.5 kJ mol^{-1}

Figure S36. Calculated (B97-D3/**I**) structures of the "σ-isomer" of [Si$_2$(H)(Idipp)$_2$]$^+$ (**1H$^+_{calc}$**), the "π-isomer" **(1H$^+$)'$_{calc}$** and the transition state of the dynamic process (**(1H$^+$)$^{TS}_{calc}$**) with their corresponding relative Gibbs energies. The H atoms, except the Si1-bonded H-atom, are omitted for clarity. Atom numbering of the experimental structure was taken over in the calculated structure.

Table S4: Comparison of selected experimental bond lengths and angles of **1** and the cation **1H$^+$** in **1H**[B(Ar^F)$_4$] with the calculated (B97-D3/**I**) bond lengths and angles of **1$_{calc}$**, **1H$^+_{calc}$**, **(1H$^+$)$^{TS}_{calc}$** and **(1H$^+$)'$_{calc}$**. Atom numbering of the experimental structures was taken over in the calculated structures.

	Si1–Si2 [Å]	Si1–C1 [Å]	Si2–C28 [Å]	Si–H [Å]	C1-Si1-Si2 [°]	C1-Si1-H [°]	Si1-Si2-C28 [°]	H-Si1-Si2 [°]	φ_{NHC1}[a] [°]	φ_{NHC2}[a] [°]
1[b]	2.229(1)	1.927(2)	1.927(2)	–	93.37(5)	–	93.37(5)	–	87.11(5)	87.11(5)
1$_{calc}$	2.237	1.921	1.921	–	96.43	–	96.43	–	91.57	91.57
1H$^+$	2.1873(8)	1.882(2)	1.940(2)	1.32(2)	116.73(7)	106(1)	95.34(6)	138(1)	8.60(6)	71.06(6)
1H$^+_{calc}$	2.198	1.869	1.937	1.486	116.83	104.85	94.77	137.94	3.63	72.60
(1H$^+$)$^{TS}_{calc}$	2.326	1.964	1.933	1.544 2.404	101.35	96.62[c]	91.27	73.71[c]	14.93	81.33
(1H$^+$)'$_{calc}$	2.301	1.935	1.939	1.716 1.710	93.33	89.58[c]	92.34	47.70[c]	76.17	107.03

[a]: The dihedral angles φ_{NHC1} and φ_{NHC2} are the respective angles between the least-square plane of the atoms C1, Si1, Si2 and C28 and the respective NHC central ring planes. [b]: The structural parameters were obtained from ref. [S1]. [c] The corresponding angles C28-Si2-H and H-Si2-Si1 are 84.16° and 38.06° (**(1H$^+$)$^{TS}_{calc}$**) and 89.72° and 47.90° (**(1H$^+$)'$_{calc}$**).

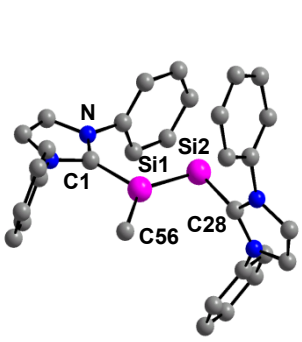

1Me$^{+}_{calc}$, 0.0 kJ mol^{-1}

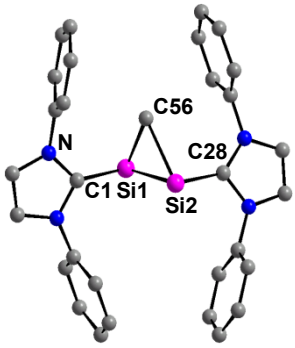

(1Me^{+})'$_{calc}$, 95.4 kJ mol^{-1}

Figure S37. Calculated (B97-D3/**I**) structures of the "σ-isomer" of $[Si_2(Me)(Idipp)_2]^+$ (**1Me$^{+}_{calc}$**) and the "π-isomer" **(1Me^{+})'$_{calc}$** with their corresponding relative Gibbs energies. The H atoms are omitted for clarity. Atom numbering of the experimental structure was taken over in the calculated structure.

Table S5: Comparison of selected experimental bond lengths and angles of the cation **1Me^{+}** in **1Me**[B(Ar^{F})$_4$] with the calculated (B97-D3/**I**) bond lengths and angles of **1Me$^{+}_{calc}$** and **(1Me^{+})'$_{calc}$**. Atom numbering of the experimental structures was taken over in the calculated structures.

	Si1–Si2 [Å]	Si1–C1 [Å]	Si2–C28 [Å]	Si–C56 [Å]	C1-Si1-Si2 [°]	C1-Si1-C56 [°]	Si1-Si2-C28 [°]	C56-Si1-Si2 [°]	φ_{NHC1}[a] [°]	φ_{NHC2}[a] [°]
1Me^{+}	2.1909(8)	1.901(2)	1.947(2)	1.885(2)	114.62(7)	111.3(1)	95.13(6)	133.71(8)	13.23(8)	79.11(7)
1Me$^{+}_{calc}$	2.198	1.883	1.937	1.891	114.76	110.39	95.11	134.54	7.83	80.31
(1Me^{+})'$_{calc}$	2.336	1.963	1.952	2.029 2.307	102.06	98.41[b]	100.21	51.81[b]	88.69	67.25

[a]: The dihedral angles φ_{NHC1} and φ_{NHC2} are the respective angles between the least-square plane of the atoms C1, Si1, Si2 and C28 and the respective NHC central ring planes. [b] The corresponding angles C28-Si2-C56 and C56-Si2-Si1 are 95.24° and 63.37°.

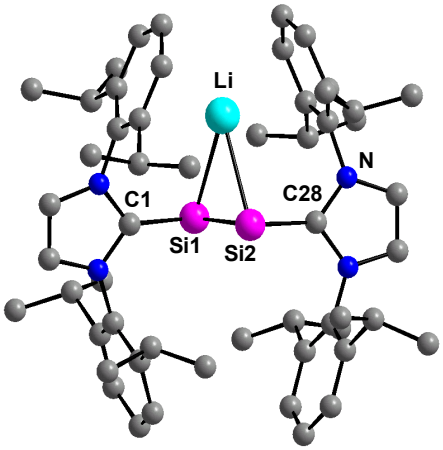

Figure S38. Calculated (B97-D3/**I**) structure of **1Li$^{+}_{calc}$**. The H atoms are omitted for clarity. Atom numbering of the experimental structure was taken over in the calculated structure.

Table S6: Comparison of selected experimental bond lengths and angles of the cation **1Li**$^+$ in **1Li**[$B(C_6F_5)_4$]·(*n*-C_6H_{14}) with the calculated (B97-D3/**I**) bond lengths and angles of **1Li**$^+_{calc}$. Atom numbering of the experimental structures was taken over in the calculated structures.

	Si1–Si2 [Å]	Si1–C1 [Å]	Si2–C28 [Å]	Si1–Li [Å]	C1-Si1-Si2 [°]	C1-Si1-Li [°]	Li-Si1-Si2 [°]	φ_{NHC1}[a]	φ_{NHC2}[a]
1Li$^+$	2.234(1)	1.941(3)	1.938(3)	2.822(6)	94.9(1)	95.9(2)	69.6(1)	79.0(1)	108.9(1)
1Li$^+_{calc}$	2.251	1.942	1.939	2.781	99.40	94.84	66.75	79.56	99.23
				Si2–Li [Å]	C28-Si2-Si1 [°]	C28-Si2-Li [°]	Li-Si2-Si1 [°]		
1Li$^+$				2.925(7)	98.7(1)	93.7(2)	64.7		
1Li$^+_{calc}$				2.804	98.25	94.56	65.71		

[a]: The dihedral angles φ_{NHC1} and φ_{NHC2} are the respective angles between the least-square plane of the atoms C1, Si1, Si2 and C28 and the respective NHC central ring planes.

5.2 Selected Kohn-Sham orbitals of the compounds $1H^+_{calc}$, $(1H^+)'_{calc}$, $1Me^+_{calc}$, $(1Me^+)'_{calc}$ and $1Li^+_{calc}$

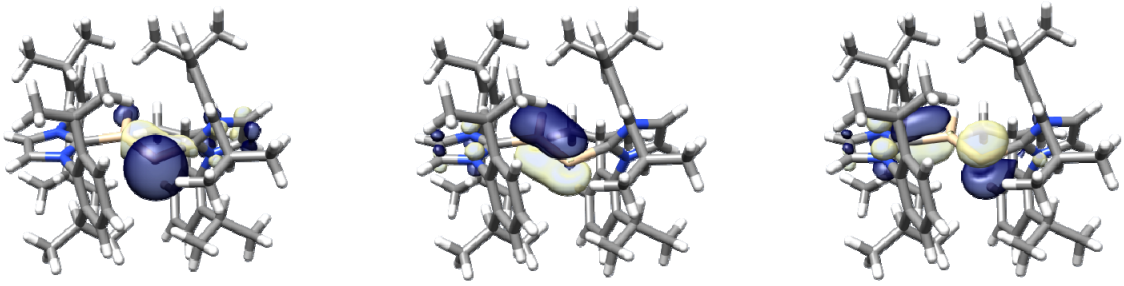

−5.34 eV
HOMO−1

−4.67 eV
HOMO

−2.83 eV
LUMO

Figure S39. Selected *Kohn-Sham* orbitals (B97-D3/**I**) of $\mathbf{1H^+_{calc}}$ and their corresponding energy eigenvalues; isosurface value: 0.05 e bohr^{-3}.

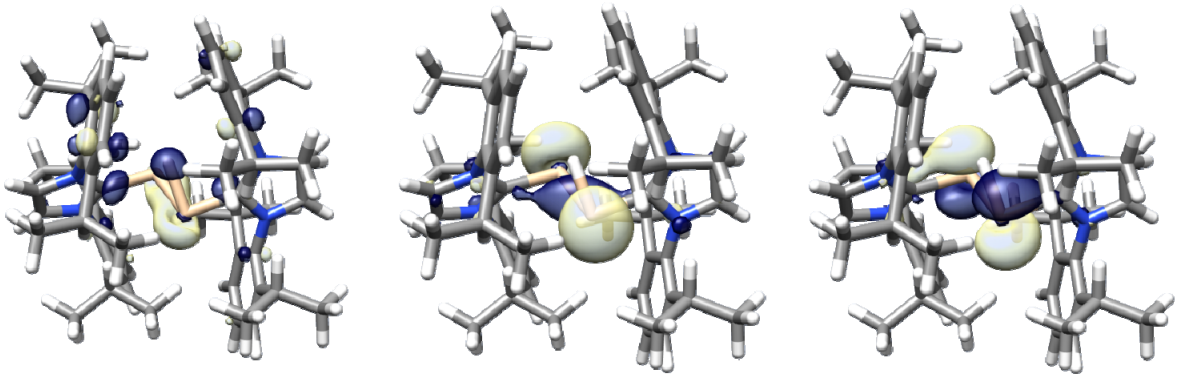

−6.27 eV
HOMO−1

−4.67 eV
HOMO

−2.71 eV
LUMO

Figure S40. Selected *Kohn-Sham* orbitals (B97-D3/**I**) of $\mathbf{(1H^+)'_{calc}}$ and their corresponding energy eigenvalues; isosurface value: 0.05 e bohr^{-3}.

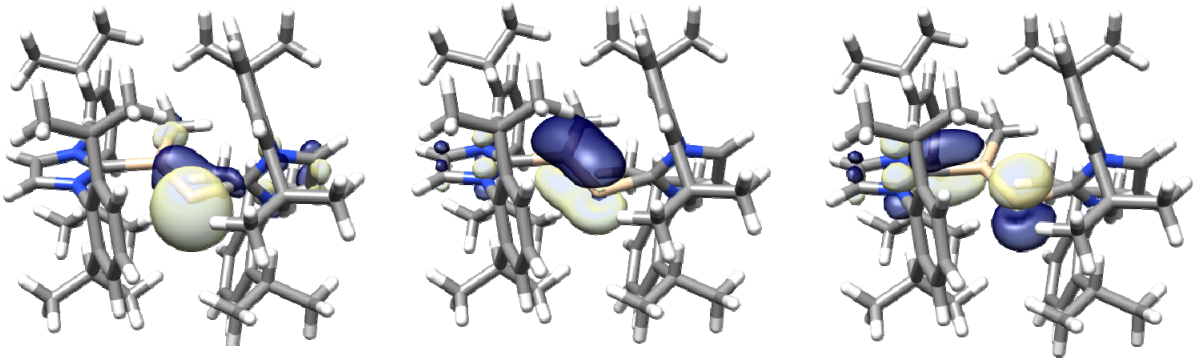

−5.14 eV
HOMO−1

−4.47 eV
HOMO

−2.66 eV
LUMO

Figure S41. Selected *Kohn-Sham* orbitals (B97-D3/**I**) of $\mathbf{1Me^+_{calc}}$ and their corresponding energy eigenvalues; isosurface value: 0.05 e bohr^{-3}.

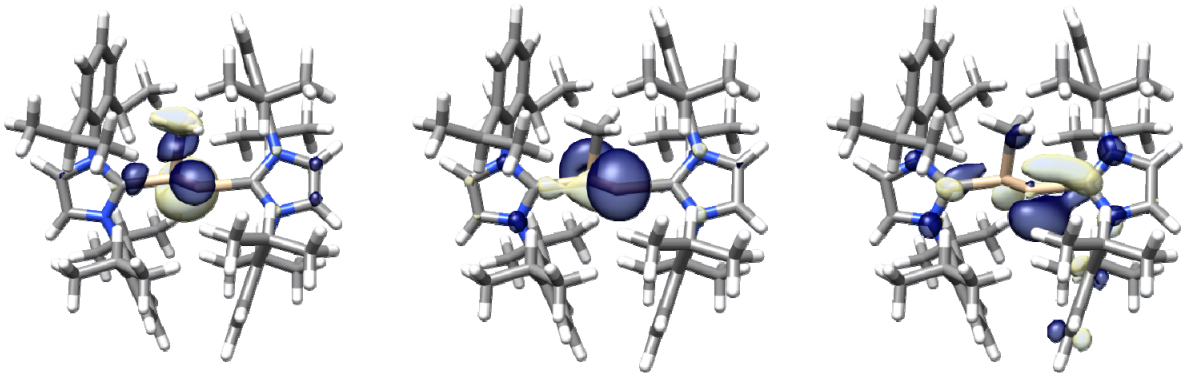

−5.73 eV
HOMO−1

−4.51 eV
HOMO

−2.30 eV
LUMO

Figure S42. Selected *Kohn-Sham* orbitals (B97-D3/**I**) of **(1Me$^+$)'$_{calc}$** and their corresponding energy eigenvalues; isosurface value: 0.05 e bohr^{-3}.

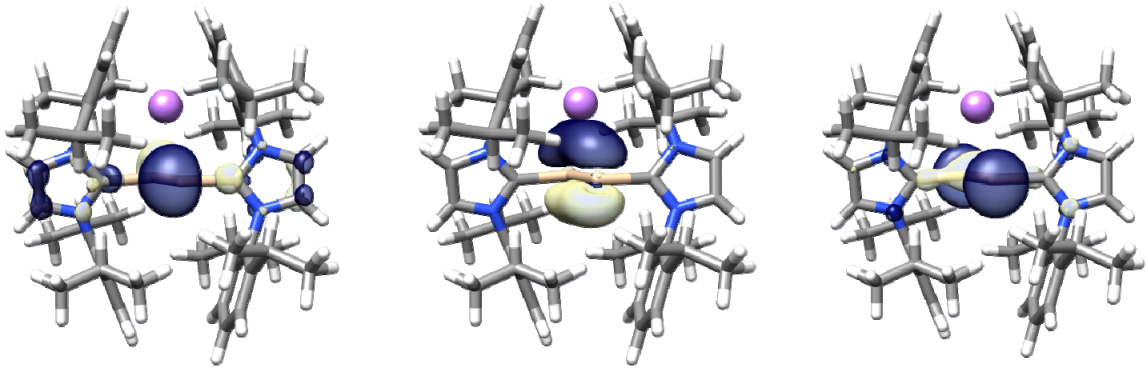

−5.93 eV
HOMO−2

−4.48 eV
HOMO−1

−3.94 eV
HOMO

Figure S43. Selected *Kohn-Sham* orbitals (B97-D3/**I**) of **1Li$^+$$_{calc}$** and their corresponding energy eigenvalues; isosurface value: 0.05 e bohr^{-3}.

5.3 Results of the natural bond orbital (NBO) and natural resonance theory analysis of $\mathbf{1}_{calc}$, $\mathbf{1H^+}_{calc}$, $\mathbf{(1H^+)^{TS}}_{calc}$, $\mathbf{(1H^+)'}_{calc}$, $\mathbf{1Me^+}_{calc}$, $\mathbf{(1Me^+)'}_{calc}$ and $\mathbf{1Li^+}_{calc}$

Table S7: Selected results of the natural bond orbital (NBO) and natural resonance theory (NRT) analyses of $\mathbf{1}_{calc}$ (B97-D3/**I**). Atom numbering of the experimental structure was taken over in the calculated structure (see Ref. [S1]).[a]

NBO analysis					NPA partial charges[b]		NRT analysis[c]	
	occ.	pol. [%]	hyb.	WBI				tot / cov / ionic
σ(Si–C1)	1.94	21.4 (Si) 78.6 (C1)	$sp^{8.04}$ (Si) $sp^{1.17}$ (C1)	0.86	C1 Σ(NHC)	0.06 0.10	Si1–C1	1.13 / 0.43 / 0.70
σ(Si#–C1#)	1.94	21.4 (Si#) 78.6 (C1#)	$sp^{8.04}$ (Si#) $sp^{1.17}$ (C1#)	0.86	C1# Σ(NHC)	0.06 0.10	Si#–C1#	1.13 / 0.43 / 0.70
σ(Si–Si#)	1.75	50.0 (Si) 50.0 (Si#)	$sp^{5.35}$ (Si) $sp^{5.35}$ (Si#)	1.70	Si	−0.10	Si–Si#	1.86 / 1.85 / 0.01
π(Si–Si#)	1.85	50.0 (Si) 50.0 (Si#)	p (Si) p (Si#)		Si#	−0.10		
n(Si)	1.82		$sp^{0.36}$					
n(Si#)	1.82		$sp^{0.36}$					

[a]: occ.: occupancy, pol.: polarization, hyb.: hybridization, WBI: Wiberg bond index, tot / cov / ionic: total bond order / covalent bord order / ionic bond order. [b]: Partial charges obtained by natural population analysis (NPA). [c]: A local NRT analysis was carried out including the Si, N, C1 and C1# atoms.

Table S8: Selected results of the natural bond orbital (NBO) and natural resonance theory (NRT) analyses of $\mathbf{1H^+}_{calc}$ (B97-D3/**I**). Atom numbering of the experimental structure was taken over in the calculated structure.[a]

NBO analysis					NPA partial charges[b]		NRT analysis[c]	
	occ.	pol. [%]	hyb.	WBI				tot / cov / ionic
σ(Si1–C1)	1.96	25.4 (Si1) 74.6 (C1)	$sp^{3.80}$ (Si1) $sp^{1.36}$ (C1)	0.89	C1 Σ(NHC)	0.03 0.33	Si1–C1	1.09 / 0.51 / 0.58
σ(Si2–C28)	1.94	20.5 (Si2) 79.5 (C28)	$sp^{9.71}$ (Si2) $sp^{1.27}$ (C28)	0.76	C28 Σ(NHC)	0.02 0.24	Si2–C28	1.09 / 0.41 / 0.68
σ(Si1–H1)	1.98	43.7 (Si1) 56.3 (H1)	$sp^{2.17}$ (Si1) s (H1)	0.91	H1	−0.14	Si1–H1	0.99 / 0.87 / 0.12
σ(Si1–Si2)	1.92	61.5 (Si1) 38.5 (Si2)	$sp^{1.10}$ (Si1) $sp^{6.32}$ (Si2)	1.61	Si1	0.31	Si1–Si2	1.85 / 1.44 / 0.41
π(Si1–Si2)	1.73	60.4 (Si1) 39.6 (Si2)	p (Si1) p (Si2)		Si2	0.26		
n(Si2)	1.84		$sp^{0.29}$					

[a]: occ.: occupancy, pol.: polarization, hyb.: hybridization, WBI: Wiberg bond index, tot / cov / ionic: total bond order / covalent bord order / ionic bond order. [b]: Partial charges obtained by natural population analysis (NPA). [c]: A local NRT analysis was carried out including the Si1, Si2, H1, N, C1 and C28 atoms.

Table S9: Selected results of the natural bond orbital (NBO) and natural resonance theory (NRT) analyses of **(1H$^+$)'$_{calc}$** (B97-D3/**I**). Atom numbering of the experimental structure was taken over in the calculated structure.[a]

NBO analysis					NPA partial charges[b]		NRT analysis[c]	
	occ.	pol. [%]	hyb.	WBI				tot / cov / ionic
σ(Si1–C1)	1.94	20.6 (Si1) 79.5 (C1)	$sp^{8.77}$ (Si) $sp^{1.26}$ (C1)	0.75	C1 Σ(NHC)	0.04 0.26	Si1–C1	1.06 / 0.40 / 0.66
σ(Si2–C28)	1.94	20.7 (Si2) 79.3 (C28)	$sp^{8.79}$ (Si2) $sp^{1.26}$ (C28)	0.75	C28 Σ(NHC)	0.04 0.26	Si2–C28	1.05 / 0.40 / 0.65
2e3c(Si1–H–Si2)	1.94	19.8 (Si1) 20.0 (Si2) 60.2 (H)	$sp^{26.66}$ (Si1) $sp^{29.49}$ (Si2) s (H)	0.45 0.46	H	−0.19	Si1–H Si2–H	0.46 / 0.20 / 0.25 0.46 / 0.21 / 0.26
σ(Si1–Si2)	1.77	50.0 (Si1) 50.0 (Si2)	$sp^{8.38}$ (Si1) $sp^{8.38}$ (Si2)	1.01	Si1 Si2	0.34 0.33	Si1–Si2	0.96 / 0.89 / 0.07
n(Si1)	1.87		$sp^{0.30}$					
n(Si2)	1.88		$sp^{0.31}$					

[a]: occ.: occupancy, pol.: polarization, hyb.: hybridization, WBI: Wiberg bond index, tot / cov / ionic: total bond order / covalent bord order / ionic bond order. [b]: Partial charges obtained by natural population analysis (NPA). [c]: A local NRT analysis was carried out including the Si1, Si2, H, N, C1 and C28 atoms.

Table S10: Selected results of the natural bond orbital (NBO) and natural resonance theory (NRT) analyses of **1Me$^+$$_{calc}$** (B97-D3/**I**). Atom numbering of the experimental structure was taken over in the calculated structure.[a]

NBO analysis					NPA partial charges[b]		NRT analysis[c]	
	occ.	pol. [%]	hyb.	WBI				tot / cov / ionic
σ(Si1–C1)	1.95	24.6 (Si1) 75.4 (C1)	$sp^{3.76}$ (Si1) $sp^{1.36}$ (C1)	0.86	C1 Σ(NHC)	0.01 0.30	Si1–C1	1.12 / 0.49 / 0.62
σ(Si2–C28)	1.94	20.6 (Si2) 79.4 (C28)	$sp^{9.65}$ (Si2) $sp^{1.24}$ (C28)	0.77	C28 Σ(NHC)	0.03 0.23	Si2–C28	1.10 / 0.41 / 0.69
σ(Si1–C56)	1.98	30.3 (Si1) 69.7 (C56)	$sp^{2.15}$ (Si1) $sp^{2.44}$ (C56)	0.84	C56 CH_3	−1.10 −0.38	Si1–C56	0.99 / 0.60 / 0.39
σ(Si1–Si2)	1.91	59.9 (Si1) 40.1 (Si2)	$sp^{1.10}$ (Si1) $sp^{5.94}$ (Si2)	1.62	Si1	0.65	Si1–Si2	1.84 / 1.51 / 0.33
π(Si1–Si2)	1.71	57.8 (Si1) 42.2 (Si2)	p (Si1) p (Si2)		Si2	0.20		
n(Si2)	1.82		$sp^{0.30}$					

[a]: occ.: occupancy, pol.: polarization, hyb.: hybridization, WBI: Wiberg bond index, tot / cov / ionic: total bond order / covalent bord order / ionic bond order. [b]: Partial charges obtained by natural population analysis (NPA). [c]: A local NRT analysis was carried out including the Si1, Si2, C56, N, C1 and C28 atoms.

Table S11: Selected results of the natural bond orbital (NBO) and natural resonance theory (NRT) analyses of **(1Me$^+$)'$_{calc}$** (B97-D3/**I**). Atom numbering of the experimental structure was taken over in the calculated structure.[a]

NBO analysis					NPA partial charges[b]		NRT analysis[c]	
	occ.	pol. [%]	hyb.	WBI				tot / cov / ionic
σ(Si1–C1)	1.94	22.3 (Si1) 77.7 (C1)	sp$^{8.66}$ (Si1) sp$^{1.25}$ (C1)	0.81	C1 Σ(NHC)	0.09 0.28	Si1–C1	1.11 / 0.44 / 0.67
σ(Si2–C28)	1.95	21.3 (Si2) 78.7 (C28)	sp$^{8.29}$ (Si2) sp$^{1.27}$ (C28)	0.77	C28 Σ(NHC)	0.04 0.25	Si2–C28	1.09 / 0.42 / 0.67
σ(Si1–C56)	1.84	23.6 (Si1) 76.4 (C56)	sp$^{10.06}$ (Si1) sp$^{2.29}$ (C56)	0.66	C56 CH_3	−1.12 −0.37	Si1–C56	0.92 / 0.44 / 0.49
σ(Si1–Si2)	1.78	49.6 (Si1) 50.4 (Si2)	sp$^{10.08}$ (Si1) sp$^{9.79}$ (Si2)	0.90	Si1 Si2	0.35 0.49	Si1–Si2	0.90 / 0.87 / 0.03
n(Si1)	1.82		sp$^{0.39}$					
n(Si2)	1.87		sp$^{0.28}$					
LV[d](Si2)	0.26		sp$^{44.91}$					

[a]: occ.: occupancy, pol.: polarization, hyb.: hybridization, WBI: Wiberg bond index, tot / cov / ionic: total bond order / covalent bord order / ionic bond order. [b]: Partial charges obtained by natural population analysis (NPA). [c]: A local NRT analysis was carried out including the Si1, Si2, C56, N, C1 and C28 atoms. [d]: LV = lone vacancy.

Table S12: Selected results of the natural bond orbital (NBO) and natural resonance theory (NRT) analyses of **1Li$^+$$_{calc}$** (B97-D3/**I**). Atom numbering of the experimental structure was taken over in the calculated structure.[a]

NBO analysis					NPA partial charges[b]		NRT analysis[c]	
	occ.	pol. [%]	hyb.	WBI				tot / cov / ionic
σ(Si1–C1)	1.94	21.6 (Si1) 78.4 (C1)	sp$^{8.71}$ (Si1) sp$^{1.20}$ (C1)	0.84	C1 Σ(NHC)	0.06 0.19	Si1–C1	1.12 / 0.43 / 0.69
σ(Si2–C28)	1.94	21.7 (Si2) 78.3 (C28)	sp$^{8.59}$ (Si2) sp$^{1.20}$ (C28)	0.84	C28 Σ(NHC)	0.06 0.19	Si2–C28	1.12 / 0.43 / 0.69
σ(Si1–Si2)	1.77	50.0 (Si1) 50.0 (Si2)	sp$^{6.33}$ (Si1) sp$^{6.45}$ (Si2)	1.75	Si1	−0.12	Si1–Si2	1.88 / 1.87 / 0.01
π(Si1–Si2)	1.89	50.2 (Si1) 49.8 (Si2)	p (Si1) p (Si2)		Si2	−0.11		
LV[d](Li)	0.13		s		Li	0.85		
n(Si1)	1.79		sp$^{0.32}$					
n(Si2)	1.79		sp$^{0.32}$					

[a]: occ.: occupancy, pol.: polarization, hyb.: hybridization, WBI: Wiberg bond index, tot / cov / ionic: total bond order / covalent bord order / ionic bond order. [b]: Partial charges obtained by natural population analysis (NPA). [c]: A local NRT analysis was carried out including the Si1, Si2, Li, N, C1 and C28 atoms. [d]: LV = lone vacancy.

Table S13: Selected results of the second order pertubation theory analysis of the Fock matrix in the NBO basis of **1Li$_{calc}^{+}$** (B97-D3/**I**). Atom numbering of the experimental structure was taken over in the calculated structure.[a]

Donor NBO	Acceptor NBO	Interaction energy [kcal/mol]
n(Si1)	LV Li	69.8
n(Si2)	LV Li	68.6
σ(Si1–C1)	LV Li	17.6
σ(Si2–C2)	LV Li	17.6
π(Si1–Si2)	LV Li	23.8
σ(C4–C5)	LV Li	11.3
σ(C5–C6)	LV Li	10.5
σ(C6–C7)	LV Li	7.53
σ(C7–C8)	LV Li	7.95
σ(C8–C9)	LV Li	10.9
σ(C4–C9)	LV Li	12.1
σ(C43–C44)	LV Li	12.1
σ(C44–C45)	LV Li	10.9
σ(C45–C46)	LV Li	7.95
σ(C46–C47)	LV Li	7.53
σ(C47–C48)	LV Li	10.5
σ(C43–C48)	LV Li	11.3

[a]: LV = lone vacancy.

Table S14: Major resonance structures **1$_{calc}$** and their percentage contribution to the resonance hybrid according to NRT theory (four other structures with percentage contributions <6.5 % were found, which are not depicted); R = dipp.

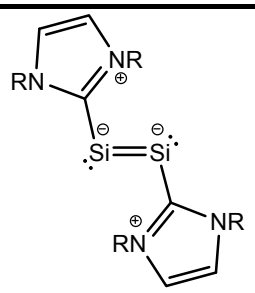	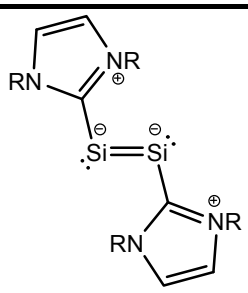	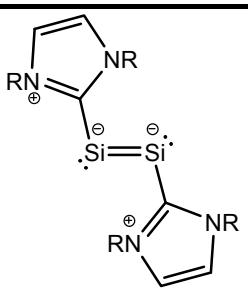
28.0 %	22.0 %	21.7 %

Table S15: Major resonance structures **1H$^{+}_{calc}$** and their percentage contribution to the resonance hybrid according to NRT theory (three other structures with percentage contributions <9.5 % were found, which are not depicted); R = dipp.

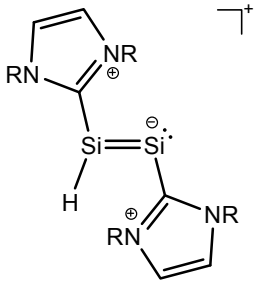	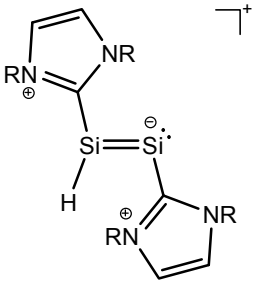	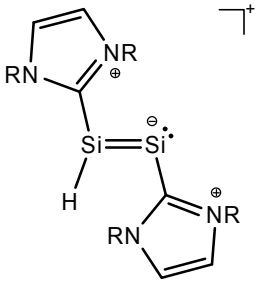
30.2 %	24.4 %	24.1 %

Table S16: Major resonance structures **(1H$^+$)'$_{calc}$** and their percentage contribution to the resonance hybrid according to NRT theory (nine other structures with percentage contributions <3.9 % were found, which are not depicted); R = dipp.

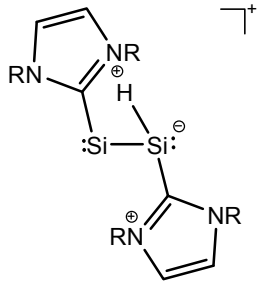	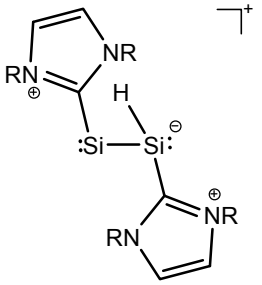	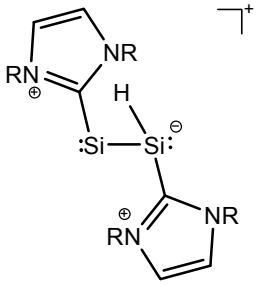
11.8 %	11.8 %	11.4 %
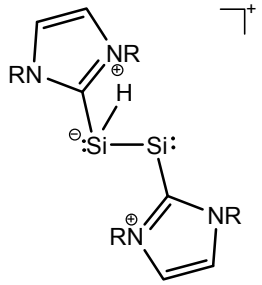	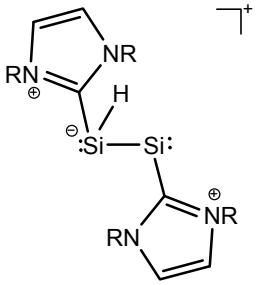	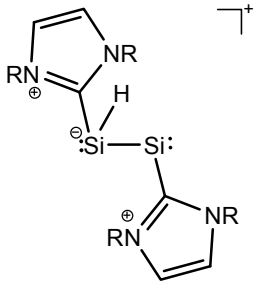
11.8 %	11.8 %	11.2 %

Table S17: Major resonance structures **1Me$^+$$_{calc}$** and their percentage contribution to the resonance hybrid according to NRT theory (three other structures with percentage contributions <12.1 % were found, which are not depicted); R = dipp.

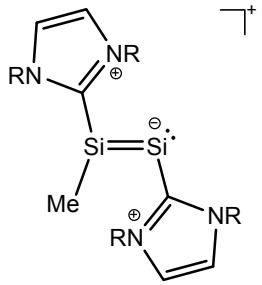	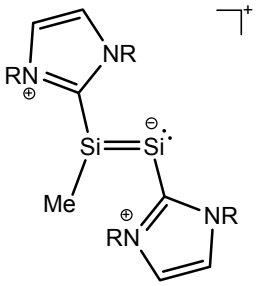	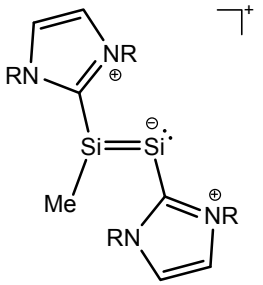
27.3 %	23.4 %	23.2 %

Table S18: Major resonance structures **(1Me$^+$)'$_{calc}$** and their percentage contribution to the resonance hybrid according to NRT theory (seven other structures with percentage contributions <6.5 % were found, which are not depicted); R = dipp.

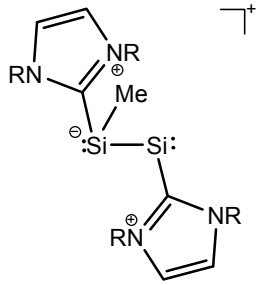	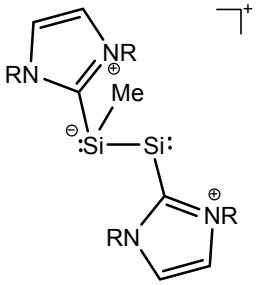	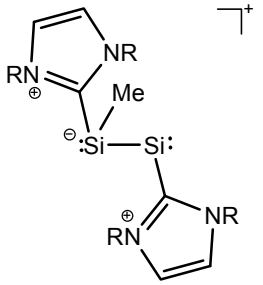
24.7 %	22.3 %	22.0 %

Table S19: Major resonance structures **1Li$^+$$_{calc}$** and their percentage contribution to the resonance hybrid according to NRT theory (four other structures with percentage contributions <7.4 % were found, which are not depicted); R = dipp.

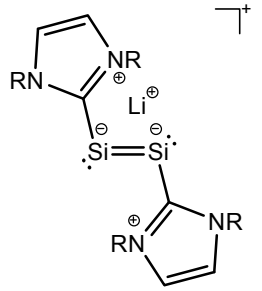	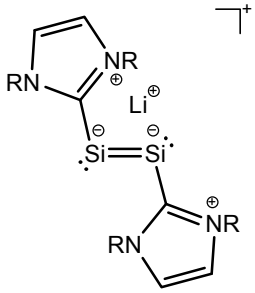	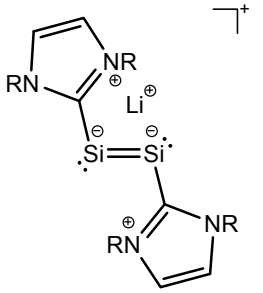
23.1 %	22.4 %	21.4 %

5.4 Cartesian coordinates [Å] and SCF energies of the calculated structures of $\mathbf{1}_{calc}$, $\mathbf{1H^+}_{calc}$, $\mathbf{(1H^+)^{TS}}_{calc}$, $\mathbf{(1H^+)'}_{calc}$, $\mathbf{1Me^+}_{calc}$, $\mathbf{(1Me^+)'}_{calc}$ and $\mathbf{1Li^+}_{calc}$

$\mathbf{1}_{calc}$
Energy: –2896.370660910749 E_H

C	1.705477	0.143220	1.578496
C	-1.705529	-0.143214	-1.578528
C	0.266471	1.427300	4.289666
C	-0.266530	-1.427441	-4.289156
C	0.591062	0.838589	-3.803475
C	-0.590995	-0.838657	3.803487
C	-0.390912	-2.202813	3.169696
C	0.390922	2.202946	-3.170098
C	0.776197	3.763965	3.465220
C	-0.777189	-3.765097	-3.467552
C	0.388351	0.163979	3.686472
C	-0.388427	-0.163884	-3.686393
C	1.700028	2.871786	-2.749533
C	-1.700134	-2.871859	2.749820
C	0.417151	-3.120863	4.105371
C	-0.416368	3.120956	-4.106489
C	0.886801	-1.675659	-5.042474
C	-0.886677	1.675123	5.043394
C	1.331235	2.502019	4.143491
C	-1.331819	-2.501688	-4.143321
C	1.730742	0.534139	-4.553777
C	-1.730496	-0.534571	4.554192
C	1.983643	2.821749	5.498311
C	-1.986020	-2.818812	-5.497899
C	1.876528	-0.707374	-5.169406
C	-1.876277	0.706721	5.170254
C	2.799543	-0.463800	3.493788
C	-2.799548	0.464442	-3.493643
C	2.622425	-2.825051	-1.956415
C	-2.622253	2.824313	1.957647
C	3.153292	-2.171665	-0.678944
C	-3.152984	2.171326	0.679907
C	3.714521	-0.457359	2.492210
C	-3.714508	0.457840	-2.492047
C	3.416543	3.777172	0.543514
C	-3.416022	-3.777068	-0.544765
C	3.690509	0.198485	0.082799
C	-3.690357	-0.198580	-0.082689
C	3.741949	-0.792419	-0.913649
C	-3.741698	0.792005	0.914124
C	4.189437	2.534792	1.010905
C	-4.189209	-2.534606	-1.011419
C	4.179108	-3.085696	0.017090
C	-4.178685	3.085655	-0.015924
C	4.261132	1.473173	-0.074568
C	-4.260811	-1.473359	0.074420
C	4.390390	-0.464369	-2.108113
C	-4.389826	0.463473	2.108621
C	4.910271	1.745535	-1.284394
C	-4.909571	-1.746229	1.284321
C	4.970625	0.788977	-2.291440
C	-4.969818	-0.790003	2.291694
C	5.592035	2.895743	1.526970
C	-5.591894	-2.895472	-1.527319
H	-0.384446	-3.520894	-2.476567
H	0.385142	3.517992	2.473992
H	-0.131929	-3.301014	5.037361
H	0.133312	3.300771	-5.038190

H	1.482151	3.784488	-2.186357
H	-1.482434	-3.784420	2.186352
H	0.026101	-4.215674	-4.061685
H	-0.028530	4.214275	4.057576
H	1.254928	3.248015	6.197536
H	-1.258468	-3.244622	-6.198607
H	1.570009	4.510749	3.348837
H	-1.571713	-4.511089	-3.351030
H	0.188924	-2.048045	2.252981
H	-0.189550	2.048499	-2.253724
H	0.598592	-4.088612	3.623524
H	-0.597908	4.088856	-3.624978
H	2.281828	2.209296	-2.105745
H	-2.282461	-2.209359	2.106526
H	1.015567	-2.644198	-5.517271
H	-1.015427	2.643512	5.518508
H	2.314302	3.154822	-3.613184
H	-2.313820	-3.155181	3.613806
H	1.387420	-2.685391	4.362463
H	-1.386560	2.685600	-4.364071
H	2.115218	2.110149	3.490463
H	-2.114793	-2.110178	-3.488897
H	2.520364	1.272096	-4.648999
H	-2.520010	-1.272648	4.649395
H	2.400203	1.918589	5.957911
H	-2.402365	-1.914595	-5.955602
H	2.794476	3.547955	5.368763
H	-2.797363	-3.544480	-5.368538
H	1.917941	-2.162465	-2.463153
H	-1.917938	2.161520	2.464356
H	2.094420	-3.749833	-1.703161
H	-2.094108	3.749105	1.704720
H	2.774359	-0.923028	-5.743964
H	-2.774009	0.922107	5.745067
H	2.293184	-2.045146	-0.011696
H	-2.292804	2.044977	0.012731
H	2.393376	3.503379	0.269634
H	-2.392718	-3.503317	-0.271345
H	2.896204	-0.682056	4.544865
H	-2.896208	0.683082	-4.544638
H	3.630820	2.117807	1.852831
H	-3.630815	-2.117204	-1.853305
H	3.370704	4.518275	1.349948
H	-3.370583	-4.517924	-1.351451
H	3.428705	-3.083536	-2.653426
H	-3.428621	3.082691	2.654604
H	3.739109	-4.070066	0.214262
H	-3.738608	4.070067	-0.212711
H	3.897393	4.246690	-0.321664
H	-3.896343	-4.246922	0.320518
H	4.510871	-2.667882	0.972172
H	-4.510370	2.668200	-0.971179
H	4.771572	-0.667752	2.491238
H	-4.771523	0.668404	-2.491039
H	4.433844	-1.194299	-2.909569
H	-4.433159	1.193126	2.910336
H	5.061633	-3.225356	-0.618316
H	-5.061257	3.225149	0.619453
H	5.520787	3.616136	2.350383
H	-5.520838	-3.615934	-2.350690
H	5.356906	2.722985	-1.442335
H	-5.355951	-2.723819	1.442099
H	6.119241	2.007034	1.891322
H	-6.119035	-2.006730	-1.891684
H	5.465590	1.022342	-3.231036
H	-5.464480	-1.023758	3.231352
H	6.203113	3.346230	0.736302

H	-6.202934	-3.345795	-0.736537
N	1.579930	-0.106251	2.928601
N	-1.579950	0.106654	-2.928577
N	3.039927	-0.095315	1.330616
N	-3.039909	0.095546	-1.330515
Si	0.407702	0.953825	0.417520
Si	-0.407762	-0.954021	-0.417936

$1H^{+}_{calc}$
Energy: −2896.874950699624 E_H

C	-0.580482	2.372023	0.063114
C	0.691950	-2.272819	0.166759
C	1.901909	-4.087977	0.797549
C	-1.096895	4.579222	-0.017755
C	-2.257284	3.891260	0.213507
C	2.146637	-3.869774	-0.531633
H	2.275566	-4.839764	1.488299
H	-0.900836	5.640373	-0.149472
H	-3.283732	4.225102	0.341734
H	2.765462	-4.403350	-1.248071
N	1.008029	-3.102609	1.199620
N	-0.081364	3.635251	-0.105664
N	-1.922158	2.545949	0.257634
N	1.402287	-2.751650	-0.894993
Si	0.356724	0.754851	0.049294
Si	-0.838339	-1.085832	0.180007
H	1.789862	1.144834	0.089071
C	1.245855	-2.235520	-2.232155
C	0.136166	-2.690992	-2.979295
C	2.170495	-1.278885	-2.709805
C	-0.044389	-2.137918	-4.261056
C	1.950610	-0.772058	-4.003124
C	0.851103	-1.188206	-4.765615
H	-0.894981	-2.458539	-4.871909
H	2.640729	-0.030398	-4.415850
H	0.692353	-0.765863	-5.764315
C	0.429144	-2.970098	2.513043
C	-0.804766	-3.611560	2.767762
C	1.116065	-2.194738	3.472217
C	-1.342466	-3.472761	4.060479
C	0.540067	-2.097850	4.751867
C	-0.674789	-2.730856	5.042578
H	-2.296232	-3.953577	4.302483
H	1.044672	-1.515381	5.529671
H	-1.111696	-2.636475	6.043670
C	1.267352	3.916324	-0.532638
C	2.277863	4.064352	0.444420
C	1.505311	4.004643	-1.921905
C	3.580746	4.320587	-0.019268
C	2.828167	4.262358	-2.330877
C	3.852039	4.419223	-1.391250
H	4.397929	4.443310	0.697975
H	3.058389	4.334372	-3.399622
H	4.875685	4.616736	-1.729514
C	-2.865349	1.465400	0.378616
C	-3.431230	0.948287	-0.809180
C	-3.141862	0.950750	1.664617
C	-4.357705	-0.101894	-0.670070
C	-4.080439	-0.093511	1.746630
C	-4.683917	-0.609981	0.592984
H	-4.823579	-0.531555	-1.562673
H	-4.331699	-0.517510	2.723890
H	-5.405779	-1.430171	0.679664
C	0.400601	3.808198	-2.954842
H	-0.560729	3.746519	-2.417659

C	1.953360	3.977919	1.931881
H	1.130537	3.247612	2.045681
C	-3.084901	1.508315	-2.184309
H	-2.227437	2.191077	-2.063442
C	-2.465668	1.508735	2.910862
H	-1.593305	2.097758	2.577980
C	-0.795825	-3.783679	-2.464845
H	-0.571537	-3.945909	-1.397517
C	3.378203	-0.851371	-1.881797
H	3.115548	-0.991107	-0.816753
C	-1.514641	-4.449586	1.711426
H	-1.032223	-4.243305	0.740643
C	2.442942	-1.520153	3.152091
H	2.566209	-1.526352	2.054655
C	-2.281771	-3.399747	-2.549642
H	-2.904624	-4.203672	-2.118419
H	-2.480828	-2.476239	-1.979889
H	-2.609086	-3.244339	-3.592762
C	-0.502771	-5.110594	-3.193526
H	-1.128516	-5.924723	-2.784373
H	-0.718406	-5.023224	-4.273914
H	0.557558	-5.400512	-3.082035
C	-2.997694	-4.069996	1.562168
H	-3.106574	-2.989697	1.363745
H	-3.446835	-4.621227	0.716637
H	-3.579446	-4.318280	2.468238
C	-1.330929	-5.952028	1.999308
H	-1.797227	-6.228144	2.962705
H	-1.802337	-6.559137	1.205712
H	-0.260996	-6.221396	2.051903
C	4.587140	-1.760833	-2.187873
H	4.887775	-1.655110	-3.246275
H	5.448729	-1.482831	-1.554975
H	4.360479	-2.825204	-2.008639
C	3.756617	0.625815	-2.070995
H	2.893730	1.292078	-1.917047
H	4.535770	0.912074	-1.343629
H	4.161229	0.818702	-3.080617
C	3.613713	-2.321674	3.754574
H	4.581170	-1.860824	3.483210
H	3.542893	-2.349478	4.857478
H	3.615444	-3.363690	3.389275
C	2.472298	-0.049226	3.594634
H	3.408740	0.425639	3.255637
H	1.625968	0.508413	3.157158
H	2.428919	0.054839	4.693525
C	-1.930082	0.397590	3.827560
H	-1.279482	-0.294697	3.267507
H	-1.336369	0.832974	4.651198
H	-2.745157	-0.190674	4.284109
C	-3.413361	2.467892	3.657214
H	-4.317489	1.934933	4.003918
H	-2.911839	2.900212	4.541871
H	-3.741118	3.298720	3.006738
C	-4.256976	2.336913	-2.744336
H	-3.986344	2.778594	-3.720285
H	-5.151506	1.705474	-2.892767
H	-4.533280	3.157980	-2.059024
C	-2.633605	0.412336	-3.164446
H	-2.338281	0.862406	-4.128263
H	-1.762485	-0.133100	-2.764603
H	-3.436924	-0.317036	-3.370150
C	3.130643	3.474848	2.779175
H	2.792107	3.260694	3.807113
H	3.558589	2.549165	2.360352
H	3.936137	4.228078	2.847665
C	1.442856	5.337018	2.458056

H	1.176393	5.259984	3.527510
H	2.226662	6.109192	2.351655
H	0.550879	5.682313	1.908620
C	0.578907	2.479158	-3.711150
H	0.552964	1.618226	-3.022158
H	-0.231630	2.342257	-4.448739
H	1.541368	2.452266	-4.250844
C	0.301765	5.005504	-3.916872
H	1.204093	5.094370	-4.548599
H	-0.565840	4.883292	-4.590077
H	0.179065	5.954711	-3.364746

$(1H^{+})^{TS}_{calc}$
Energy: −2896.856169506304 E_H

C	-0.533414	2.360824	0.141905
C	0.670682	-2.216800	0.046708
C	1.907839	-4.027839	0.624051
C	-1.099039	4.562307	0.128390
C	-2.234835	3.845569	0.394614
C	2.097318	-3.811680	-0.713109
H	2.305852	-4.782471	1.297653
H	-0.927773	5.629668	0.012436
H	-3.262633	4.155011	0.567361
H	2.687829	-4.344500	-1.453733
N	1.030134	-3.040014	1.068674
N	-0.078577	3.636944	-0.021617
N	-1.865177	2.508459	0.390828
N	1.342179	-2.691241	-1.042879
Si	0.703014	0.840104	0.018481
Si	-0.780303	-0.947750	-0.099175
H	0.513475	0.338577	1.466630
C	1.123507	-2.142576	-2.358499
C	-0.052135	-2.536500	-3.043551
C	2.053160	-1.208134	-2.873639
C	-0.298468	-1.931782	-4.291171
C	1.763051	-0.651504	-4.131685
C	0.595688	-0.997305	-4.825031
H	-1.195812	-2.204032	-4.855933
H	2.454366	0.073526	-4.571492
H	0.384936	-0.536221	-5.796470
C	0.488371	-2.962001	2.402274
C	-0.739317	-3.617263	2.655980
C	1.222085	-2.272933	3.393668
C	-1.227329	-3.575513	3.975335
C	0.698909	-2.281340	4.699747
C	-0.511029	-2.925103	4.987126
H	-2.175495	-4.067858	4.216353
H	1.240360	-1.769901	5.501756
H	-0.905194	-2.910730	6.010153
C	1.265145	3.971416	-0.436126
C	2.273286	4.099418	0.546749
C	1.490874	4.151860	-1.817627
C	3.563432	4.426891	0.093771
C	2.802459	4.473648	-2.215753
C	3.825040	4.611305	-1.271326
H	4.380097	4.535428	0.813880
H	3.025230	4.611001	-3.279470
H	4.839762	4.863071	-1.600713
C	-2.807999	1.425643	0.496580
C	-3.475461	1.021656	-0.679815
C	-2.994474	0.810289	1.753965
C	-4.398909	-0.034524	-0.558612
C	-3.932595	-0.235655	1.819574
C	-4.630787	-0.648985	0.676771
H	-4.933209	-0.387599	-1.446687

H	-4.111867	-0.739466	2.774056
H	-5.350588	-1.472083	0.748800
C	0.391846	3.947425	-2.855525
H	-0.574620	3.902945	-2.325057
C	1.962102	3.907898	2.027376
H	1.174315	3.134424	2.095931
C	-3.210167	1.665749	-2.036626
H	-2.434462	2.438827	-1.905544
C	-2.228114	1.276556	2.984361
H	-1.332709	1.813231	2.627009
C	-0.958344	-3.648237	-2.522394
H	-0.742214	-3.785341	-1.449969
C	3.344156	-0.871089	-2.135153
H	3.173227	-1.071115	-1.061878
C	-1.478168	-4.396216	1.574407
H	-1.026271	-4.130106	0.604303
C	2.544095	-1.584814	3.078970
H	2.597819	-1.447204	1.984763
C	-2.455091	-3.321717	-2.630773
H	-3.050537	-4.132985	-2.175886
H	-2.691361	-2.388444	-2.091202
H	-2.782556	-3.217112	-3.680189
C	-0.610214	-4.973271	-3.231369
H	-1.216333	-5.802258	-2.822490
H	-0.811850	-4.902360	-4.315856
H	0.456565	-5.229334	-3.101268
C	-2.964196	-4.015753	1.486523
H	-3.078050	-2.930618	1.326413
H	-3.440263	-4.537180	0.637043
H	-3.517637	-4.296254	2.401040
C	-1.279851	-5.911549	1.769079
H	-1.726114	-6.250377	2.721814
H	-1.762763	-6.472109	0.948506
H	-0.207533	-6.176150	1.783934
C	4.479133	-1.800744	-2.615708
H	4.698000	-1.620939	-3.684131
H	5.402261	-1.613459	-2.038216
H	4.215602	-2.866674	-2.503819
C	3.757052	0.603821	-2.256732
H	2.956735	1.271277	-1.898008
H	4.650632	0.791052	-1.635923
H	4.014303	0.879066	-3.294813
C	3.731849	-2.473554	3.500660
H	4.689843	-1.995344	3.225894
H	3.729209	-2.634058	4.594475
H	3.692222	-3.462761	3.014637
C	2.643917	-0.187781	3.710494
H	3.561876	0.315692	3.361576
H	1.781766	0.438004	3.423160
H	2.690715	-0.235839	4.812868
C	-1.731147	0.109153	3.847747
H	-1.154343	-0.614894	3.249346
H	-1.070999	0.483536	4.649756
H	-2.560292	-0.435256	4.331806
C	-3.072669	2.275524	3.800287
H	-3.993588	1.794023	4.176410
H	-2.500185	2.647120	4.669357
H	-3.373517	3.144472	3.188602
C	-4.468903	2.376038	-2.569409
H	-4.252309	2.875443	-3.530980
H	-5.290928	1.657968	-2.738777
H	-4.828180	3.140654	-1.857240
C	-2.655829	0.646173	-3.047853
H	-2.425478	1.139805	-4.007830
H	-1.726110	0.180633	-2.679015
H	-3.382028	-0.160441	-3.249057
C	3.161807	3.396998	2.837780

H	2.838223	3.122359	3.856190
H	3.608629	2.504505	2.368693
H	3.946737	4.167930	2.939873
C	1.399849	5.208301	2.641075
H	1.137822	5.051215	3.702803
H	2.152981	6.015692	2.586284
H	0.494551	5.553446	2.114058
C	0.576339	2.598463	-3.575461
H	0.569950	1.756860	-2.862311
H	-0.233593	2.430659	-4.307127
H	1.539026	2.567167	-4.114609
C	0.302853	5.116390	-3.851250
H	1.201120	5.175991	-4.491940
H	-0.569533	4.983299	-4.516089
H	0.193378	6.083375	-3.327984

$(1H^{+})'_{calc}$
Energy: −2896.864484796281 E_H

C	-0.710611	2.161795	0.351007
C	0.717026	-2.145052	-0.403663
C	1.611550	-4.074770	0.385968
C	-1.336005	4.283930	-0.157805
C	-2.360951	3.706856	0.538112
C	2.212402	-3.805459	-0.811112
H	1.742892	-4.889337	1.093102
H	-1.216454	5.276170	-0.584563
H	-3.328913	4.089470	0.847639
H	2.977727	-4.333096	-1.374339
N	0.699259	-3.046232	0.619222
N	-0.339751	3.320123	-0.259793
N	-1.959667	2.406456	0.838562
N	1.649370	-2.622657	-1.273330
Si	0.549190	0.727388	0.664682
Si	-0.432062	-0.659839	-0.886364
H	-0.754992	-0.382030	0.769649
C	2.032820	-1.932279	-2.477380
C	1.372690	-2.261017	-3.682088
C	3.065732	-0.969598	-2.387561
C	1.812452	-1.609768	-4.850061
C	3.457782	-0.341325	-3.583445
C	2.845918	-0.666904	-4.801359
H	1.332743	-1.836929	-5.807923
H	4.254110	0.410288	-3.562914
H	3.168556	-0.166788	-5.721423
C	-0.096954	-2.933699	1.816452
C	-1.468905	-3.276226	1.748211
C	0.544364	-2.509765	3.001849
C	-2.211347	-3.174652	2.937350
C	-0.243825	-2.450001	4.167753
C	-1.604784	-2.770999	4.134153
H	-3.276457	-3.419180	2.933478
H	0.215647	-2.146162	5.113819
H	-2.202674	-2.704242	5.050575
C	0.917091	3.491535	-0.942507
C	2.006641	4.025338	-0.218593
C	0.985624	3.132538	-2.309027
C	3.200331	4.246057	-0.931076
C	2.204511	3.367379	-2.970148
C	3.293713	3.930290	-2.291516
H	4.070245	4.661186	-0.410954
H	2.303191	3.108801	-4.029208
H	4.233345	4.109357	-2.827266
C	-2.769866	1.446143	1.545674
C	-3.795353	0.785829	0.832891
C	-2.504070	1.226183	2.917528

C	-4.600259	-0.113308	1.558018
C	-3.319983	0.295414	3.584656
C	-4.360833	-0.360298	2.914354
H	-5.422077	-0.629266	1.051474
H	-3.142634	0.081889	4.642032
H	-4.988616	-1.077343	3.455764
C	-0.222331	2.566740	-3.045428
H	-0.924857	2.186277	-2.283594
C	1.902693	4.367685	1.262824
H	0.931996	3.990961	1.629578
C	-4.064173	1.063909	-0.643195
H	-3.172414	1.567615	-1.056235
C	-1.415354	2.006845	3.648564
H	-0.606281	2.203293	2.922504
C	0.243131	-3.282711	-3.731395
H	0.004178	-3.572005	-2.693206
C	3.766149	-0.671036	-1.067054
H	3.111038	-1.024912	-0.252746
C	-2.094030	-3.783720	0.450544
H	-1.642291	-3.207775	-0.379633
C	2.033475	-2.178419	3.054550
H	2.395492	-2.080573	2.015571
C	-1.041142	-2.682817	-4.334235
H	-1.863852	-3.419272	-4.285613
H	-1.350299	-1.782344	-3.774408
H	-0.901021	-2.403575	-5.393473
C	0.685827	-4.557993	-4.474053
H	-0.121339	-5.313275	-4.460593
H	0.928649	-4.338911	-5.529560
H	1.582050	-5.001714	-4.004494
C	-3.608660	-3.553505	0.368634
H	-3.867450	-2.508531	0.598127
H	-3.967248	-3.781994	-0.650518
H	-4.163575	-4.207324	1.064894
C	-1.756670	-5.272967	0.226487
H	-2.191042	-5.890846	1.033566
H	-2.177855	-5.622473	-0.733822
H	-0.669277	-5.455151	0.205716
C	5.089645	-1.456251	-0.971642
H	5.791663	-1.134136	-1.762513
H	5.574278	-1.282132	0.007257
H	4.925388	-2.542184	-1.085221
C	3.979533	0.830728	-0.838464
H	3.031495	1.383451	-0.937522
H	4.371139	1.009428	0.178379
H	4.702263	1.261973	-1.552786
C	2.819753	-3.328782	3.717683
H	3.904641	-3.119301	3.694572
H	2.517222	-3.448551	4.774080
H	2.644213	-4.292738	3.209506
C	2.324162	-0.839491	3.754209
H	3.404323	-0.613072	3.697147
H	1.775878	-0.013947	3.268485
H	2.046319	-0.864995	4.822313
C	-0.785766	1.228409	4.812055
H	-0.459734	0.228394	4.486863
H	0.096454	1.771910	5.193522
H	-1.490468	1.105659	5.653812
C	-1.953318	3.372993	4.124124
H	-2.771505	3.232558	4.853820
H	-1.149103	3.952128	4.614002
H	-2.345324	3.975509	3.286716
C	-5.260034	2.025256	-0.799788
H	-5.419144	2.277404	-1.863377
H	-6.185462	1.558865	-0.416054
H	-5.105297	2.965281	-0.243345
C	-4.273488	-0.215830	-1.468233

H	-4.391048	0.042692	-2.535678
H	-3.405522	-0.891332	-1.377149
H	-5.179851	-0.765578	-1.157553
C	2.994191	3.664931	2.089505
H	2.846475	3.869159	3.165583
H	2.958619	2.570965	1.937617
H	4.003431	4.021979	1.816672
C	1.912925	5.893072	1.476742
H	1.783871	6.134081	2.547380
H	2.868752	6.334837	1.141917
H	1.098846	6.382175	0.913083
C	0.140183	1.378033	-3.945877
H	0.700946	0.612012	-3.386706
H	-0.776683	0.906980	-4.339947
H	0.754579	1.684840	-4.810044
C	-0.944757	3.676910	-3.834055
H	-0.282530	4.094877	-4.614609
H	-1.845866	3.273731	-4.330358
H	-1.257443	4.505891	-3.175432

1Me$^{+}_{calc}$
Energy: −2936.189716704963 E_H

C	-0.56325786845140	2.40658874413522	0.13187887667684
C	0.74003305494678	-2.23316177715345	0.09267242140199
C	1.93693168347376	-4.05245589144903	0.74531220427901
C	-1.18392460580642	4.59402584194073	0.05924134373616
C	-2.31786282607514	3.84894330542850	0.22602116822153
C	2.12864677671947	-3.89415070792731	-0.59976986908716
H	2.32014736281292	-4.78792114253200	1.44829412844912
H	-1.03096042747754	5.66443084700377	-0.05058539396286
H	-3.36428731374687	4.13103459284783	0.31134335337579
H	2.70601005983147	-4.47251187662843	-1.31606577694027
N	1.08362100014557	-3.02989001608387	1.14636172868192
N	-0.12211585820025	3.69998987195571	0.00831621006563
N	-1.92247537268038	2.52069994120812	0.26610038154296
N	1.39506718081285	-2.77342517909152	-0.97983053439815
Si	0.43135345706738	0.80741273185808	0.12439353877389
Si	-0.77690721085131	-1.02797012940002	0.08820976169667
C	1.17895972840685	-2.32990468055499	-2.33766458957326
C	-0.01212091058990	-2.74514386699350	-2.98012231646971
C	2.14352421290046	-1.50253683013505	-2.95743632394243
C	-0.24352403839346	-2.26394095188654	-4.28147884623217
C	1.86216160479589	-1.05344181511512	-4.26134147282676
C	0.67677035257495	-1.41776395808952	-4.91109533101004
H	-1.15559377969960	-2.55964478392450	-4.80919128784275
H	2.58084710835252	-0.40747179947144	-4.77505995728343
H	0.47371872063911	-1.04724840922365	-5.92225724051985
C	0.50800389201276	-2.89985898861692	2.46371768627005
C	-0.71114723789782	-3.56911565718359	2.72311529346992
C	1.18551241184240	-2.12669595583824	3.43172537255608
C	-1.24277468353040	-3.45722443957109	4.02084551200027
C	0.61691312854251	-2.05808957438382	4.71670888767194
C	-0.58327973030748	-2.71684756081226	5.00879142282184
H	-2.18577099834348	-3.95947481610650	4.26208625772881
H	1.11719244218529	-1.47778403876332	5.49862716805397
H	-1.01445575521951	-2.64398506623028	6.01417047944518
C	1.22622869381124	4.06831828231600	-0.34147237952326
C	2.13317401082844	4.39809834166394	0.69102204499829
C	1.57354525361998	4.04410955585365	-1.71054798044639
C	3.45207528245502	4.70123980390089	0.30861570373515
C	2.91200191735463	4.33569165048510	-2.03601161480126
C	3.83964350187037	4.65864209118980	-1.03833195640684
H	4.19178196260484	4.96105511420859	1.07207296405073
H	3.22918240887832	4.31327677418641	-3.08448520383281
H	4.87652046448577	4.88442491454028	-1.31242799591343

C	-2.84165805488888	1.41624166079260	0.33951750623691
C	-3.38351754508413	0.92782403708045	-0.87095512402691
C	-3.14134077712871	0.87076967229381	1.60686445394702
C	-4.30962763392231	-0.12734139114158	-0.77569046150066
C	-4.07125911692412	-0.18349251551045	1.64476521264455
C	-4.65203857098403	-0.67225309269685	0.46740519903150
H	-4.76149228740753	-0.53241706759300	-1.68690619743599
H	-4.33671504696912	-0.63487338648797	2.60598074325706
H	-5.36944555901007	-1.49929887520463	0.51940951107608
C	0.55965571548009	3.72196138303949	-2.80441038714105
H	-0.43201529694069	3.63626636047443	-2.32958625574567
C	1.69220113470128	4.43739420504301	2.15058442793382
H	0.84933704870023	3.72974559429266	2.26033208065069
C	-3.01093692272027	1.52637762721595	-2.22260079838442
H	-2.15161980184580	2.19822615272417	-2.06279996396245
C	-2.50579822347195	1.41345395465983	2.88069488013904
H	-1.63837455446992	2.02854391962891	2.58304948598237
C	-0.96696624457884	-3.74862230284067	-2.34238208367409
H	-0.76118828978490	-3.76688316072336	-1.26054175197801
C	3.47081906160250	-1.17128651797508	-2.28550083492030
H	3.31927562019105	-1.24687675018156	-1.19427870204209
C	-1.41566204889686	-4.41249568742652	1.66824674543703
H	-0.93259211815233	-4.20681166179654	0.69873027925860
C	2.50062798796856	-1.42722203368173	3.11970188610270
H	2.60054485279140	-1.38490236360908	2.02160715070856
C	-2.44693620794322	-3.37086255679430	-2.49892109831866
H	-3.08046759389894	-4.09992298080045	-1.96444493136600
H	-2.64165597023619	-2.37491641556603	-2.06833783578405
H	-2.76361038026758	-3.36508357288260	-3.55684535296678
C	-0.67761159406090	-5.16383693888559	-2.88249518882824
H	-1.30849066599694	-5.91022156277495	-2.36654272268393
H	-0.88989875247282	-5.22362319006181	-3.96596094659069
H	0.38057269340379	-5.44278733106970	-2.73015641706373
C	-2.89867611000055	-4.03619372267244	1.51355352784496
H	-3.00756415753751	-2.96032707568194	1.29365008390055
H	-3.34849554606608	-4.60350757862077	0.67959921183350
H	-3.47908389125341	-4.26703781150727	2.42513564910051
C	-1.22860251732091	-5.91413316073168	1.95656451188033
H	-1.70151571292069	-6.19463670586785	2.91550045126554
H	-1.69117490488328	-6.52147696136620	1.15784754514371
H	-0.15817730576830	-6.17966037099345	2.01665040702023
C	4.54215124294858	-2.21027783458786	-2.68195971309291
H	4.72498240813858	-2.17414630630974	-3.77129609005815
H	5.49492445565290	-1.99937301041595	-2.16399162681050
H	4.23763945110929	-3.23899220008367	-2.42760978472446
C	3.97676115776399	0.24762710181567	-2.59240802085063
H	3.19661977762809	1.00459599848036	-2.42390087856126
H	4.83602531757288	0.48951340603180	-1.94338259515258
H	4.31958899379368	0.33720113316765	-3.63847396879320
C	3.69001552106416	-2.24477716811829	3.66139895841488
H	4.64834039505812	-1.76276966279837	3.39391723806684
H	3.63979438994841	-2.32489637018071	4.76280757644162
H	3.69372248537441	-3.26820106912425	3.24799680083011
C	2.52908729376761	0.02142457185643	3.63316904296028
H	3.44153515185135	0.52953132205425	3.27539957135431
H	1.65139887920075	0.58421252693131	3.27043790105871
H	2.53731498762694	0.07016844289791	4.73660205249454
C	-1.96799480598666	0.29299445002513	3.78366527625577
H	-1.28280536117022	-0.36424788780480	3.22374329649998
H	-1.41079846124107	0.72053583229952	4.63625524705778
H	-2.77991517103632	-0.32873475615584	4.20010869155684
C	-3.49236798231280	2.33477506608137	3.62413636042532
H	-4.39211133084593	1.77450189059233	3.93800263062050
H	-3.02210247791246	2.75875486810245	4.52974683447731
H	-3.82328327427873	3.17248870391554	2.98384905202709
C	-4.16772077921116	2.37784478989209	-2.77987321991105
H	-3.87615035837480	2.84686739371425	-3.73704153225190

H	-5.06207489415846	1.75554863897155	-2.96441549504968
H	-4.45361231356795	3.17974664259058	-2.07636044711000
C	-2.54698392230370	0.45871452695136	-3.22675391814045
H	-2.23073281783349	0.93499261620991	-4.17146317072196
H	-1.68772379673535	-0.10433913741274	-2.82614164181139
H	-3.35069622642335	-0.25856700269054	-3.46871999288692
C	2.78977184475891	4.00064418528937	3.13473260088446
H	2.36432554386246	3.89310013886118	4.14757901793259
H	3.23606038096463	3.03340147101722	2.84932300593133
H	3.60491359175954	4.74359633718730	3.19888798303087
C	1.16654013531952	5.84139212783539	2.51877206442738
H	0.81505363502574	5.85733144294659	3.56612939277439
H	1.96949425834858	6.59362386364819	2.41274963437580
H	0.32776041996780	6.15044838690059	1.87265407243001
C	0.85272183974906	2.37120844838301	-3.48295209296384
H	0.83151412784443	1.54140030482538	-2.75486537257011
H	0.09151242872310	2.15304070446441	-4.25169345483722
H	1.84105391354755	2.37332200689758	-3.97414273100660
C	0.46396884548675	4.86521452455871	-3.83152737187500
H	1.40708623981444	4.98514079592709	-4.39459125871020
H	-0.33723802933096	4.65300271461620	-4.56187886899343
H	0.23697577320456	5.82809617213699	-3.33972290815748
C	2.27531875027691	1.17756665361736	0.31730425521556
H	2.47488166495803	1.71977336519882	1.24305335646510
H	2.80647031028645	0.22367806764267	0.36612452468062
H	2.68433762259352	1.75754845549139	-0.50938301832132

(1Me^{+})'$_{calc}$
Energy: −2936.153786022380 E_H

C	-0.908210	2.274642	0.361230
C	0.859180	-2.277921	-0.312627
C	1.783761	-4.268430	0.288418
C	-1.186779	4.474702	-0.176708
C	-2.233813	4.114703	0.620804
C	2.392918	-3.868788	-0.866265
H	1.914660	-5.148664	0.912113
H	-0.926762	5.416498	-0.652010
H	-3.097756	4.667986	0.980290
H	3.177689	-4.320269	-1.467198
N	0.855103	-3.282803	0.614474
N	-0.396177	3.342605	-0.321911
N	-2.048867	2.772719	0.939418
N	1.813061	-2.657292	-1.213731
Si	0.203535	0.735519	0.858608
Si	-0.319590	-0.805887	-0.816482
C	2.179602	-1.858742	-2.352982
C	1.535480	-2.108784	-3.586458
C	3.190143	-0.885421	-2.176890
C	1.954886	-1.342834	-4.689667
C	3.559938	-0.138920	-3.309963
C	2.953229	-0.370376	-4.551545
H	1.488266	-1.502819	-5.666755
H	4.337314	0.626715	-3.223698
H	3.258112	0.220451	-5.422806
C	0.029580	-3.342560	1.791812
C	-1.276023	-3.866126	1.665293
C	0.556614	-2.837757	3.001183
C	-2.074751	-3.881324	2.823194
C	-0.281599	-2.883744	4.131211
C	-1.583206	-3.394321	4.041523
H	-3.095415	-4.273001	2.772982
H	0.084747	-2.505394	5.090886
H	-2.223352	-3.408937	4.931223
C	0.822155	3.326812	-1.087738
C	1.988896	3.849400	-0.490119

C	0.765951	2.859376	-2.421605
C	3.141209	3.923471	-1.295657
C	1.949766	2.940141	-3.175775
C	3.120671	3.476364	-2.621302
H	4.069156	4.320230	-0.870114
H	1.953404	2.588715	-4.210899
H	4.031295	3.536461	-3.228934
C	-3.025812	2.020836	1.684067
C	-4.158983	1.548614	0.985019
C	-2.792204	1.768450	3.055809
C	-5.096174	0.793807	1.716885
C	-3.760578	1.011170	3.738286
C	-4.899836	0.530385	3.077048
H	-5.983483	0.397492	1.211495
H	-3.620590	0.782567	4.798837
H	-5.638652	-0.062714	3.628958
C	-0.545839	2.374082	-3.030161
H	-1.163207	1.976465	-2.205973
C	2.014031	4.331214	0.956814
H	1.023101	4.130342	1.399080
C	-4.339160	1.765334	-0.514454
H	-3.580563	2.492276	-0.849277
C	-1.536730	2.283220	3.750730
H	-0.732250	2.311971	2.992189
C	0.473535	-3.192463	-3.730749
H	0.157737	-3.487107	-2.714509
C	3.899798	-0.716982	-0.839322
H	3.258111	-1.166858	-0.062130
C	-1.795670	-4.406203	0.336176
H	-1.151035	-4.003239	-0.464441
C	1.973230	-2.279954	3.093696
H	2.322894	-2.083869	2.064693
C	-0.784760	-2.697865	-4.463730
H	-1.551799	-3.493423	-4.475271
H	-1.210073	-1.815343	-3.956515
H	-0.569866	-2.428634	-5.512837
C	1.075077	-4.441133	-4.408300
H	0.326471	-5.252534	-4.460481
H	1.400248	-4.208707	-5.438375
H	1.953014	-4.814826	-3.851984
C	-3.230098	-3.947557	0.022382
H	-3.321519	-2.847659	0.072138
H	-3.513693	-4.267740	-0.995914
H	-3.966237	-4.384475	0.720039
C	-1.669769	-5.941880	0.298849
H	-2.299213	-6.406194	1.079541
H	-1.993827	-6.335182	-0.681837
H	-0.626726	-6.261767	0.468793
C	5.235015	-1.489500	-0.843532
H	5.924655	-1.069478	-1.598608
H	5.725272	-1.417349	0.144954
H	5.086689	-2.558202	-1.077286
C	4.098211	0.752610	-0.452512
H	3.141051	1.294820	-0.478330
H	4.506428	0.821204	0.571113
H	4.804966	1.266755	-1.126842
C	2.921821	-3.324475	3.716698
H	3.957302	-2.939626	3.741094
H	2.619121	-3.556099	4.754237
H	2.918079	-4.269264	3.146415
C	2.040857	-0.940775	3.847767
H	3.072158	-0.545090	3.816031
H	1.377468	-0.190340	3.381587
H	1.760176	-1.046976	4.910544
C	-1.043227	1.356606	4.872521
H	-0.951072	0.314412	4.520628
H	-0.048931	1.686979	5.218993

H	-1.717923	1.365609	5.747094
C	-1.746640	3.722830	4.261575
H	-2.551006	3.751466	5.019686
H	-0.820358	4.107223	4.725611
H	-2.026605	4.407807	3.442664
C	-5.716590	2.362432	-0.853419
H	-5.777722	2.588942	-1.932875
H	-6.534505	1.659301	-0.614277
H	-5.897797	3.297071	-0.293721
C	-4.080758	0.458122	-1.289622
H	-4.174874	0.628842	-2.377337
H	-3.063276	0.070196	-1.103428
H	-4.801972	-0.327094	-0.999717
C	3.039580	3.553653	1.800737
H	3.018085	3.911564	2.845849
H	2.803872	2.475937	1.798648
H	4.067548	3.688452	1.418162
C	2.248591	5.851697	1.027675
H	2.209448	6.199342	2.075774
H	3.239596	6.121920	0.619780
H	1.485367	6.404280	0.451615
C	-0.365108	1.233281	-4.037424
H	0.199547	0.397054	-3.597015
H	-1.351613	0.849202	-4.350332
H	0.166205	1.560569	-4.947987
C	-1.315093	3.555129	-3.659785
H	-0.742111	3.985696	-4.501229
H	-2.291798	3.214358	-4.047073
H	-1.498634	4.359538	-2.927427
C	-1.282127	-0.583446	1.268556
H	-1.532797	-1.494402	0.658556
H	-2.234749	-0.068313	1.293155
H	-1.031483	-1.006726	2.239091

$1Li^{+}_{calc}$
Energy: −2903.842666821888 E_H

C	18.35360953561810	38.70415497684752	29.30369934105416
C	17.81247667858898	39.95706722627968	31.14341034445683
C	17.91834227583649	40.80782375572000	30.08119938698703
C	18.00662833517249	37.46723090587859	31.41423523468093
C	16.74408162794007	36.83428384528534	31.54971071895904
C	16.71513199446632	35.58642579283314	32.21018151882103
C	17.89297249620431	35.00357605991068	32.70362745447289
C	19.12825560686763	35.66024826991876	32.56489642174171
C	19.21496581007612	36.91242116612403	31.91620551415348
C	15.46847562670076	37.48730422223893	31.02829928214912
C	14.49704052794333	36.49936237099468	30.36664511210928
C	14.78050864048302	38.27413676391333	32.16415949156279
C	20.54037489777052	37.65275869860629	31.76600943540484
C	20.72000701989621	38.65617812540390	32.92538470344066
C	21.75217721361592	36.71860451144216	31.64572397316298
C	18.46202083950743	40.54815741883146	27.65299761142915
C	19.74884263318215	41.03122510671255	27.33041911415087
C	19.92453284464770	41.58250677893260	26.04733759622031
C	18.86598868090977	41.62284761861678	25.13222751667168
C	17.60647270911252	41.11625754259606	25.47872528389950
C	17.37289343313695	40.56941634270166	26.75320822806505
C	20.90294204693049	40.97946795344418	28.32457896568595
C	22.12925180944836	40.25400216741719	27.74206046876975
C	21.25218229633008	42.39275586109214	28.82985639210746
C	15.99027611755463	40.08445297106975	27.17003897893477
C	15.28202694044030	39.28249410180530	26.07250006163377
C	15.12950169272697	41.27139363330144	27.64969711262774
C	17.99490728775686	34.98591224022088	26.32947119390329
C	18.19458565273179	33.82798104828503	24.36982117632211

C	18.56994789584897	32.98396064480072	25.37493457162931
C	17.42563755182271	36.20706396893102	24.24922382552780
C	18.39100838139203	37.19528064553614	23.94222840826198
C	17.95027060922151	38.31532214324317	23.21558373988663
C	16.61460243652882	38.42648546384827	22.80344308848558
C	15.68594983030480	37.42994856412039	23.12347551932771
C	16.06989980740548	36.29809020142424	23.86866406134225
C	19.85321703635950	37.01193517245750	24.33236707081990
C	20.60971179389150	36.23158635220978	23.23742282583234
C	20.56508742809229	38.32717911931999	24.66467694555564
C	15.05012826902177	35.22921307704426	24.24515329327353
C	14.51550089050165	34.50551048179506	22.99457791505560
C	13.91244370439183	35.80934592876510	25.10531803564700
C	18.84207996996519	33.24127779044800	27.85805870880499
C	17.84671385822439	32.69921214695739	28.71493239436822
C	18.24208837609208	32.35575396997017	30.02748155701755
C	19.56727982649398	32.54728333924466	30.45483304407146
C	20.53138866258562	33.06941044167074	29.57747233862973
C	20.19139994118575	33.43013121814471	28.25527376633296
C	16.41697166499209	32.48622029245198	28.22778375831660
C	16.27846476796563	31.08449068451533	27.59571725639683
C	15.36322801434966	32.70809018261536	29.32356040464906
C	21.24058873988358	33.96593060580926	27.28660211721099
C	22.00338163016049	32.78952443120718	26.64180163218185
C	22.20702900949012	34.97373998334103	27.92613465548613
Li	18.45864591030649	35.20970612062731	29.81525299434231
N	18.07835976293580	38.68011469501994	30.65255014569093
N	18.24358091837512	40.02869516007249	28.97678333233149
N	17.85734278188109	35.03747730764861	24.96793662401060
N	18.44895844867970	33.70649822768043	26.56012695758772
Si	19.14213600436373	37.35943840573342	28.15047754003341
Si	17.25026611636133	36.29316416725523	27.55674245319488
H	17.56770246592418	40.13190302693133	32.18753798378894
H	17.79530783913208	41.88530261929724	30.00368858592207
H	15.76383871337532	35.06002815047847	32.33220196170610
H	17.84992229585421	34.02745656909558	33.19871602644876
H	20.03349898137842	35.18914747801237	32.95828265186152
H	15.76708220626990	38.21181652309533	30.25172518886970
H	14.08111279108197	35.77251220790844	31.08731120640917
H	14.99467997025899	35.95237302804491	29.54638819010214
H	13.64625350340965	37.05265053934142	29.93156882732207
H	13.89440794630198	38.80687910725716	31.77570068819796
H	15.45745473042377	39.01950803460525	32.61650466471762
H	14.44589979814603	37.59015951005069	32.96513617069592
H	20.48085130729203	38.22774739212601	30.82475028127366
H	20.77270663204695	38.12692356649758	33.89437816821707
H	19.88497712157910	39.37547753704929	32.97548147247106
H	21.65623796088686	39.22711715575468	32.79304743434851
H	22.65612816485835	37.30972232517549	31.41722379960060
H	21.61507165413242	35.98308441198511	30.83408044065882
H	21.94955219077688	36.16929013259170	32.58403661714559
H	20.90637284933871	41.97067543082932	25.75659642055710
H	19.02605280645654	42.04536896665610	24.13353016739153
H	16.79175469710689	41.14825515451377	24.74836680945621
H	20.57158640110892	40.38858422123647	29.19602000645172
H	22.54545746584879	40.79051496209189	26.87057644938173
H	21.85302804060850	39.23355505347325	27.42724856924741
H	22.92569735008333	40.17856365230062	28.50481321264338
H	22.05854886077049	42.34681403848383	29.58485967178150
H	20.37391488428946	42.87987826802913	29.29043346194318
H	21.59744567814119	43.03706274172324	28.00036411500194
H	16.12466335897590	39.40011304127837	28.02559955634680
H	15.89981552126650	38.42869693285581	25.75087528857442
H	15.05299095145385	39.89878174755252	25.18537237458298
H	14.32658577346285	38.88152770927289	26.45316394348593
H	14.95121873903965	41.98549243204607	26.82440119241302
H	15.61769262869588	41.82196771317067	28.47341851617335

H	14.14744690050952	40.91577002967924	28.01066522690392
H	18.13038864555392	33.68571220087973	23.29355744927576
H	18.91577910153669	31.95419031599948	25.36354079261406
H	18.65889738468080	39.11075568871718	22.96752423178899
H	16.29265494061280	39.30843453157856	22.23683928449582
H	14.64215881298125	37.54017902955403	22.80938697361477
H	19.86815744364745	36.40554267112906	25.25500301375514
H	20.63807846388952	36.81258396378141	22.29717514217230
H	20.13453349844689	35.25991020537091	23.01876383733336
H	21.65133583901968	36.03701351617809	23.55197366492362
H	21.57422269134077	38.11772582654969	25.06064952450384
H	20.01261363104659	38.89035155594784	25.43174907391432
H	20.68635604580024	38.97148457262811	23.77538032592665
H	15.56380373417900	34.47534094925894	24.86628037640208
H	15.33999016946439	34.06043922382848	22.40843532261281
H	13.96828233271374	35.20260836162613	22.33355317456140
H	13.81868084188985	33.69727668889584	23.28234323523483
H	13.20640480662304	35.00829417720627	25.39062951089581
H	13.34428237023868	36.58329347107922	24.55793010267550
H	14.31784643315499	36.26072023133127	26.02696296424863
H	17.50609969858866	31.94547505346674	30.72491345069830
H	19.85009050815824	32.28750206256714	31.48053735913326
H	21.55944177245067	33.20529107773265	29.92692534004665
H	16.22810974615142	33.23530714864200	27.43822197426728
H	16.47289483446563	30.29807208354629	28.34761861391857
H	16.98829356926128	30.94224953957862	26.76327595923773
H	15.25570893581834	30.94146951241391	27.20386529958615
H	14.35278834018477	32.68855574362350	28.87946421136721
H	15.49397794489078	33.68735034468583	29.81512598790373
H	15.39800036230071	31.92269902929056	30.10001397243970
H	20.70386265623280	34.49909636590946	26.48325522999669
H	21.31799847947216	32.07752193108297	26.15025288796544
H	22.57780975058562	32.23334615206654	27.40556801185579
H	22.71406453668783	33.16268835039896	25.88227974974034
H	22.84494378490265	34.50629104505098	28.69783763957956
H	21.65239720630143	35.81608195086559	28.37577045208707
H	22.87564819576921	35.38871560671281	27.15144190225191

5.5 Cartesian coordinates [Å] and SCF energies of the calculated structures of $[(NHC^{Me})(Me)Si=Si(NHC^{Me})]^+$, $(NHC^{Me})(Me)Si=SiMe$, $Me_2Si=Si(NHC^{Me})$, $[Me_2Si=SiMe]^-$, $Me_2Si=PMe$ and $[Me_2P=PMe]^+$ (NHC^{Me} = C[N(Me)CH]$_2$

$[(NHC^{Me})(Me)Si=Si(NHC^{Me})]^+$
Energy: −1228.211705080193 E_H

C	-0.611300	2.333557	0.098470
C	0.545311	-2.275068	-0.038143
C	2.121424	-3.714638	0.711271
C	-1.029079	4.555750	-0.000502
C	-2.222574	3.920954	0.150323
C	2.217894	-3.671523	-0.645871
H	2.680890	-4.278059	1.441419
H	-0.794705	5.604840	-0.090170
H	-3.225938	4.310400	0.218013
H	2.877863	-4.190180	-1.323617
N	1.090321	-2.860919	1.066340
N	-0.051962	3.580533	-0.033147
N	-1.958159	2.568280	0.210194
N	1.243151	-2.793401	-1.088539
Si	0.220944	0.637120	0.109645
Si	-1.047940	-1.160974	-0.120376
C	2.094685	0.776998	0.393592
H	2.338427	1.320978	1.312855
H	2.479151	-0.242297	0.507382
H	2.638456	1.237524	-0.436704
C	1.362239	3.871957	-0.258188
H	1.469212	4.946938	-0.404431
H	1.961039	3.566235	0.600729
H	1.710920	3.353563	-1.154099
C	-2.987369	1.545862	0.344342
H	-2.730935	0.868807	1.164869
H	-3.939147	2.036077	0.549510
H	-3.062646	0.963463	-0.579390
C	1.014442	-2.434987	-2.485655
H	1.503967	-1.485445	-2.719223
H	1.414716	-3.225589	-3.122344
H	-0.059461	-2.331355	-2.658089
C	0.657321	-2.596838	2.435560
H	-0.434844	-2.573594	2.470488
H	1.029057	-3.393835	3.081465
H	1.042841	-1.632260	2.775945

$(NHC^{Me})(Me)Si=SiMe$
Energy: −963.505757125125 E_H

C	0.528383	-2.306265	0.119652
C	1.811363	-4.049053	0.816392
C	2.303930	-3.632931	-0.380445
H	2.139095	-4.835866	1.477842
H	3.136613	-3.995006	-0.962742
N	0.731678	-3.236385	1.115079
N	1.514850	-2.577423	-0.802660
Si	-0.008185	1.254887	0.035937
Si	-0.694788	-0.877133	0.055160
C	1.885491	1.038948	-0.429127
H	2.438337	1.866760	0.032635
H	2.357315	0.103926	-0.109222
H	2.018737	1.144541	-1.515149
C	1.648745	-1.926913	-2.099317
H	2.498776	-1.240653	-2.102111

H	1.780790	-2.688791	-2.873208
H	0.734096	-1.352611	-2.279940
C	0.002242	-3.245623	2.372191
H	-0.051625	-2.219721	2.753904
H	-1.013372	-3.626172	2.234404
H	0.535544	-3.878161	3.084236
C	-2.377418	-1.464119	0.744925
H	-2.745761	-2.355396	0.225161
H	-2.380071	-1.664411	1.821809
H	-3.095000	-0.654919	0.563124

$Me_2Si=Si(NHC^{Me})$
Energy: −963.525467746306 E_H

C	0.495435	-2.298581	-0.121986
C	2.077439	-3.647784	0.801269
C	2.287350	-3.635696	-0.543021
H	2.603721	-4.157354	1.592838
H	3.031356	-4.133672	-1.145200
N	0.978514	-2.839131	1.042179
N	1.312322	-2.819954	-1.092333
Si	0.120557	0.564742	0.067855
Si	-1.078403	-1.212256	-0.391899
C	1.972266	0.699998	0.514475
H	2.101192	1.187702	1.490342
H	2.452464	-0.283297	0.557227
H	2.512442	1.309044	-0.222381
C	1.199723	-2.479788	-2.502933
H	1.551142	-1.457497	-2.673181
H	1.793945	-3.188114	-3.084214
H	0.149272	-2.529925	-2.801927
C	0.433540	-2.547599	2.359792
H	-0.653103	-2.462504	2.280364
H	0.707324	-3.357669	3.041236
H	0.821813	-1.595033	2.731647
C	-0.605527	2.319350	0.004893
H	-0.507165	2.826730	0.974081
H	-0.091312	2.936694	-0.742781
H	-1.668878	2.280892	-0.253925

$[Me_2Si=SiMe]^-$
Energy: −698.698498749281 E_H

Si	0.012414	1.392027	0.196756
Si	-0.539424	-0.747467	0.175790
C	2.001784	1.220815	0.158900
H	2.431047	1.719447	1.041224
H	2.394029	0.195429	0.135134
H	2.399094	1.748622	-0.721428
C	-2.365648	-1.362113	0.200984
H	-2.614909	-1.958467	-0.690275
H	-2.579478	-1.990361	1.079417
H	-3.041684	-0.498925	0.230151
C	0.529464	-2.359766	0.136450
H	1.598329	-2.112850	0.118330
H	0.344332	-2.989279	1.020519
H	0.310093	-2.972107	-0.751883

$Me_2Si{=}PMe$
Energy: −750.577152623410 E_H

C	0.766111	-2.262019	0.184355
Si	0.271141	0.797099	-0.031578
P	-0.672782	-1.059620	-0.043226
C	2.103671	1.199351	0.153790
H	2.257476	1.883303	0.997833
H	2.708088	0.303606	0.318604
H	2.472494	1.702068	-0.749393
C	-0.766899	2.352178	-0.233678
H	-0.667845	3.004173	0.643488
H	-0.442751	2.928159	-1.109783
H	-1.823171	2.095022	-0.358201
H	0.579891	-2.861646	1.081742
H	1.747167	-1.790369	0.279726
H	0.790170	-2.940889	-0.674855

$[Me_2P{=}PMe]^+$
Energy: −802.202980964709 E_H

C	0.760117	-2.191362	0.187788
P	0.314992	0.811978	-0.024346
P	-0.613112	-0.970978	-0.027277
C	2.074938	1.210542	0.142862
H	2.201809	1.894927	0.989185
H	2.661050	0.305283	0.308282
H	2.411484	1.705546	-0.775289
C	-0.719212	2.279811	-0.224888
H	-0.619907	2.921040	0.657965
H	-0.395710	2.836073	-1.111681
H	-1.760885	1.970261	-0.341908
H	0.485276	-2.827048	1.037880
H	1.753557	-1.774148	0.350356
H	0.768366	-2.821510	-0.710107

6. References

[S1] Y. Wang, Y. Xie, P. Wei, R. B. King, H. F. Schaefer III, P. v. R. Schleyer, G. H. Robinson, *Science* **2008**, *321*, 1069.

[S2] a) M. Brookhart, B. Grant, A. F. Volpe, Jr., *Organometallics* **1992**, *11*, 3920; b) R. Taube, S. Wache, *J. Organomet. Chem.* **1992**, *428*, 431.

[S3] a) A. G. Massey, A. J. Park, *J. Organomet. Chem.* **1964**, *2*, 245; b) M. Lehmann, A. Schulz, A. Villinger, *Angew. Chem. Int. Ed.* **2009**, *48*, 7444; *Angew. Chem.* **2009**, *121*, 7580.

[S4] a) H. Nishida, N. Takada, M. Yoshimura, T. Sonoda, H. Kobayashi, *Bull. Chem. Soc. Jpn.* **1984**, *57*, 2600; b) S. R. Bahr, P. Boudjouk, *J. Org. Chem.* **1992**, *57*, 5545; c) R. Taube, S. Wache, *J. Organomet. Chem.* **1992**, *428*, 431; d) D. L. Reger, C. A. Little, J. J. S. Lamba, K. J. Brown, J. R. Krumper, R. G. Bergman, M. Irwin, J. P. Fackler, Jr., *Inorg. Synth.* **2004**, *34*, 5; e) N. Yakelis, R. G. Bergman, *Organometallics* **2005**, 24, 3579.

[S5] *gNMR*, Version 5.0.6.0, P. H. M. Budzelaar, IvorySoft, Centennial, USA, **2006**.

[S6] J. Sandström, *Dynamic NMR Spectroscopy*, Academic Press, London, **1982**.

[S7] A. Steigel, J. Sauer, D. A. Kleier, G. Binsch, *J. Am. Chem. Soc.* **1972**, *94*, 2770.

[S8] P. M. Morse, M. D. Spencer, S. R. Wilson, G. S. Girolami, *Organometallics* **1994**, *13*, 1646.

[S9] K. Brandenburg, DIAMOND 2.1c, Crystal Impact GbR, Bonn, Germany, **1999**.

[S10] G. M. Sheldrick, *SHELXS97* and *SHELXL97*, University of Göttingen, Germany, **1997**.

[S11] F. Neese, *WIREs Comput. Mol. Sci*. **2012**, *2*, 73.

[S12] a) S. Grimme, S. Ehrlich, L. Goerigk, *J. Comp. Chem*. ***2011***, *32*, 1456; b) S. Grimme, J. Antony, S. Ehrlich, H. Krieg, *J. Chem. Phys*. **2010**, *132*, 154104; c) S. Grimme, *J. Comp. Chem*. **2006**, *27*, 1787.

[S13] A. Klamt, G. Schüürmann, *J. Chem. Soc., Perkin Trans. 2* **1993**, 799.

[S14] a) F. Neese, *J. Comput. Chem.* **2003**, *24*, 1740; b) F. Neese, F. Wennmohs, A. Hansen, U. Becker, *Chem. Phys.* **2009**, *356*, 98.

[S15] a) A. Schäfer, H. Horn, R. Ahlrichs, *J. Chem. Phys*. **1992**, *97*, 2571; b) F. Weigend, R. Ahlrichs, *Phys. Chem. Chem. Phys.* **2005**, *7*, 3297.

[S16] J. B. Foresman, Æ. Frisch, *Exploring Chemistry with Electronic Structure Methods*, 2nd ed., Gaussian, Inc. Pittsburgh, PA, **1996**.

[S17] NBO 6.0 Program. E. D. Glendening, J. K. Badenhoop, A. E. Reed, J. E. Carpenter, J. A. Bohmann, C. M. Morales, C. R. Landis, F. Weinhold, Theoretical Chemistry Institute, University of Wisconsin, Madison, **2013**.